Roles of the Stemness Factor SOX2 in Melanoma

and

Multicolor Lineage Tracing to Address Clonality in Melanoma

Dissertation

zur

Erlangung der naturwissenschaftlichen Doktorwürde

(Dr. sc. nat.)

vorgelegt der

Mathematisch-naturwissenschaftlichen Fakultät

der

Universität Zürich

von

Simon Manuel Schäfer

Von Luzern LU

Promotionskomitee

Prof. Dr. Onur Boyman (Vorsitz)

Prof. Dr. Ian Frew

Prof. Dr. Michael Detmar

Prof. Dr. Lukas Sommer (Leitung der Dissertation)

Zürich, 2017

Acknowledgements

I would like to express my gratitude for the following persons:

Prof. Dr. Lukas Sommer,
I would like to thank you for the provided mentorship and creative working environment eventually leading to the performed work.

Prof. Dr. Onur Boyman, Prof. Dr. Ian Frew and Prof. Dr. Michael Detmar
For the scientific inputs and ideas during the committee meetings and for co-reviewing my PhD thesis.

All members and alumni of the Sommer laboratory,
For long-standing scientific support and inputs. Most importantly, thank you for creating a friendly, enthusiastic and inspiring environment leading to many outstanding moments.

Dr. Olga Shakhova and Dr. Daniel Zingg,
For your competent supervision during my master thesis.

Nicole Bachelin and Monika Jenny,
For your support regarding administrative matters, especially nerve-racking expense forms.

Corina Segalada,
For being a highly enthusiastic master student.

Dr. Mario Bonalli, Dr. Phil Cheng, Vadims Parfejevs, Prof. Mitchell Levesque, Prof. Reinhard Dummer, Prof. Silvia Nicolis,
For a fruitful collaboration leading to the published work.

Dr. Susanna Dolci
For an excellent collaboration and counterchecking the submitted manuscript.

My family and my friends,
For encouraging support and good times.

Table of contents

1. Summary

Malignant melanoma, which is the most deadly type of skin cancer, is characterized by its high efficiency to form regional and distant metastases. Melanomas often present with a high degree of genetic and phenotypic heterogeneity, which makes treatment of evolved and metastasized tumors extremely challenging. During my PhD. thesis, I therefore studied and analyzed mechanisms how intratumor heterogeneity can be established. To shed more light into mechanisms of melanoma initiation and progression, we additionally studied the role of Sox2, which appeared to be a promising factor mediating those oncogenic processes.

1.1. The role of Sox2 in primary melanoma and metastasis formation

SOX2 is a transcription factor containing a high-mobility group DNA binding site, through which it binds the minor groove of the DNA and affects target gene transcription. It is highly expressed in the inner cell mass of the embryo, where it plays an essential role in maintaining a pluripotent cell state. In the human and mouse skin, SOX2 is not expressed in differentiated melanocytes but gets upregulated upon malignant transformation in a subset of melanoma patients. A growing body of evidence suggests that SOX2 plays a role in melanoma initiation and invasion, although most studies were performed solely *in vitro*. Hence, we decided to shed more light on this issue, by depleting *Sox2* in a mouse model which spontaneously develops melanoma.

Unexpectedly, Tamoxifen-induced conditional ablation of *Sox2 (Sox2* cKO*)* in the melanocytic lineage did not affect tumor initiation, growth nor metastasis formation. Moreover, we did not observe differences in melanoma-specific survival comparing *Sox2* cKO mice to the control group. To analyze the role of SOX2 in human melanoma cells, we genetically depleted *SOX2* using the CRISPR-Cas9 genome editing technology. Consistent with the obtained *in vivo* results, *SOX2* KO and control cells showed similar growth pattern upon xenotransplantation into immunocompromised mice. Moreover, the transcript levels of melanocyte differentiation genes did not differ comparing control and *SOX2* KO tumors. Using bioinformatics and data from the cancer genome atlas, we did not observe a link between SOX2 expression and overall patient survival, strengthening the obtained results. In summary, we conclude that SOX2 is functionally not involved in melanoma formation and progression.

1.2. Multicolor lineage tracing to address clonality in primary mouse melanomas and metastases

In the scientific community, it is widely accepted that tumors originate from one mutated clone, which acquires additional mutations as the tumor evolves. This is mainly based on studies

analyzing female cancer patients heterozygous for certain X-chromosome-linked markers. However, it remains highly controversial if tumors originate from one or multiple clones, especially since mouse adenomas were found to be polyclonal. To bring more knowledge into this field, we applied a multicolor lineage tracing strategy to monitor the development of premalignant melanocytes, which were stochastically labelled in four different fluorescent colors. Applying this experimental setup, monoclonal tumors would be exclusively unicolored while multiple colors within tumors would point towards polyclonality.

Surprisingly, we discovered that 80% of all analyzed mouse melanomas were polyclonal. Using a fluorescent-activated cell sorting approach, we were able to isolate and separate the differently colored intratumor clones from one tumor. All isolated clones expressed transcripts specific for the melanocytic lineage, confirming their melanocytic origin. Further, we observed that all clones initiated tumors and expanded upon reinjection into immunocompromised recipient mice, demonstrating the tumorigenicity of each clone. Last, we detected multiple different colored cancer clones within lymph nodes and distant organs, speaking for polyclonal metastasis formation. In summary, most primary mouse melanomas and metastases were surprisingly polyclonal, contradicting the widely accepted view that tumors originate from one mutated cell.

2. Zusammenfassung

Metastasierender schwarzer Hautkrebs (Melanom) ist der tödlichste Typ aller Hautkrebse und zeichnet sich durch seine enorme Effizienz aus, regionale und distale Metastasen zu bilden. Charakteristisch für diese Art Tumore ist die häufig vorhandene hohe genetische und phänotypische Heterogenität, wodurch sich die Behandlung von metastasierten und weit entwickelten Tumore als enorm schwierig gestaltet. Aus diesen Gründen habe ich während meiner Doktorarbeit Mechanismen studiert, welche zu dieser Heterogenität beitragen. Um die Melanom Entstehung und Entwicklung besser zu verstehen habe ich zusätzlich die Rolle des Sox2 Genes studiert, welches unserer Ansicht ein vielversprechender Faktor war, der an diesen onkogenen Prozessen beteiligt sein könnte.

2.1. Der Einfluss von Sox2 auf die Entstehung und Metastasierung vom schwarzen Hautkrebs

SOX2 ist ein Transkriptionsfaktor und bindet die kleine Furche der DNS durch eine HMG (*high mobility group,* Englisch) Domäne. Das Protein ist stark exprimiert in der inneren Zellmasse des sich entwickelnden Embryos und erfüllt dort eine entscheidende Rolle in der Erhaltung des pluripotenten Status. Obwohl differenzierte Melanozyten der humanen und murinen Haut SOX2 nicht exprimieren wird die Expression in einigen Patienten mit schwarzem Hautkrebs hochreguliert. Des Weiteren konnte anhand Versuchen mit humanen Melanoma Zellen gezeigt werden, dass SOX2 einen entscheiden Einfluss auf das Wachstum der Krebszellen hatte. Weil diese Studien hauptsächlich in der Zellkultur (*in vitro)* durchgeführt wurden habe ich während meiner Doktorarbeit den Einfluss von Sox2 auf die Entstehung und Metastasierung vom schwarzen Hautkrebs anhand transgener Mäusen (*in vivo*) studiert.

Erstaunlicherweise führte die Melanozyten-spezifische und Tamoxifen-induzierte *Sox2* Deletion im Melanom Mausmodell im Vergleich zu Kontrolltieren zu keiner veränderten Anzahl Primärtumoren und Metastasen. Zusätzlich konnten wir keinen statistisch signifikanten Unterschied in der Melanom spezifischen mittleren Überlebenszeit zwischen den zwei Gruppen feststellen. Durch den Gebrauch der CRISPR-Cas9 Technologie konnten wir ausserdem *SOX2* in humanen Melanomzellen ablatieren. Wir konnten zeigen, dass *SOX2* KO und Kontrollzellen ein ähnliches Wachstumsmuster aufwiesen nachdem Sie in immunkomprimierte Mäuse injiziert wurden. Ferner unterschieden sich die Tumore nicht in ihrem Differenzierungsgrad, was anhand der Transkriptlevels von spezifischen Melanozyten Differenzierungsgenen bestimmt wurde. Mit Hilfe bioinformatischer Analyse von TCGA Daten (The Cancer Genome Atlas, *Englisch)* konnten wir zeigen, dass keine Korrelation zwischen SOX2 Expression und dem Gesamtüberleben von

Melanom Patienten bestand. Zusammenfassend haben unsere Daten gezeigt, dass SOX2 keinen Einfluss auf die Entstehung, das Wachstum und Metastasierung vom schwarzen Hautkrebs hat.

2.2. Klonalitätsbestimmung von Melanomen und deren Metastasen

Es wird weitgehend akzeptiert, dass sich Tumore aus einer mutierten Zelle entwickeln, welche im Verlaufe der Onkogenese zusätzliche Mutationen akquiriert. Dieses Denken stützt sich hauptsächlich auf Studien, in welchen heterozygote X-chromosomale Marker in weiblichen Krebspatientinnen studiert wurden. Weil gezeigt wurde, dass sich intestinale Adenokarzinome aus mehreren Zellen bilden können (polyklonal), bleibt die Frage höchst kontrovers, ob sich Tumore aus einer (mono) oder multiplen (poly) Klonen entwickeln. Deshalb haben wir in einem Melanom Mausmodell prämaligne Melanozyten in vier unterschiedlichen fluoreszierenden Farben markiert, um deren Entwicklung zur Onkogenese zu verfolgen. Falls sich Melanome aus einem Klon entwickeln würden, könnte man davon ausgehen, dass die Tumore einfarbig wären (monoklonal). Anderseits würden mehrfarbig Tumore darauf hindeuten, dass multiple Zellen einen Tumor geformt haben (polyklonal).

Überraschenderweise waren 80% der untersuchten Maus Melanome polyklonal. Mit Hilfe der auf Fluoreszenz basierender Durchflusszytometrie konnten wir die unterschiedlich farbigen Klone eines Tumors voneinander separieren. Da alle isolierten Klone Transkripte von Melanozyten spezifischen Genen exprimierten, konnten wir davon ausgehen, dass die Klone tatsächlich einen melanozytären Ursprung hatten. Des Weiteren konnten wir beobachten, dass alle Klone Tumore bildeten nachdem Sie in immunkomprimierte Mäuse injiziert wurden. Die Analyse von Lymphknoten und Lungenmetastasen zeigte, dass sich mehrere unterschiedlich farbige Klone innerhalb dieser Metastasen befanden, was darauf schliessen lässt, dass diese Ableger vermutlich von mehreren Klonen gebildet wurden. Zusammenfassend zeigen unsere Experimente, dass Maus Melanome und Metastasen polyklonal sein können. Diese Daten widersprechen der etablierten Meinung, dass sich Tumore aus einer mutierten Zelle entwickeln.

3. Introduction

3.1. Stem cells

3.1.1. Embryonic stem cells and induced pluripotent stem cells

Embryonic stem cells (ESCs) are derived from the inner cells mass of the blastocyst and are characterized by following properties: 1) They are pluripotent, which enables them to differentiate into all germ layers (endoderm, mesoderm and ectoderm) and 2) They have the capacity to self-renew and therefore maintain a copy of themselves (Moore et al. 1973; McCulloch 1961; Weissman 2000; Martello & Smith 2014). The first successful isolation and culturing of mouse ESCs (mESCs) was achieved in the year 1981, while human ESCs (hESCs) were cultured for the first time in the year 1998 (Evans & Kaufman 1981; Thomson et al. 1998). It was shown that hESC maintained their potency even after 4-5 month of culturing with the potential to differentiate into all three germ layers, making this culture system a potent tool for researchers. Therefore, ESCs can be used for transplantation assays, tissue engineering and many other potential clinical applications (Levenberg et al. 2002). For example, ES-derived cells were successfully used to treat several diseases in mouse models (Shamblott & Clark 2004). Nevertheless, ethical issues arise from the fact that the early embryo, and therefore a potential life, has to be destroyed to obtain ESCs. Scientists developed therefore a method to produce pluripotent cells from differentiated skin fibroblasts. These so-called induced pluripotent stem cells (iPSCs) are generated by the overexpression of the four "Yamanaka" transcription factors *Sox2*, *Oct3/4*, *Klf4* and *c-Myc* (Takahashi & Yamanaka 2006). They elegantly showed that the generated stem cells carried the same markers as ESCs and, moreover, xenografting iPSCs caused growth of tumors of various tissues of all three germ layers. Nevertheless, the efficiency of generating iPSCs from fibroblasts remains very low, calling for new optimization protocols enhancing this reprogramming process.

Another potent application of iPSCS is disease modelling (Figure 3.1.). The ground-breaking paper by Park and colleagues described the generation of iPSCs from patients carrying genetic disorders like muscular dystrophy, Parkinson disease, Huntington disease or early onset, type I diabetes mellitus. (Park et al. 2008). The patient-derived generated stem cells can be reprogrammed into disease-specific cell types and serve therefore as a useful model system enabling investigations into human diseases (Figure 3.1).

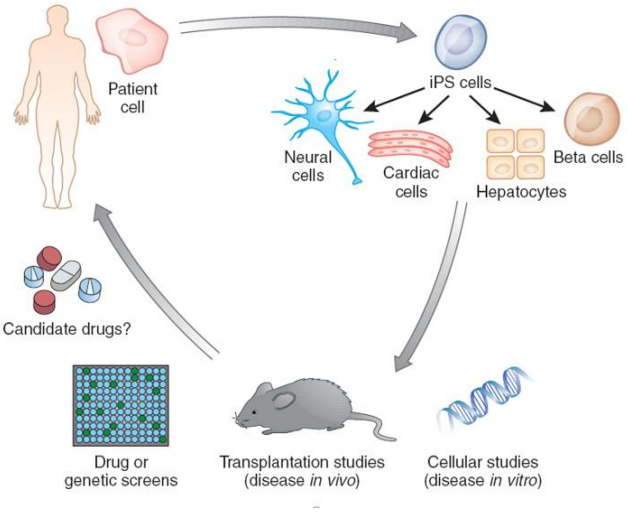

Figure 3.1. Disease modelling with IPSCs. Patient-derived cells harboring specific mutations are reprogrammed to iPSCs and subsequently differentiated towards disease-specific cell types. This allows phenotype analysis, disease mechanism elucidation, toxicity and efficacy screening and drug discovery. Adapted from (https://www.mskcc.org/sites/default/files/node/35635/images/disesae-modeling.jpg.). Lorenz Studer Lab, MSKCC).

3.1.2. Neural crest stem cells

Neural crest stem cells (NCSCs) are a transient embryonic cell population emerging from the dorsal part of the neural tube and display multipotent properties *in vitro* and *in vivo* (Baggiolini et al. 2015; Bronner-Fraser & Fraser 1989; Crane & Trainor 2006; Shakhova & Sommer 2010; Sommer 2001) (Figure 3.2.). NCSCs undergo epithelial-to-mesenchymal transition (EMT), migrate extensively towards many different parts of the body and eventually differentiate into specialized cells. They differentiate towards most cells of the peripheral nervous system (PNS), melanocytes, smooth muscle cells of the cardiovascular system, craniofacial cartilage, connective tissue and bones. While most cartilage and bone structures of the face originate from the cranial neural crest, the trunk neural crest gives rise to melanocytes of the skin and sensory and sympathetic ganglia of the PNS. Interestingly, isolation of NCSCs was not only possible from an embryonic structure but also from adult tissue. Namely, neural crest lineage traced cells (*Wnt1::Cre/ R26R)* found in the adult mouse skin expressed the NCSC markers Sox10 and $p75^{NTR}$, formed spheres upon isolation in culture and differentiated into neural crest derivatives *in vitro* (Wong et al. 2006).

NCSCs can be cultured as relatively pure population after explanting the cells from avian or rodent embryos at stages before emigration. Therefore, this culture system display a potent tool for differentiation studies *in vitro.* By adding specific growth factors (TGF-β, BMP-2, NRG-1, Wnt-1), NCSCs are able to differentiate into specific neural crest derivatives *in vitro*, demonstrating their multipotent properties in the culture system (Shakhova & Sommer 2010). They can be kept in a

pluripotent state by activated combinatorial Wnt/BMP signaling and are characterized by the expression of the two neural crest stem cell markers $p75^{NTR}$ and Sox10 (Stemple & Anderson 1992; Paratore et al. 2001; Kléber et al. 2005). To demonstrate the multipotentiality of NCSCs *in vivo*, Baggiolini and colleagues performed multicolor lineage tracing experiments labeling and following the fate of premigratory and migratory NCSCs in mouse embryos. (Baggiolini et al. 2015).

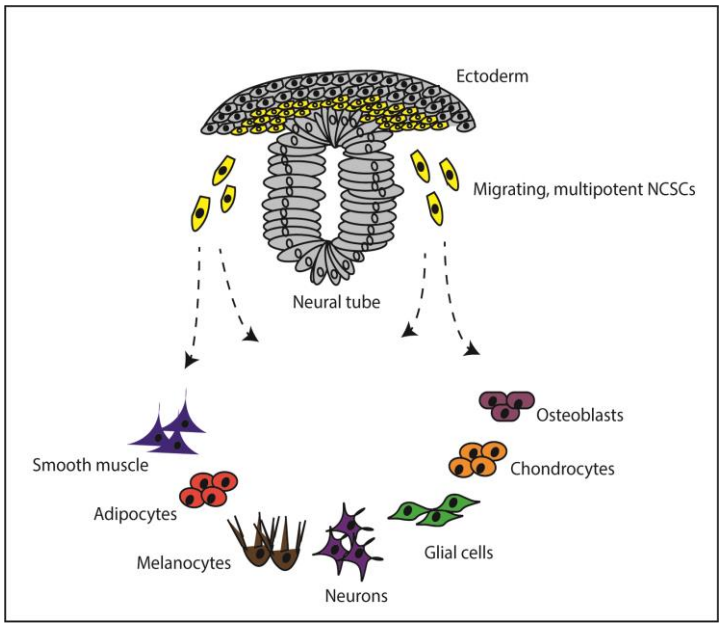

Figure 3.2. NCSCs and differentiated derivatives. Multipotent NCSCs (yellow) and emerge from the dorsal part of the neural tube, undergo EMT and migrate via different routes to specific parts of the embryo where they differentiate to specialized cell types. Drawn by Simon Schäfer, adapted from (Shakhova & Sommer 2010).

3.1.3. Cancer stem cells

Cells with stem cell properties not only exist in a physiological but also in a pathophysiological malignant context. John E. Dick performed pioneer work in this field, demonstrating that only a subset of acute myeloid leukemia (AML) cells (CD34-positive/CD38-negative) was able to initiate new tumors upon xenotransplantation into immunocompromised nude mice (Lapidot et al. 1994). Hence, cancer stem cells were defined as a small subset of cells within a tumor which have the unique capabilities to self-renew and maintain tumor growth (Clarke et al. 2006). Therefore, they are able to divide and expand the cancer stem cell pool due to their self-renewal potential and manage to differentiate into non-tumorigenic, proliferating tumor bulk cells due to their (multi)potentiality (Clarke et al. 2006; Reya et al. 2001). Experimentally, this hypothesis is tested by transplanting maker-based cancer cell subpopulation into immunocompromised mice. Those cells should be tumorigenic over several passages and able to phenocopy the parental tumor

(Visvader & Lindeman 2008). First proper evidence for the existence of CSCs in solid tumors came from Al-Hajj and colleagues in the year 2003. The authors showed that a subpopulation of breast cancer cells harboring the surfacemarker phenotype CD44-positive/CD24$^{-/Low}$ had enriched tumor initiating capacities (Al-Hajj et al. 2003). As few as 100 cells carrying this particular phenotype were able to initiate tumorigenesis whereas more than 10000 cells carrying different phenotypes did not grow upon xenotransplantations. Among several other surface markers, the glycoprotein CD133 (prominin-1) has been identified as glioma-CSC marker in several studies (Bao et al. 2006; Bao, et al. 2006; Beier et al. 2007). One study elegantly demonstrated that the percentage of CD133-positive cells was enriched after radiotherapy and those cells survived ionizing radiation in increased proportions compared to the CD133-negative fraction (Bao et al. 2006). Mechanistically, CD133-positive CSCs activated DNA damage checkpoints in response to radiation. Another study elegantly showed that colon cancer initiating cells were always CD133-positive while CD133-negative tumor bulk cells did not initiate tumor growth upon xenotransplantation (O'Brien et al. 2007).

Regardless of these studies, it has to be questioned if xenograft mouse models represent a faithful tool accurately representing tumor initiation in patients. For example, Kelly and colleagues hypothesized that the low frequency of human AML cells initiating tumor growth in NOD/*scid* mice could rather reflect how well the cells adapt to a foreign (mouse) milieu (Kelly et al. 2007). Next, it is known that immune cells have a defined roles in tumor initiation and progression (Visvader & Lindeman 2008). A study highlighted this point by demonstrating that the percentage of melanoma CSCs seemed to be dependent on the degree of immune deficiency in recipient mice (Medema 2013; E Quintana et al. 2008).

Since CSCs are the only tumorigenic cells driving cancer growth, selective targeting of this particular subpopulation might have profound clinical consequences. Albeit existing challenges to exclusively target CSCs, Guzman and colleagues demonstrated that the small molecule parthenolide (PTL) preferentially targets AML progenitor and stem cell populations (Guzman et al. 2005). In summary, there is substantial evidence for the existence of CSCs in many cancers, which might drive tumorigenesis and promote drug resistance. Nevertheless, experimental setups only partially reflect endogenous tumor formation and specific targeting of CSC remains challenging.

3.2. Transcription factor Sox2

3.2.1. Sox2 and its role in maintaining pluripotency in embryonic stem cells

Sex determing region Y-Box 2 (*SOX2*) is a member of the SoxB1 transcription factor family (Sox1,2 and 3), is located on Chromosome 3 in the human genome and possesses one exon (Zhang

& Cui 2014). It has a high-mobility group (HMG) domain and interacts with the minor groove of the DNA (Remenyi 2003). In the early mouse embryo, Sox2 is expressed in the inner cell mass (ICM) and the epiblast. Consistent with the findings that Sox2 is the only SoxB1 gene expressed before implantation, *Sox2*-null homozygous mouse embryos were lethal and died around embryonic day 5.5 (Lovell-badge 2015; Avilion et al. 2003). Another study could show that *Sox2* knockdown (KD) in a 2-cell stage mouse embryo arrested its development in the morula stage and let to increased apoptosis (Keramari et al. 2010). A recent publication highlighted the importance of Sox2 posttranslational regulations in fate determination of ESCs (Fang et al. 2014). Set7 can monomethylate Sox2 at K119 and is therefore inhibiting its transcriptional activity. On the other hand, Sox2 is phosphorylated by Akt1 at T118 leading to protein stabilization. Subsequently, Akt1 activity is higher in murine ESCs than Set7. During early development, Set7 expression is upregulated leading to lower Sox2 expression and proper differentiation (Fang et al. 2014). Further, it has been shown that Sox2 forms a complex with Oct3/4, binds to the FGF-4 enhancer and therefore controls early processes in development like limb patterning and growth (Yuan et al. 1995). Therefore, many different published studies postulate Sox2 as an essential guiding factor for maintaining pluripotency in the early mouse embryo.

3.2.2. Sox2 and its role in induced pluripotent stem cells (iPSCs)

In the year 2006, Kazutoshi Takahashi and Shinya Yamanaka published a study named “induction of pluripotent stem cells from mouse embryonic and adult fibroblast cultures by defined factors (Takahashi & Yamanaka 2006). By overexpressing the four factors *Sox2, Oct3/4, Klf4* and *c-Myc*, they succeeded in reprograming fibroblasts towards stem cells if cultured under ESCs conditions (see 3.1.). Interestingly, single cell gene expression analysis during reprogramming revealed endogenous *Sox2* activation as a relatively early event (Buganim et al. 2012). The authors of the study postulate that activation of endogenous *Sox2* can be seen as a first step driving a subsequent chain of events leading to correct cellular reprogramming (Buganim et al. 2012). In contrary, it has been shown that *Sox2* can be replaced by other factors of the SoxB1 family (*Sox1* and *Sox3*) for successful reprogramming (Nakagawa et al. 2008). Further, Hochedlinger and colleagues demonstrated that *Sox2* is dispensable for reprogramming melanocytes and melanoma cells into IPSCs (Utikal et al. 2009). Next, it was shown that Sox2 can be replaced by the glycogen synthase kinase 3 (GSK3) inhibitor CHIR99021 for generation of iPSCs, making exogenous Sox2 dispensable for the reprogramming under certain experimental settings (Chalovich & Eisenberg 2009) .

3.2.3. Sox2 and its role in adult tissues and stem cells

In the adult organism, Sox2 expression has been reported in several tissues (Arnold et al. 2011). The transcription factor is highly expressed in multipotent neural progenitors cells in the brain (Ellis et al. 2004). The authors generated a *Sox2::EGFP* transgenic reporter mice, labelling all Sox2 expressing cells in green. Fluorescent cells were detected in proliferating neural progenitor cells and formed neurospheres upon isolation. Those spheres were passaged repeatedly and had the potential to differentiate into neurons, astrocytes and oligodendrocytes (Ellis et al. 2004). Further, Sox2 expression was observed in the trachea (Que et al. 2007) , the retina (Taranova 2006), the tongue epithelium (Okubo et al. 2006) and dermal papilla of the hair follicle (Ryan R Driskell et al. 2009a). Although Sox2 was expressed in all dermal papillae of E16.5 mouse embryos, its expression got restricted to guard/awl/auchenne follicles in postnatal skin. On the contrary, zigzag follicles showed CD133-positive/Sox2-negative dermal papillae. Interestingly, Sox2-positive and Sox2-negative hair follicles displayed distinct expression of gene sets with different activated pathways specifying different types of follicles (Ryan R Driskell et al. 2009a). Arnold and colleagues showed Sox2 expression in several adult epithelial tissues, including stomach, cervix, anus, testes, lens and multiple glands (Arnold et al. 2011) (Figure 3.3.). Lineage tracing and transplantation assays of labelled Sox2-positive cells were able to give rise to mature cell types within these particular tissues. Moreover, Sox2 depletion let to disrupted epithelial tissue homeostasis and cell death (Figure 3.3).

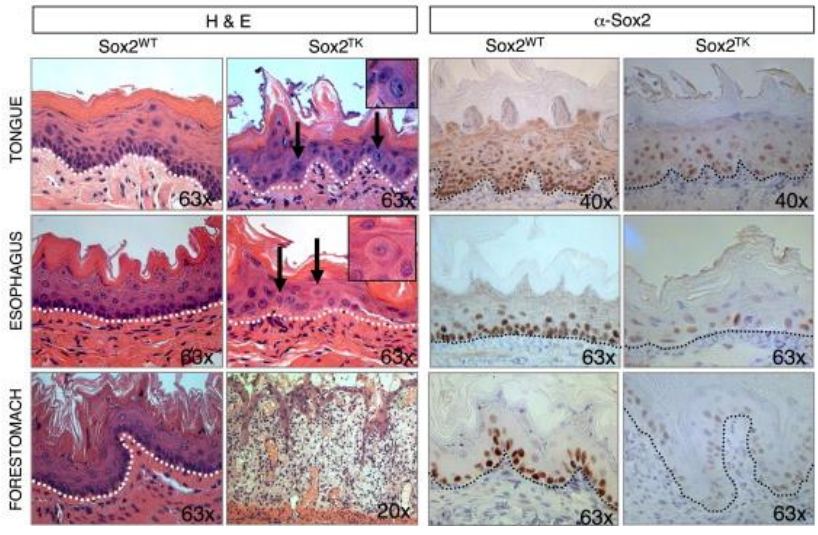

Figure 3.3 *Sox2* depletion leads to disruption of adult epithelial tissue. Left panel: H&E pictures of different epithelial tissue in *Sox2*^{wt} and *Sox2*^{TK} (*Sox2* knockout) mice. In the tongue, esophagus and forestomach, the epithelial tissue is disrupted and loss of the basal membrane was observed (dashed line). Right panel: Sox2 immunostaining confirms *Sox2* loss. Adapted from (Arnold et al. 2011).

3.2.4. Sox2 and its role in cancer

Sox2 has not only been studied under a physiological context but also extensively in malignant diseases. It is amplified in many cancers and associated with regulations of specific cellular pathways (Wnt/β-Catenin, AMPK/mTOR, BMP, Hedgehog-GLI) leading to altered cellular functions (Fang et al. 2010; Chen et al. 2008; Corominas-Faja et al. 2013; Santini et al. 2014; Weina & Utikal 2014). An interesting study by Bouhmadi and colleagues deciphered an essential role of Sox2 in the formation and maintenance of murine squamous cell carcinoma (Boumahdi et al. 2014). Despite Sox2 absence in the mouse epidermis, it started to be upregulated and being heterogeneously expressed upon chemically induced carcinogenesis. Consistent with these findings, Tamoxifen (TM)-based conditional *Sox2* deletion in the mouse epidermis significantly decreased the formation of skin squamous cell carcinomas (Boumahdi et al. 2014). In medulloblastoma, it has been shown that Sox2 is expressed in rare quiescent and tumor propagating cells (Vanner et al. 2014). Lineage tracing experiments using *Sox2::CreER*^{T2} stop$^{lox/lox}$ tdtomato transgenic mice elegantly proofed the tumor propagation potential of Sox2-positive cells. Moreover, the tracings revealed that the Sox2-positive cells were able to differentiate into doublecortin (Dcx)-positive and NeuN-positive proliferating tumor bulk cells (Vanner et al. 2014). A recent study showed that prostate cancer cells lacking *TP53* and *RB1* are able to develop resistance to the antiandrogen drug enzalutamide by phenotypic shifting from luminal to basal-like cells (Mu et al. 2017). The authors demonstrated that the phenotypic switching is mediated by increased SOX2 expression and can be reversed by *SOX2* inhibition. Andoniadou and colleagues presented strong evidence for the role of Sox2 in paracrine signaling in pituitary tumors (Andoniadou et al. 2013). Overexpressing the oncogenic β-catenin in Sox2-positive cells (*Sox2::Cre*^{ERT2} *Ctnnb1*$^{lox(ex3)/+}$) let to reliable pituitary tumor formation. Interestingly, the tumors did not derive from those Sox2-positive cells, suggesting a paracrine role of Sox2-positive cells in pituitary tumorigenesis (Andoniadou et al. 2013). Next, *PRKCI* and *SOX2* are coamplified in lung squamous cell carcinoma (LSCC) and cooperate to drive a stem-like phenotype (Justilien et al. 2014).

In summary, Sox2 has been attributed to have an oncogenic role in many cancers. However, Sarkar and colleagues recently showed that Sox2 can act as a tumor suppressor in a gastric cancer mouse model (Sarkar et al. 2016). In this particular context, Sox2 acts as tumor suppressor by inhibiting Wnt signaling through Tcf/Lef dependent genes. TM-based *Sox2* loss in *Sox2::Cre*$^{ERT2/flox}$ *Apc*$^{flox/flox}$ mice enhanced Wnt-driven tumor formation. Therefore, the role of Sox2 in cancer cannot be attributed to a typical tumor suppressor or oncogenic role, but stays complex under different cellular contexts.

3.3. Melanocyte and nevus biology

3.3.1. Melanocyte biology

3.3.1.1. Melanocyte development and its master transcription factors

Melanocytes are derived from NCSCs, a highly migratory stem cell population delaminating from the dorsal part of the neural tube (see 3.1.2) (Mort et al. 2015). A study by Erickson showed that Fluoro-Gold-labeled quail NCSCs, which have previously been cultured for 12 hours, differentiated into neurons and glia and followed the ventral pathway upon grafting into chick embryos (Erickson & Goins 1995). On the other hand, quail NCSC that have been cultured for at least 20 hours were enriched in melanoblasts and migrated dorsolaterally. Cell populations depleted of melanoblasts were not able to migrate the dorsolateral pathway, confirming that only melanoblasts migrate along the dorsolateral pathway during embryogenesis.

The microphtalmia-associated transcription factor (MITF) presents as master regulator and specifier of the melanocytic lineage identity (Mort et al. 2015). It was demonstrated that ectopic expression of MITF converted NIH/3T3 fibroblasts into cells with melanocytic properties (Tachibana et al. 1996). Moreover, mice lacking *MITF* or *MITF* loss-of-function mutants could not form melanocytes (Steingrímsson et al. 2004). Additionally, *MITF*-deficient mice not only lost hair pigmentation, but also presented with reduced eye size, failure of secondary bone formation, reduced number of mast cells and early onset of deafness (Hodgkinson 1993). Consistent with these findings, many direct *MITF* downstream target genes are involved in melanin synthesis (*Tyrosinase, DHICA oxidase* (*Tyrp1*) and *dopachrome tautomerase (DCT*) (Cheli et al. 2010). In the promoter regions of these genes, a conserved GTCATGTGCT motif mediated most of the MITF responses (Lowings et al. 1992; Cheli et al. 2010). Nevertheless, MITF also orchestrates genes like *BCL2, CDK2, CDKN1a, MET* and *HIF1a* which are involved in more general cellular processes (Cheli et al. 2010).

Other transcription factors required for proper migration, survival and differentiation of the melanocyte lineage are *Sox10* and *Pax3* (Bondurand et al. 1998; Britsch 2001; Lang et al. 2005; Paratore et al. 2001; Southard-Smith et al. 1998). Mutations in *Sox10* can lead to a Waardenburg syndrome type IV (Hirschsprung disease), a congenital disorder characterized by pigmentary abnormalities, hearing loss and absence of ganglion cells in the myenteric and submucosal plexus of the gastrointestinal tracts (Sánchez-Mejías et al. 2010). Consistent with those findings, mice heterozygous for a targeted mutation ($Sox10^{LacZ}$) were characterized by hypopigmentation in the head and belly region (bellyspot). Co-labeling experiments using *Dct::LacZ* mice showed nuclear Sox10 expression from E18.5 to p4 stages in the epidermis and in the bulge regions of the hair

follicles (Osawa 2005). Further, Sox10 expression persists in peripheral glia cells and the melanocytic lineage into adulthood (Aoki et al. 2003; Harris et al. 2013). Moreover, *Sox10* KO in *Tyr::Cre*^{ER} *Sox10*$^{lox/lox}$ adult mice caused loss of differentiated melanocytes as well as melanocyte stem cells, demonstrating that Sox10 plays a crucial role in maintaining the adult melanocytic lineage (Harris et al. 2013).

3.3.1.2. Physiological role of melanocytes and pigment production

In the adult human skin, pigment producing melanocytes are mainly located in the basal layer of the epidermis, where they divide less than twice per year (Shain & Bastian 2016; Jimbow 1975). Melanocytes produce pigment, which is subsequently passed on to keratinocytes to protect the organism from Ultraviolet (UV) radiation-induced DNA damage (Costin & Hearing 2007). Release of α-melanocyte stimulating hormone (α-MSH) in UV-radiation-induced and DNA-damaged keratinocytes enhances pigment production in melanocytes (Cui et al. 2007). Hydroxylation of the amino acid tyrosine serves as first step in melanin production, followed by a series of enzymatic reaction and oxidations (Cichorek et al. 2013). The central enzymes involved in the pigment production are tyrosinase (TYR), DCT and TRP-1. Melanin is synthesized in cellular organelles called melanosomes, which undergo four different maturation steps before the melanin containing melanosomes can be passed on to the surrounding keratinocytes (Cichorek et al. 2013). Although mainly located in the epidermis, melanocytes are also found in hair follicles, the uveal tract of the eye, the meninges and in the urogenital tract (Shain & Bastian 2016). In contrast differentiated mouse melanocytes are mainly located in bulb regions of the hair follicles, the eyes, the herderian gland, the ear but not in the epidermal/dermal junction of the skin (Aoki et al. 2009) (Figure 3.4).

3.3.1.3. Hair follicles, melanocyte stem cell and hair cycle in mice

Hair follicles develop from the embryonic epidermis and are structured in three cylinder-like structures, the shaft (center), the inner root sheat (IRS) and the outer root sheath (ORS) (Stenn & Paus 2001). Whilst differentiated and pigmented melanocytes are located in the bulb region of the hair follicle, undifferentiated and unpigmented melanocyte stem cells (MSC) are found in the bulge regions (Figure 3.4). The location of the slow cycling and self-maintaining MSCs have been determined by means of transgenic *Dct::LacZ* tracer mice (Nishimura et al. 2002). Hair follicles are not static entities but undergo constant cycling in three phases (Alonso & Fuchs 2006) (Figure 3.5). First, they undergo a growth phase (anagen), in which a new hair shaft is formed (Schneider et al. 2009). This process is highly dependent on a complex interplay between epithelial stem cells (EpSCs) and MSCs (Rabbani et al. 2011). In early anagen, MSCs are activated, migrate and

differentiate towards pigmented-producing bulb melanocytes. Second, the hair follicles go through an apoptosis-mediated regression phase (catagen), where the lower 'non-permanent' part of the follicle completely deteriorates (Alonso & Fuchs 2006). Third, the hair follicles enter a resting, dormant state called telogen (Figure 3.5). In a worldwide study, it has been calculated that 74% of people between 45 and 65 years of age are affected by hair greying (Panhard et al. 2012). An elegant by Nishimura and colleagues showed that defective self-maintenance of MSCs led to hair greying (Nishimura et al. 2005). The authors demonstrated that *Bcl2*$^{-/-}$ mice displaying a hair greying phenotype exhibited increased apoptosis in MSCs but not in differentiated bulb melanocytes.

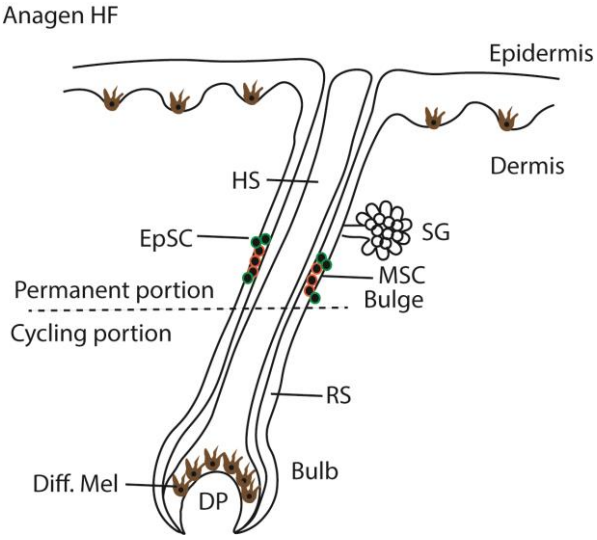

Figure 3.4. Scheme of a hair follicle (anagen) and melanocyte locations. In human skin, differentiated and pigmented melanocytes (Diff. Mel.) are located in the basal layer of the epidermis and the bulb region of the hair follicles. In the mouse skin, Diff. Mel. Are exclusively located in the bulb regions of the hair follicle. The bulge region, which serves as a permanent stem cell niche, contains MSCs and EpSCs in human and mice and is located under the sebaceous gland (SG). The follicle is composed of a hair shaft (HS), root sheath (RS) and a dermal papilla (DP) and has a permanent and a cycling portion. Drawn by Simon Schäfer, adapted from (Falabella 2009).

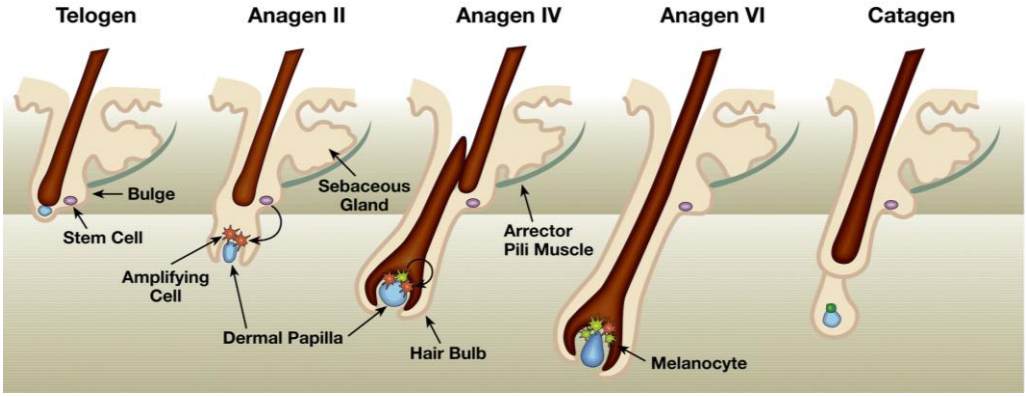

Figure 3.5. The phases of the hair follicle cycle. The hair cycle consists of three main phases, a resting phase (telogen), a growing phase (anagen) and a regression phase (catagen). In early anagen, the MSCs (violet) are activated, proliferate and produce amplifying cells (orange). Those cells further differentiate into mature melanocytes (green) in the hair bulb during mid to late anagen. During the catagen phase, the hair shaft regresses thereby ending one cycle. Adapted from (Steingrímsson et al. 2005).

3.3.2. Nevus biology

The common acquired/banal melanocytic nevus is defined as a benign proliferation of melanocytes with a low probability of progression to melanoma (Shain & Bastian 2016). A cross sectional study analyzed that most nevi significantly increased before and decreased after the fourth decade of life (Zalaudek et al. 2011). Interestingly, 63 of 77 (82%) of nevi carried a specific mutation (V599E) in the a *v-raf murine sarcoma virus oncogene homolog B1* (*BRAF)* gene, a mutation which is also often present in melanocytic neoplasms (Pollock et al. 2003). This suggests that the $BRAF^{V600E}$ oncogenic mutation is not sufficient for melanomagenesis but for nevogenesis. In agreement, a study by Patton et al. showed that expression of $BRAF^{V600E}$ under a melanocyte-specific mitfa promoter led to dramatic patches of ectopic melanocytes also called "fish-nevi" (Patton et al. 2005). A study conducted by Shain and colleagues analyzed the genetic evolution of melanoma from precursor lesions (Shain et al. 2015). Around 80% of benign lesions carried a $BRAF^{V600E}$ mutation and 20% were positive for diverse *NRAS* mutations. Expectedly, the number of mutation per megabase was very low and no other additional mutations were detected in most benign lesions. Acquired melanocytic nevi are located more commonly on sun-exposed anatomical sites, highlighting the importance of UV radiation in the formation of this benign lesions (Breitbart et al. 1997; Shain & Bastian 2016). $BRAF^{V600E}$ mutations usually result from thymine (T) to adenine (A) transitions, which are surprisingly not associated with UV radiation-induced DNA damage. It is possible that nevi can still originate from error prone replication/DNA polymerases of UV-damaged DNA (Thomas et al. 2006). After a limited round of oncogene-driven cell divisions, nevi enter a "senescent-like" state and rarely progress into malignant tumors. Moreover, the vast majority of nevi do not change in size for many years (Shain & Bastian 2016). A study by Michaloglou demonstrated that the "senescent-like" state is driven by a mosaic induction of the tumor suppressor $P16^{INK4a}$ which protects against BRAF-mediated proliferation (Michaloglou et al. 2005). In agreement, the authors showed that nevus cells expressed high levels of the senescence marker SA-β-GAL and low levels of the proliferation marker KI-67. Further, they did not observe loss of telomere in nevi. Nevertheless, other studies showed that nevus cells still had the potential to

proliferate in response to stimuli like UV radiation, pregnancy or immunosuppression (Chan et al. 2010; Richert et al. 1996; Rudolph et al. 1998; Kornberg 1975). Giant congenital melanocytic nevi (GCMN) represent a relatively rare special form of melanocytic nevi, defined as congenital melanocytic lesions reaching a size of at least 20 cm in adulthood (Viana et al. 2013). This can result in major psychosocial stress for patients. Moreover, it is surveyed that 5-10% of people carrying GCMN develop melanoma in their life (Hale et al. 2005; Ka et al. 2005; Zaal et al. 2004).

3.4. Cutaneous melanoma

3.4.1. Epidemiology and survival

Cutaneous malignant melanoma (MM) is a relatively frequent diagnosed cancer in the USA, with around 5% (total numbers: 34260 men and 27930 women) of all new estimated cancer cases per year (Jemal et al. 2006). Moreover, the incidence rate of MM has dramatically increased and risen faster than any other cancer (Erdei & Torres 2010). The incidence rates are higher in light skinned people than in darker skinned individuals with a median age of 52 at diagnosis. Solid tumors are classified in the Tumor (T) Nodus lymphoides (N) and metastases (M) (TNM staging) system. According the American Joint Committee on Cancer (AJCC), the 10-year survival rate of stage I melanoma patients ranked as T1N0M0 (Thickness $\leq$ 1 mm, no lymph nodes afftect, no metastases persent) is 93% (Balch et al. 2009). For stage II melanoma patients ranked as T4N0M0 (Thickness $\leq$ 4 mm, no lymph nodes affect, no distant metastases present) the survival drops to 39%. The 5-year survival of Stage IV melanoma patients (with distant metastases) is even lower, calling for new and effective treatment options.

3.4.2. Risk factors

Exposure to UV radiation is one of the biggest, and above all most modifiable risk factor for melanoma development (Mark Elwood & Jopson 1997; Rastrelli et al. 2014; Gandini et al. 2005). One study found a positive association between intermittent sun exposure and melanoma development (Gandini et al. 2005). Further, sunburns during childhood and exposure to "sun-tanning beds" enhanced the risk of developing MM (International Agency for Research on Cancer Working Group on artificial ultraviolet (UV) light and skin cancer 2007; Mark Elwood & Jopson 1997). Another major risk factor for a person developing MM is the total number of melanocytic nevi (see 1.3.2) and the genetic predisposition (Grob et al. 1990; Holly et al. 1987). It was calculated that people with a high number of melanocytic nevi (100-120) have an almost 7 fold risk increase than people with low numbers (0-15) (Gandini et al. 2005). A subset of MM are inherited

in a autosomal dominant manner with mutations in the two genes *CDKN2* and *CDK4*, highlighting the role of family history as risk factor (Tsao & Niendorf 2004). Further, red hair, light eyes, inability to tan, fair skin and numerous freckles greatly enhances the risk for MM development (Gandini et al. 2005).

3.4.3. Melanoma classifications

Accounting for 70% of all cases, superficial spreading melanoma (SSM) represent by far the most common type of all MM. Mostly located on the back and legs, they show a variety of colors and either arise in association with a nevus or de novo (Rastrelli et al. 2014). It is characterized by lateral spreading of melanoma cells, which are haphazardly distributed (Smoller 2006). Another typical feature of SMM is pagetoid (upwards in epidermis) spread of malignant cells, which expand over the breadth of the lesion. Nodular melanoma (NM) represent another type of MM and account for around 20% of all cases.

Although NM share many features with SMM, they do not show poor but sharp lateral circumscription (Smoller 2006). Since NM do not spread radially, they tend to enter vertical growth faster and are therefore associated with a more aggressive phenotype and worse prognosis (Bergenmar et al. 1998). Lentigo malignant melanoma (LMM), which is almost exclusively seen on sun damaged head and neck regions of elderly patients, represents the last subtype of melanoma (Smoller 2006). They arise form benign lesion called lentigo maligna (LM)/melanoma in situ and share the invasive phenotype of all MM (Juhász & Marmur 2015). Increasing variation of colors, border irregularity, elevation and expanding surface areas might be indicators for progression from LM to LMM (McKENNA et al. 2006).

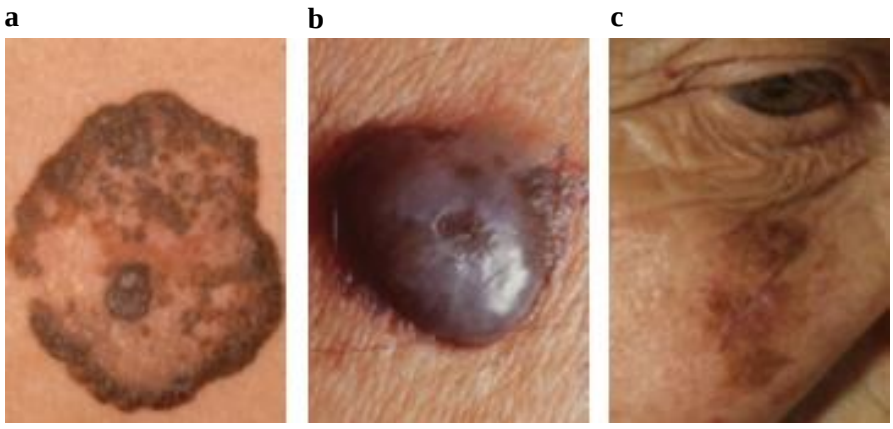

Figure 3.6. Different subtypes of melanoma. (a) Superficial spreading melanoma (SSM) **(b)** Nodal melanoma (NM) and **(c)** Lentigo malignant melanoma (LMM). Adapted from **(**http://www.skindermatologists.com/melanoma.html)

3.4.4. Melanoma biology – Oncogenes: The Ras/Raf/MAPK pathway

MM is a highly complex genetic disease, often presenting with a number of different mutations within (intra) and between (inter) different melanomas (V Gray-Schopfer et al. 2007). It has been shown that mutations associated with Ras/Raf/MEK/ERK signaling (Ras-MAPK pathway), which often preexist in benign nevi, are also present in 90% of all melanomas (Cohen et al. 2002). In this signaling pathway, a ligand binds and activates the receptor tyrosine kinase (RTK), which triggers the dimerization of the two subdomains and catalyzes their autophosphorylation (Lemmon & Schlessinger 2010) (Figure 3.7.). This causes guanosine triphosphate (GTP) loading of the Ras GTPase, which can subsequently activate the protein kinase RAF. Once stimulated, Raf phosphorylates MEK1/2 and ERK1/2 which leads to a variety of altered cellular functions (Dhillon et al. 2007). 15-30% of all melanomas carry *NRAS* and 50-70% *BRAF* mutations, highlighting the importance of this signaling pathway in melanomagenesis (V Gray-Schopfer et al. 2007). While the most common alteration in *NRAS*-mutated melanomas displays a substitution of a leucine to a glutamine at position 61 (Q61L), *BRAF*-mutated melanomas most often present with substitution of glutamic acid to valine at position 600 (V600E) (Davies et al. 2002). These mutations lead to constitutively active signaling and therefore altered proliferation, differentiation, apoptosis and migration (Dhillon et al. 2007). Since benign nevi also harbor mutations in the Ras/Raf/MEK/ERK pathway, additional alterations are required for a malignant transformation.

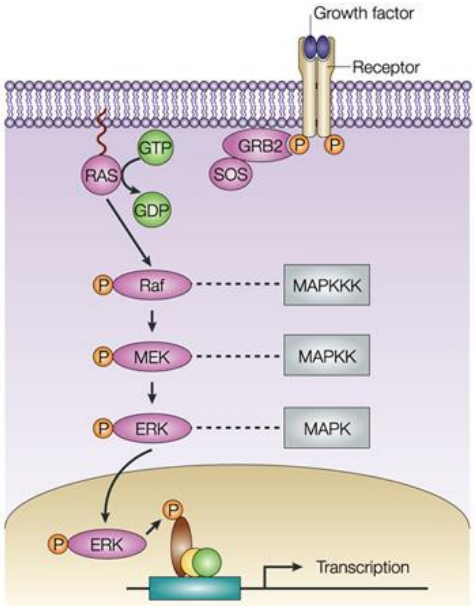

Figure 3.7 The Ras/Raf/MAPK signaling pathway. A growth factor (blue) binds and activates the receptor, leading to a dimerization of the two subdomains. This catalyzes autophosphorylation of the heterodomains and activates the growth factor receptor-bound protein 2 (GRB2)/Son of sevenless (SOS)

complex which mediates the phosphorylation of Ras-GDP to Ras-GTP. This leads to a subsequent chain of phosphorylation reactions, namely Raf, MEK and ERK. The pathway controls genes involved in proliferation, differentiation, apoptosis and migration and is constitutively active in many cancers. Around 50-70% of human melanomas harbor a $BRAF^{V600E}$ mutations while around 15% carry alterations in the *NRAS* gene. From (Kim & Bar-Sagi 2004).

3.4.5. Melanoma biology – Tumor suppressors: TERT, CDKN2A, NF1, PTEN, TRP53

It has been shown that two recurrent mutations in the promoter regions of the telomerase reverse transcriptase (TERT) occurred in 71% of all melanomas (Huang et al. 2013). Further, bi-allelic inactivation of the *CDKN2A* gene was observed in high percentage of melanomas but not in benign precursor lesion (Krauthammer et al. 2012; Hodis et al. 2012; Shain et al. 2015). Germline mutations of this gene, which encodes the cell cycle inhibitor $p16^{CDKN2A}$, have been found in patients with familial atypical multiple mole/melanoma (Foulkes et al. 1997). Moreover, a *Tyr::Nras*^{Q61K} $Cdkn2a^{INK4a-/-}$ mouse model developed by Ackermann and colleagues showed high penetrance in primary melanoma and metastasis formation (Ackermann 2005). Those mouse melanomas developed at 6 month, were melanotic, multifocal and disseminated as metastases to lymph nodes, lung and liver, making it an important tool to study melanoma biology *in vivo.*

Neurofibromin 1 (NF-1) acts as tumor suppressor and negatively controls RAS signaling by stimulating the GTPase activity, which leads to an accumulation of the RAS-GDP inactive form (Cichowski & Jacks 2001; Gibney & Smalley 2013). Inherited inactivating mutations in *NF-1* can lead to multiple neurofibromas, café-au-lait macules, freckling, iris hamartomas and an increased cancer incidence for patients. Further, loss-of-function *NF-1* mutations cause an enriched activity of phosphoinositide 3-kinase (PI3K)/ protein kinase B (AKT)/mechanistic target of rapamycin (mTOR) signaling, which strongly enhances a proliferative phenotype (Gibney & Smalley 2013). To test the role of NF-1 in melanomagensis functionally, Maertens and colleagues developed a mutant $BRAF^{CA/+}$ $NF\text{-}1^{flox/flox}$ mouse model (Maertens et al. 2013). While $BRAF^{CA/+}$ $NF\text{-}1^{+/+}$ showed a very mild hyperpigmentation, $BRAF^{CA/+}$ $NF\text{-}1^{flox/flox}$ mice presented with darkening of the paws, the ears and the tail. Importantly, lesions derived from $BRAF^{CA/+}$ $NF\text{-}1^{+/+}$ mice strongly expressed the senescence marker β-Gal as seen in benign nevi (see 1.3.2). In contrast, this senescence was not observed in $BRAF^{CA/+}$ $NF\text{-}1^{flox/flox}$ mice. Furthermore, Whittaker and colleagues proved that shRNA-mediated *NF-1* KD in cell lines originally sensitive to the BRAF-inhibitor PLX4720 abrogated the growth inhibitory effect of PLX4720 (Whittaker et al. 2013; Gibney & Smalley 2013). Mechanistically, the observed effect was driven by derepression of RAS signaling leading to CRAF-mediated activation of MAPK signaling, not only highlighting the role of NF-1 in melanomagenesis but also in resistance formation.

Phosphatase and tensin homolog deleted in from chromosome ten (PTEN) is another important tumor suppressor often mutated in many cancers, including melanoma (Wu et al. 2003). The lipid phosphatase activity of PTEN decreases AKT activity and arrests progression of the cell cycle in G1/S, which is partially mediated by upregulation of the cyclin-dependent kinase inhibitor p27. Further, PTEN has a crucial role in mediating apoptosis by upregulation of different caspases and BID, a pro-apoptotic member of the Bcl-2 protein family (Wang et al. 1996; Wu et al. 2003). Consistent with this data, $PTEN^{+/-}$ heterozygous mice developed various tumors in endometrium, thyroid, prostate and gastrointestinal tract (Podsypanina et al. 1999). Guldberg and colleagues identified that 43% of all melanoma cell lines harbored either homozygous (17%) or heterozygous (26%) PTEN mutations (Guldberg et al. 1997). On the contrary, another study failed to detect PTEN mutations in the corresponding coding regions of 25 primary melanoma (Poetsch et al. 2001). Nevertheless, Dankort and colleagues elegantly showed that mice carrying the genotype $Tyr::Cre^{ERT2}$ $BRAF^{V600E}$ $PTEN^{flox/flox}$ developed tumors in short latency and 100% penetrance, while $Tyr::Cre^{ERT2}$ $BRAF^{V600E}$ $PTEN^{+/+}$mice displayed no signs of melanoma formation (Dankort et al. 2009). These results clearly demonstrate a cooperative effects of $BRAF^{V600E}$ and *PTEN* loss in melanoma formation.

TRP53, "the guardian of the genome", serves a prominent tumor suppressor by inducing cell cycle arrest, apoptosis, senescence and DNA repair and its inactivation is therefore often seen as a hallmark of cancer formation (Houben et al. 2011; Dankort et al. 2009). Consistently, approximately 50% of all tumors harbor *TRP53* mutations, which mostly occur in the DNA binding domain therefore destructing its transcriptional capability (van Oijen & Slootweg 2000; Roemer 1999). Terzian and colleagues crossed the $Mdm4^{+/-}$ ('high p53') mouse to the TP-$RAS^{0/+}$ mouse to study the effect of trp53 in melanoma formation (Terzian et al. 2010). Upon dimethylbenzanthracene (DMBA) treatment, 'high trp53' mice developed fewer tumors with delay in the age of onset, emphasizing the role of trp53 in melanomagenesis. Further, it was shown that 4/14 melanoma cells had mutations in the *TRP53 gene* (Houben et al. 2011). Another study by Viros et al demonstrated that $BRAF^{V600E}$ mice exposed to UV-radiation showed clonal expansions of melanocytes and melanomoagenesis (Viros et al. 2014). Interestingly, those melanomas showed increased numbers of mutations in the *TRP53* gene, therefore identifying TRP53 as an UV radiation target.

3.4.6. Melanoma biology – Transcription factors

3.4.6.1. SOX10 and SOX9

Sry-related HMG-Box gene 10 (Sox10) is a nuclear transcription factor and carries a critical role in the differentiation of neural crest derived melanocytes and peripheral glia (Mollaaghababa & Pavan 2003). Several different studies showed high SOX10 expression in human and mouse melanomas, suggesting a functional role of the transcription factor in melanomagenesis (Mohamed et al. 2013; Shakhova et al. 2012; Shin et al. 2012; Agnarsdóttir et al. 2010). Shakhova and colleagues elegantly showed that *Sox10* haploinsufficiency counteracted *Tyr::NRas*^{Q61K}-mediated hyperpigmentation and melanoma formation (Shakhova et al. 2012). Further, the authors showed that stable *SOX10* KD in human melanoma cells completely abrogated tumor growth upon xenotransplantation. Moreover, *SOX10* KD cells showed increased apoptosis, decreased proliferation and reduced melanocytic differentiation, highlighting its important role in melanomagenesis. Consistently, Cronin and colleagues obtained similar results and additionally showed elevated expression of the two tumor suppressors p21WAF1 and p27KIP2 (Cronin et al. 2013). Another study identified Sox9 as an important factor mediating the anti-tumorigenic effect of the Sox10 haploinsufficiency (Shakhova et al. 2015). The authors demonstrated SOX9 binding to the *SOX10* promoter. Further, *SOX9* overexpression resulted in cell cycle arrest, apoptosis and a gene expression profile resembling the *SOX10* KD signature. Therefore, an antagonistic cross-regulation between Sox9 and Sox10 controls an anti-tumorigenic program in melanoma (Shakhova et al. 2015). Further, Cheng and colleagues showed that *SOX9* overexpression induced invasion and metastasis formation in human melanoma cultures and decreased patient survival using patient data from TCGA (Cheng et al. 2015).

3.4.6.2. MITF

Although MITF is higher expressed in melanocytes than in melanoma, amplification are often observed in melanocytic malignancies (10-16%) and strongly correlate with decreased overall patient survival (Garraway et al. 2005). Moreover, ectopic MITF expression in *BRAF* ^{V600E}-mutant melanocytes causes malignant transformations, identifying MITF as a potent oncogene. In contrast, several studies using different experimental set-ups showed that MITF can suppress invasion and metastasis formation (Cheli et al. 2012; Pinner et al. 2009; Levy et al. 2010; Shah et al. 2010; Thurber et al. 2011). One study by Cheli et al. demonstrated that *MITF* silencing in both mouse and human melanoma cells increased their metastatic potential and resulted in an upregulation of the two mesenchymal markers FIBRONECTIN and SNAIL (Cheli et al. 2012). The authors further showed that a hypoxic environment decreased MITF expression by a hypoxia-inducible factor 1

(HIF1) α-dependent mechanism resulting in increased numbers of metastases in distant organs. Gray-Schopfer and colleagues propose a model in which MITF is regulating different cellular functions at different levels of expression (Gray-Schopfer et al. 2007). In their model, intermediate MITF levels favors proliferation while high levels supports differentiation cell cycle arrest (Levy et al. 2006). On the other hand, low MITF levels leads to cell cycle arrest, apoptosis and invasion. Hence, MITF acts on the one hand as a potent oncogene which is amplified in a subset of melanomas. On the other hand, its downregulation promotes metastasis formation and is therefore a challenging target for therapeutics.

3.4.7. Melanoma biology – Disease progression and metastasis formation

As indicated, the 5-year survival sharply decreases with increased thickness of the tumor and existing regional or distant metastases at stage of diagnosis, asking for a better understanding of melanoma progression (Figure 3.8.). While *BRAF/NRAS/NF1* mutations most often occur in the tumor initiation phase, *TERT/CDKN2A/PTEN/TRP53* mutations are often associated with invasive melanomas (Shain & Bastian 2016). After having acquired initial mutations, the transformed cells spread laterally (radial growth phase - RGP) near to the epidermis. Additional mutations cause a transition from the RGP to the vertical growth phase (VGP). In this phase, the cells penetrate the basal lamina and invade the dermis. As a final step, the cancer cells intravasate into lymphatic and/or blood vessels to form locoregional (skin), regional (lymph nodes) and distant (lung, brain, bones and other sites) metastases (Elder 2016). Since it is assumed that melanoma cells first disseminate to the lymph nodes of the draining areas of the primary tumor, most surgeons recommend completion lymph node dissection (CLND) in patients with sentinel positive lymph nodes (Pasquali et al. 2012). Interestingly, patients who undergo CLND do not experience prolongation of life expectancy, suggesting a parallel rather than serial metastasis model (Morton et al. 2014). In agreement, circulating tumor cells (CTCs) can be detected in the blood of patients even if no regional metastases are present (Shain & Bastian 2016; Reid et al. 2013; Ulmer 2004). Another indication supporting the “parallel model” came from a study comparing the exome of primary tumors with the exome of adjacent metastases (Sanborn et al. 2015). According a serial progression model, the same “phylogenetic history” should be observed in all analyzed metastases. However, the authors showed that genetically distinct cell populations within a primary tumor, which were derived from a common ancestor, formed independent metastases at different anatomic sites. For some of the patients, two different founder populations were found in one particular metastasis, advocating for a multiclonal dissemination. Moreover, the exome sequencing also revealed that no additional mutations were detected in the metastases compared to the

corresponding founder populations, suggesting no requirement for additional mutations for metastasis formation in that particular context. Melanoma metastases have the highest proliferation index of all stages (Straume et al. 2000).

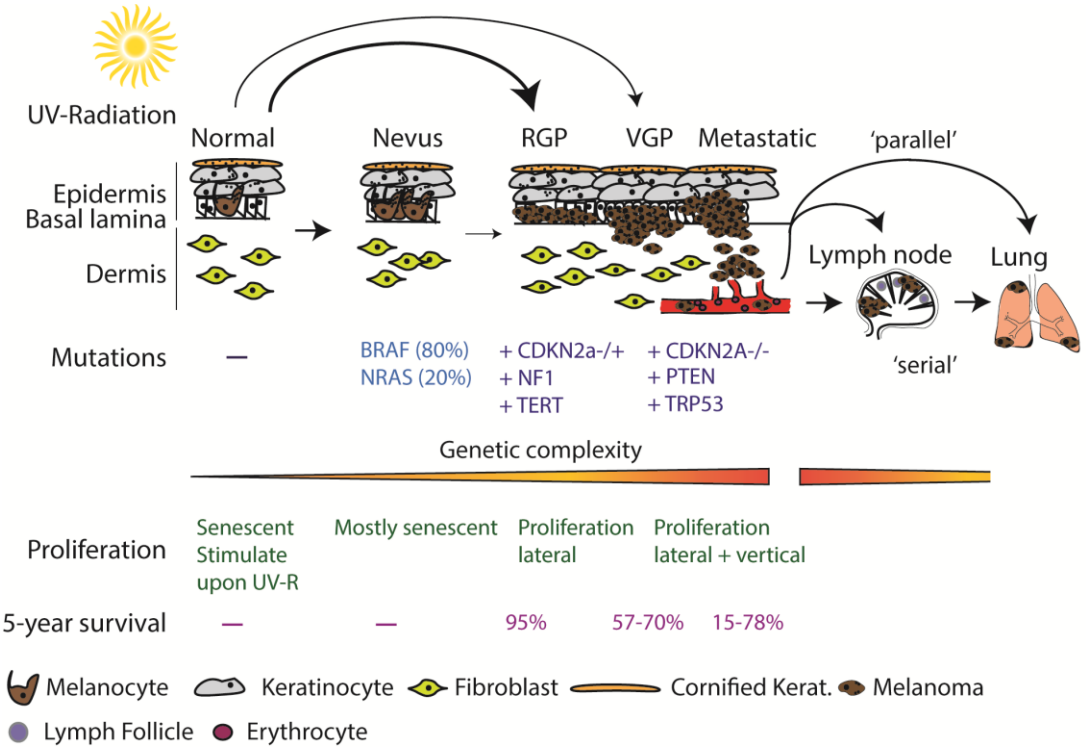

Figure 3.8. Melanoma progression and metastasis formation. Melanocytes are located in the basal layer of the epidermis, surrounded by keratinocytes. To protect the organism from UV-radiation-induced DNA damage, melanocytes start to proliferate and enhance the production of pigment, which is delivered to keratinocytes. After acquisition of *BRAF* or *NRAS* mutations, the melanocytes proliferate several times, form a nevus and subsequently senesce. The vast majority of nevi do not progress into melanoma. However, some nevi acquire additional loss-of-function mutations in tumor suppressor genes and start to proliferate radially (RGP) in the epidermis to form a melanoma in situ. Although a small proportion of melanoma in situ originate from nevi (thin arrow), the majority derives from normal melanocytes (thick arrow). Since the disease is restricted to the epidermis, the 5-year-survival is very high. The genetic complexity of localized melanomas increases over time and the cells eventually penetrate vertically (VGP) through the basal lamina to enter the dermis. Some cells escape the tumor bulk, enter the lymphatic or cardiovascular system and form metastases in the skin, lymph nodes and distant organs. New evidence favors a "parallel model" of metastasis formation rather than a "serial model". In the parallel model, genetically diverse cells disseminate from the primary tumor to form metastases at different sites. The 5-year survival drastically decreases if melanoma cells are present in the dermis or in different organs. Drawn by Simon Schäfer, adapted from (Gaggioli & Sahai 2007).

3.4.8. Melanoma biology – Cancer stem cells in melanoma

Although accumulating evidence supports the presence of CSCs (for definition see 3.1.3) in melanoma, a definitive proof for their existence is still required (Santini et al. 2014; Quintana et al. 2010; Frank 2005; Schatton et al. 2008; Civenni et al. 2011; Boiko et al. 2010). Boiko and colleagues isolated melanoma samples from patients and detected heterogeneous expression of the NCSC-marker CD271 ($p75^{NTR}$) in 9/10 tumors, suggesting a possible CSC role (Boiko et al. 2010). Therefore, the authors separated the CD271-positive from a CD271-negative fraction by fluorescence-activated cell sorting (FACS) and subsequently injected both fractions into $Rag2^{-/-}yc^{-/-}$ immunodeficient recipient mice. Interestingly, the CD271-positive fraction was highly tumorigenic (70%) while the CD271-neagtive cells rarely formed melanomas (7%). Moreover, the CD271-positive population rarely expressed the differentiation markers TYR, MART and MAGE, labeling the CD271-positive fraction as highly undifferentiated and stem cell-like. Consistent, Civenni and colleagues demonstrated that CD271-positive cells initiated tumors and fully mirrored the heterogeneity of the parental tumors upon xenotransplantation into NOD/SCID or nude mice (Civenni et al. 2011). While the CD271-negative fraction did not grow in nude mice, both fractions initiated tumor growth in fully immunocompromised NOD/SCID/$Il2r\gamma^{null}$ mice, highlighting the role of the immune system in studying CSCs. In sharp contrast, Quintana and colleagues were unable to find subpopulations that lacked tumorigenic potential and, moreover, all cell populations had an unlimited tumorigenic capacity on serial transplantation assays (Quintana et al. 2010; Quintana et al. 2008). The CD271-positive cells did not show elevated tumorigenesis compared to the CD271-negative, pointing against a hierarchical organization of melanomas. Quintana and Morrison argue that the observed differences could lie in the different experimental set-ups: Different recipient mice (NSG vs. $Rag2^{-/-}yc^{-/-}$) and altered enzymatic dissociation methods (25min vs 3h) could explain the observed variations. Civenni et al. argue that cell dissociation with trypsin can yield to loss of the surface epitope and therefore influence and falsify the results. In disagreement, Morrison states that the different dissociation methods lead to similar results with CD271-positive and CD271-negative melanoma cells (Magee et al. 2012; Quintana, Eskiocak U, Morrison SJ, unpublished). If CD271 serves as a reliable marker for melanoma stem cells is therefore still highly debated.

Another study identified another subpopulation expressing the chemoresistance mediator ABCB5 in melanoma initiating cells (MIC) (Schatton et al. 2008). They demonstrated that ABCB5-positive fractions, which recapitulated clinical tumor heterogeneity, showed greater tumor initiation capacity than ABCB5-negative patient-derived melanoma cells. Interestingly, lineage tracing experiment revealed that ABCB5-positive cells gave rise to both ABCB5-positive and ABCB5-negative cells which goes in agreement with multipotentiality of stem cells.

3.4.9. Melanoma biology – The role of SOX2 in melanoma formation and progression

Since I investigated the *in vivo* role of Sox2 in melanoma formation, I summarize hereby what has been publishing concerning this topic.

Using an immunohistochemical approach, Laga and colleagues found SOX2 expression in 9/26 (35%) patient-derived melanomas (Laga et al. 2010). While only ≤ 5% of melanoma cells expressed SOX2 in certain tumors, ≥ 50% of total cells presented with strong nuclear immunoreactivity in others, demonstrating a highly heterogeneous expression pattern. Next, the authors performed shRNA-mediated *Sox2* KD experiments. While control and *shSOX2* melanoma cells showed similar growth rates *in vitro*, the stably infected *shSOX2* A2058 cells grew significantly slower upon xenotransplantation *in vivo.* Another study showed SOX2 binding to enhancer regions of the *NESTIN* gene (Laga et al. 2011). While SOX2/NESTIN co-expression was observed in a small subset of benign nevi (11%), the fraction of SOX2/NESTIN-positivity strongly increased in MM (65%), highlighting its potential role in melanoma progression. Another study linked high SOX2 expression to an invasive phenotype *in vitro* (Girouard et al. 2012). *SOX2* KD decreased melanoma cell invasion, which was analyzed by means of "matrigel invasion chambers". In agreement, *SOX2* overexpression (OE) increased invasion by 3.8 fold. Further, the authors demonstrated that the invasion phenotype was mediated by SOX2 controlling matrix metalloproteinase-3 (MMP-3) expression levels. Santini and colleagues identified SOX2 as a crucial factor regulating self-renewal and tumorigenicity of melanoma initiating cells (Santini et al. 2014). The authors showed that SOX2 is highly expressed in melanoma spheres compared to adherent cultures and enriched in an $ALDH^{high}$ stem-like population. Further, *SOX2* KD in $ALDH^{high}$ cells reduced the number and self-renewal of melanoma spheres. *SOX2* silencing in two patient-derived human melanoma cell lines caused decreased proliferation *in vitro* and in *vivo* and led to increased apoptosis, identifying SOX2 as a potent melanoma driver (Figure 3.9.). Nevertheless, quantitative real-time PCR (qRT-PCR) measurements showed low to absent SOX2 expression in many human melanoma lines, questioning if this observed oncogenic effect includes all cell lines. A recently published study analyzed the role of Sox2 in melanomagenesis *in vivo* (Cesarini et al. 2017). Using the $Tyr::Cre^{ERT2}$ $BRAF^{V600E}$ $PTEN^{flox/flox}$ $Sox2^{lox/lox}$ mouse model, the authors did not detect differences in melanoma initiation, growth, metastasis formation and survival comparing *Sox2* cKO and control animals. Further, tumor-derived control and *Sox2* KO cells showed similar sensitivity to the BRAF inhibitor vermurafenib.

Source	*In vitro/in vivo*	Invasion	Proliferation	Apoptosis	Stemness/Initiation
Santini et al, 2014	*In vitro* and Xenografts	n/A	Increased	Decreased	Increased
Girouard et al, 2012	*In vitro*	Increased	n/A	n/A	n/A
Laga et al, 2010	Xenografts *In vitro*	n/A	Increased Unchanged	n/A	n/A
Cesarini et al, 2017	*In vitro* and mouse models	Unchanged	Unchanged	n/A	Unchanged

Figure 3.9. Summary of Sox2 functions in melanoma. Sources (papers), model systems and cellular functions of Sox2 in melanoma.

3.4.10. Melanoma treatment

3.4.10.1. Surgery, chemotherapy and adjuvant therapies

Surgical excision of the primary melanomas is the most effective and the only curative treatment option if the disease is detected in early stages (Molife & Hancock 2002). Surgeons usually resect the melanoma with a certain safety margin to avoid recurrence of the tumor. Based on different clinical studies, recommendations propose a 0.5 cm margin for melanoma in situ, a 1cm margin for melanomas less than 1mm thickness and a 2 cm margin for melanomas greater than 2mm thickness (Rigel & Carucci 2000; Wargo & Tanabe 2009). Interestingly, even patients with stage IV melanoma benefited from surgical removal of the primary tumor (Sosman et al. 2011). For accurate staging, sentinel lymph nodes (SLN) are resected and immunostained for the melanoma markers HMB45/PMEL17 and S100. It has been shown that patients presenting with SLN-negative biopsies have an increased overall survival compared to patients with positive SLNs (Gershenwald et al. 1998). Another treatment option which is often successfully applied for malignancies is chemotherapy. In melanoma however, this option has uniformly disappointed (Rigel & Carucci 2000). Dacarbazine (DTIC) is the only approved drug for treating MM with a response rate lower than 25% (Serrone et al. 2000). The authors showed that for those 25%, the median response duration was just about 5-6 month. Other adjuvant therapies include interferon alpha 2b (IFN alpha-2b), which is approved for the treatment of stage II & III melanoma. Although a study concluded that high-dose IFN alpha-2b prolonged survival, it was also associated with profound toxicity and adverse reactions (Kirkwood et al. 1996; Rigel & Carucci 2000). Surgical excision remains

therefore the cornerstone treatment option for melanoma and is often curative if the disease was diagnosed at early stages. Other options treating MM include chemotherapy or IFN alpha treatment, which are either ineffective or show high toxicity.

3.4.10.2. Targeting the MAPK pathway

The high occurrence of *BRAF*^{V600E} mutations in melanoma suggested a drug development strategy specifically targeting the mutant BRAF kinase activity. PLX 4032 (vemurafenib, genentech) was the first selective BRAF inhibitor approved in the United states in August 2011 (Bollag et al. 2012). A phase III study from the year 2010 with 675 patients compared the safety and efficacy of PLX4032 compared to DTIC in previously untreated *BRAF*^{V600E} patients with unresectable stage III or IV melanoma (Chapman et al. 2011). The authors showed that at 6 month, overall survival was 84% in the vemurafenib group and 64% in the DTIC group. The response rate for vemurafenib was 48% while only 5% responded on DTIC treatment. Common adverse reactions were arthralgia, rash, fatigue, alopecia, nausea, squamous cell carcinoma, photosensitivity and diarrhea. Despite side effects, this data shows that vemurafenib significantly prolongs the survival of patients with *BRAF*^{V600E}-mutated melanomas. Another study analyzed images of vemurafenib-treated advanced melanoma patients using the ^{18}Fluorodeoxyglucose (FDG) positron emission tomography (PET) technique (McArthur et al. 2012). The authors showed that FDG-PET scans can be used as reliable tool the measure the implications of PLX4032 treatment in melanoma patients harboring the *BRAF*^{V600E} mutation. Patients with melanoma metastases showed a clear decrease in signal upon inhibitor treatment, demonstrating the effectiveness of PLX4032 for treating metastatic melanoma. The promising results from the clinical studies opened the door for basic research investigations. Several studies demonstrated that PLX4032 selectively targets *BRAF*^{V600E}-mutant cell line but not *BRAF*^{wt} or *NRAS*^{mut} cell lines (Joseph et al. 2010; Lee et al. 2010). Expectedly, vemurafenib inhibited pERK signaling in *BRAF*-mutant cells, strongly reducing the activity of the MAPK signaling pathway and therefore potently inhibiting cell proliferation (Joseph et al. 2010). Another study performed xenografts of *BRAF*^{V600E}-mutant melanoma cells (Yang et al. 2010). The authors showed that PLX4032 treatment caused either partial or total regression of the tumor in a dose-dependent manner. In addition, no toxicity was observed in the xenograft model. Despite the observed promising results, clinical data shows that most patients developed a drug resistance within 6-7 month (Joseph et al. 2014) (Figure 3.10.). One possible mechanism explaining resistance formation is the reactivation of the MAPK pathway. A study by Prahallad and colleagues elegantly demonstrated that BRAF^{V600E} inhibition caused a rapid feedback activation of the epidermal growth factor receptor (EGFR) in colon cancer cells, which supported sustained proliferation (Prahallad et

al. 2012). Moreover, they found that ectopic expression of EGFR was sufficient to generate resistance in melanoma cells. Another study revealed the genetic landscape of pre and post RAF inhibitor treated melanomas by means of whole exome sequencing (Van Allen et al. 2014). Genetic alterations were observed in 23 of 45 patients (51%). Those mutations often occurred in the *NRAS* gene (17.8%), as amplifications of *BRAF* (8.9%) or in the *MAP2K1* (15.6%) gene. Hence, most resistance alterations were associated with the MAPK signaling pathway and occurred in 44% of all patients. Interestingly, one patient showed *MITF* amplifications after treatment. Melanoma cells overexpressing *MITF* were indeed resistant to inhibitor treatments, emphasizing a potential new resistance mechanism. Another important study by Heidorn et al. showed that BRAF inhibition drives RAS-dependent BRAF binding to CRAF, which subsequently activates and drives MEK-ERK signaling (Heidorn et al. 2010). Besides activation of the MAPK pathway, resistance formation can also be established through the PI3K/AKT/mTOR pathway. As an example, loss of *PTEN* contributes to intrinsic BRAF inhibition via suppression of BIM-mediated apoptosis (Paraiso et al. 2011).

3.4.10.3. Immunotherapy

Although specific targeting of the MAPK pathway shows high response rates, most tumors become resistant over time. Other promising treatment strategies, which enhance the immune response to cancer cells, have been established lately. Most cancer cells express antigens which are usually recognized by CD8-positive cytotoxic T cells (Gajewski et al. 2013). Therefore, cancer cells have to escape the immune response to grow progressively. To do so, they decrease the expression of antigen-presenting proteins on the cell surface, making them imperceptible for CD8-positive T-cells (Zindl & Chaplin 2010; Meissner 2005). Further, tumor cells establish an immune-suppressive environment by the expression of certain cytokines like VEGF, Il-10, TGFβ or increase resistance and survival (Mittal et al. 2014; Muenst et al. 2016). Some tumor cells express certain proteins on their surface which inhibit T-cell proliferation, which are referred as immune checkpoints (Pardoll 2012). Cytotoxic T-lymphocyte antigen-4 (CTLA-4), an immune checkpoint molecule, is a key negative regulator of T-cell activity (Hoos et al. 2010). This led to the development of the monoclonal antibody ipilimumab. Completed phase III clinical studies including 676 patients with stage III or VI melanoma showed a significant improvement in overall survival (Hodi et al. 2010). They observed a 34% risk reduction of death in the drug treated vs the control group and the median overall survival was 10 month for the ipilimumab treatment vs 6.4 month for the control. Immune related adverse events mainly occurred in the skin (rash) and gastrointestinal tract (diarrhea). Although the response rates were rather low with 10-15%, some patients achieved long

term progression free survival which was not observed in the PLX 4032 treatment (Figure 3.10.). By upregulating another immune checkpoint inhibitor named PD-L1 on their surfaces, melanoma cells often achieve to inactivate the immune response of the adaptive immune system. Therefore, an additional monoclonal antibody named nivolumab was generated, which binds the T-cell PD-1 receptor and restores the host's immune response. 418 patients with advanced melanoma without *BRAF* mutations were treated with nivolumab (Robert et al. 2015). At one year, the overall survival was 72.9% in the nivolumab group compared with 42.1% in the control (DTIC) group. The response rate was 40% and therefore significantly higher compared to iplimumab. Common adverse effects were fatigue, pruritus and nausea. Combination treatments using ipilimumab and nivolumab were tested in 945 stage III or IV melanoma patients (Larkin et al. 2015). The median progression-free survival 11.5 month in the combination group as compared with 2.9 month in the ipilimumab only and 6.9 month in the nivolumab only. Although the combination treatment significantly increased survival of the patients, it showed the most grade 3 or 4 adverse effects with 55% while only 16.3% in the nivolumab and 27.3% in the ipilimumab group were observed. In summary, immunotherapies, either administered as mono or as combination treatment, significantly increase the overall survival for stage III or VI melanoma patients (Figure 3.10).

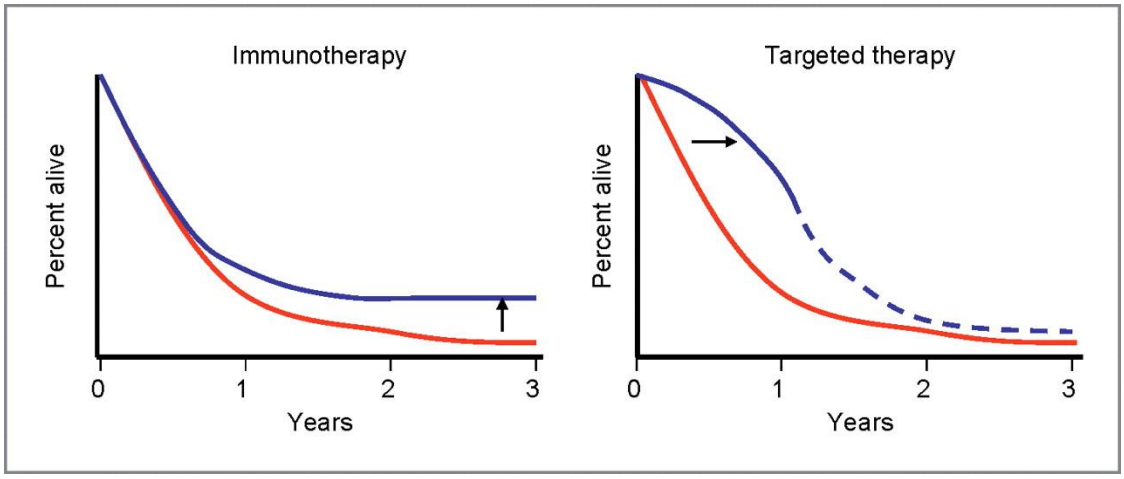

Figure 3.10. Survival curves of stage III/IV melanoma patients treated with immunotherapy or targeted therapy. Immunotherapies show a rather low overall response rates but some patients have long term benefits from the treatment. Targeted therapy blocking oncogenes like BRAF shows high response rates and rapid tumor regression but effects are not durable. From (Ribas et al. 2012).

3.5 Tumor heterogeneity and clonality

3.5.1. Tumor heterogeneity

3.5.1.1. Development of tumor heterogeneity

Cancers are usually very heterogeneous entities, both between different tumors (intertumor) and within a particular tumor (intratumor). Altered cellular morphology, metabolism, gene expression, motility, proliferation, immunogenicity, genetic landscapes and metastatic potential are often observed within a particular tumor, highlighting the degree of intratumor heterogeneity (Marusyk & Polyak 2010; Heppner 1984; Fidler & Hart 1982). Cancer formation and progression are often compared to the Darwinian evolution model, with cancer clones as the equivalent of asexually reproducing quasi-species (Greaves & Maley 2012; Nowell 1976). Genetic variations of reproductive individuals, who are united by a common ancestor, lead to natural selection of fittest variations (Greaves & Maley 2012; Darwin 1859). Cancer cells acquiring different genetic mutations can be seen as genetic variation of reproductive individuals. The fittest cancer clone will asexually reproduce and become the dominant clone within a cancer, until other randomly occurring mutations favor the growth of the next clone. Therefore, this clonal evolution model proposes that intratumor heterogeneity is based on genetic and epigenetic differences between different clones. The existence for clonal heterogeneity has been widely described in various types of cancers (Campbell et al. 2008; Fujii et al. 2000; González-García et al. 2002; Konishi et al. 1995; Macintosh et al. 1998; Shah et al. 2009; Shipitsin et al. 2007; Teixeira et al. 1996).

The linear evolution model predicts one dominant subclone within a tumor at a given time, which can be overgrown by other intratumor clones upon acquisition of additional beneficial mutations. In contrast, the branched evolution model predicts coexistence of several clones at the same time. Multiregional sequencing of 100 early non-small-cell lung cancer patients clearly demonstrated evidence supporting the branched evolution model (Jamal-Hanjani et al. 2017). Hence, the authors found a high degree of intratumor heterogeneity, with genetically different subclones carrying diverse mutations and copy-number alterations in various anatomical sites of the primary tumor. Given the large cohort size of this study and other evidence showing branched evolution in renal carcinomas (Gerlinger et al. 2012), we assume that branched evolution might be the dominant mechanism promoting intratumor heterogeneity. Several clones coexisting besides each other might increase the genetic diversity of the cancer, maybe comparable to genetic differences within sexually reproducing species (Figure 3.11.).

Another possible mechanism leading to intratumor heterogeneity can be explained by the cancer stem cell model. Only a small sub-fraction of cells within a tumor is tumorigenic and harbors the

potential to differentiate into non-tumorigenic and proliferating bulk cells. Hence, they are able to self-renew and fully phenocopy the parental tumor upon injection into immunocompromised mice. The differences between tumorigenic and non -tumorigenic cells are largely epigenetically determined (Shackleton et al. 2009). Differentiated non-tumorigenic cells represent therefore evolutionary "dead ends" (Marusyk & Polyak 2010). According this model, intratumor heterogeneity originates therefore rather from cell-intrinsic biological differences between cancer cells. However, it is still possible that CSC-derived non-tumorigenic cells acquire additional mutations which make them tumorigenic again, therefore unifying both models (Kreso & Dick 2014). Another alternative approach explaining heterogeneity is phenotypic plasticity, meaning that cancer cells are able to alter their phenotype in response to specific microenvironmental conditions (Marusyk & Polyak 2010).

Several different techniques are used to detect intra and inter tumor heterogeneity. For example multiregional whole exome sequencing displays an elegant tool revealing tumor heterogeneity on a genetic level (Jamal-Hanjani et al. 2017; Ding et al. 2012; Gerlinger et al. 2012). The fluorescence in-situ hybridization (FISH) method detecting amplification of certain chromosomal regions represents another possibility to detect heterogeneity (Mora 2001; Shipitsin et al. 2007). Further, single cell RNA sequencing displays a compelling tool to study gene expressions of single cancer cells (Li et al. 2012; Potter et al. 2013; Xu et al. 2012).

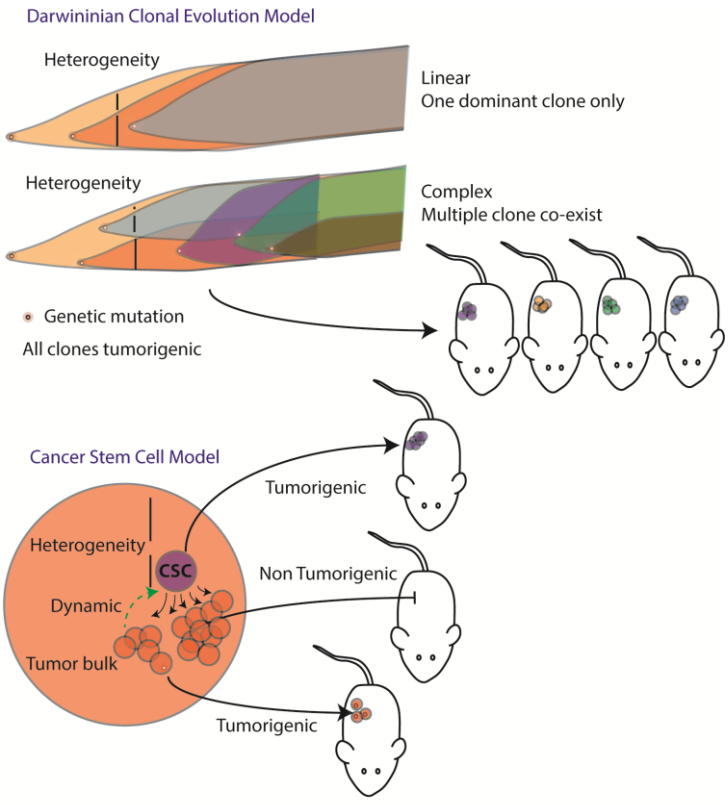

Tumorigenic vs non-tumorigenic often epigenetically determined

Figure 3.11. Different models explaining tumor heterogeneity. In the clonal evolution model, different genetic mutations occur over time (flare). The fittest clone gains advantage over the others and becomes dominant. In the linear model, only one dominant clone exists. While one clone becomes dominant but the old one still exist within the tumor, heterogeneity can be observed (indicated by black lines). In the complex model, several clones co-exist at a particular time, explaining the heterogeneity. The clones are genetically different and tumorigenic. The cancer stem model follows a steep hierarchy. The highly tumorigenic CSCs (violet) represent a small subpopulation of the whole tumor (red) while their differentiated progenitor cells do not form tumors upon xenotransplantation in immunocompromised mice, displaying a heterogeneous tumor (black lines). The differences between tumorigenic and non-tumorigenic cells is often epigenetically determined. It is also possible that differentiated cancer cells can become more stemness-like, dynamically switching their phenotype. To combine both models, CSCs-derived non tumorigenic tumor bulk cells can potentially acquire mutations reverting them into tumorigenic cells. Drawn by Simon Schäfer, adapted from (Marusyk & Polyak 2010).

3.5.1.2. Biological and therapeutic relevance of tumor heterogeneity

An elegant study by Gerlinger and colleagues examined intratumor heterogeneity by means of exome sequencing, chromosome aberration analysis and ploidy profiling from different tumors regions (Gerlinger et al. 2012). Surprisingly, 63-69% of all somatic mutations were not detectable across every renal tumor region. Mutational intra-tumor heterogeneity was observed in the tumor suppressors *SETD2*, *PTEN* or *KDM5C*. These genes underwent distinct and spatially separated inactivating loss-of-function mutations, suggesting a convergent evolution, which defined as genetically distinct "species" (clones with different mutations) possessing similar features (loss-of-function) (Gerlinger et al. 2012). Interestingly, the authors observed that mRNA expression signatures associated with both good and bad prognosis were detected within the same tumor. These observations have obvious consequences concerning treatment strategies using specific inhibitors which target individual genetic alterations. Additionally, predicted patient prognosis might be incorrect if only one single tumor biopsy was analyzed.

Another study developed two different algorithms deconvoluting tumor metagenomes, which are defined as aggregate genomes of all the clones that coexist within one sample (Andor et al. 2016). The algorithms "expanding the allele frequency on nested subpopulations' (EXPANDS) and PyClone were used to estimate the cellular prevalence of mutations to quantify data from the cancer genome atlas (TCGA). Using those bioinformatical tools, the authors detected high degree of heterogeneity in all analyzed tumor types. Interestingly, the mortality was significantly increased when more than 2 clones co-existed within a particular tumor. In contrast, more than 4 clones co-existing within a cancer decreased mortality, suggesting a trade-off between the costs and benefits of genetic instability (Andor et al. 2016).

Genetically diverse tumors can generate larger variety of variants to be tested by natural selection, therefore enhancing the probability that a particular clone reaches greater fitness (Marusyk & Polyak 2010) (Figure 3.12). This might be particular important for clinical treatments. A genetically diverse landscape of clones enables the tumor to maintain and eventually evolve treatment-resistant clones, while other clones are erased by the treatment. Chronic myelogenous leukemia (CML), which is caused by translocation of the *Bcr-Abl* translocation, can be treated with the inhibitor imatinib. However, some patients relapse from the disease. Roche-Lestienne showed that specific mutations found in resistant patients already existed in a small fraction of the original tumor, suggesting that genetic variability might enhance the fitness upon environmental changes (Roche-Lestienne 2002).

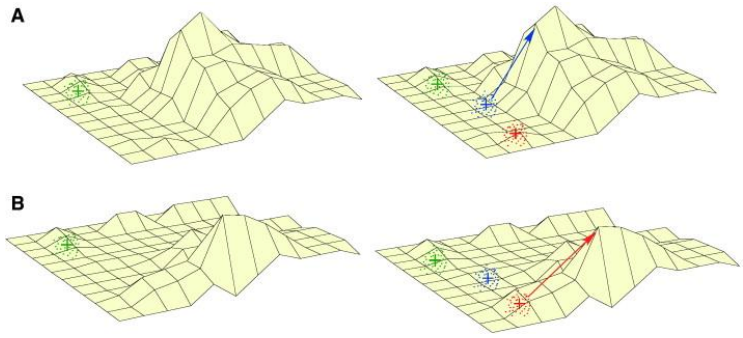

Figure 3.12. Biological relevance of tumor heterogeneity. A) Colored crosses represent genotypes of tumor clones. Small dots represent new mutations branching from the parental genotype. Peak height represent the level of fitness, while the highest elevation represent also the highest fitness in the "fitness landscape". Left: Offsets of the green clone probably never reach a very high peak of fitness since the genotypic vicinity only includes small peaks. Right: Different clones greatly enhance the probability that a clones offsets climbs a high peak. B) The fitness landscape might change after treatment. Multiple clones have a higher probability to climb a high peak in the newly altered landscape. From: (Marusyk & Polyak 2010)

If studied from an ecological perspective, distinct genetic cancer clones can be seen as asexually reproducing species interacting with each other. Therefore, infiltrating stromal cells, extracellular matrix and blood/lymphatic vessel represent the ecosystem of the species (Marusyk & Polyak 2010). It is therefore hypothesized that different tumor clones can communicate with each other in various ways, similar to species within a given ecosystem. Leith et al tested this hypothesis by injecting either two single clones or an admixture of the two clones into nude mice (Leith et al. 1987). The authors calculated growth curve kinetics for the two single clones and predicted the growth outcome if the two clones were admixed in a particular ratio. Interestingly, they could not predict the growth kinetics of the mixed clones, strongly speaking for clonal interactions.

A landmark paper by Marusyk analyzed the interaction of different breast cancer clones in regard to growth and metastasis formation (Marusyk et al. 2014). The authors used a specific breast cancer line (MDA-MB-468) which produced indolent tumors and showed very low growth rates upon transplantation into nude mice. Marusyk overexpressed 16 different factors which have been shown to be involved in tumorigenesis and combined each single clone with the parental cells (monoclonal) or pooled all clones (multiclonal). They observed that only 2/16 single clones, namely overexpressing *Il-11* and *CCl-5*, showed enhanced tumor formation when combined with the parental cells and neither of the tumors were metastatic. Intriguingly, the polyclonal fraction strongly increased tumor growth kinetics and metastasis formation. Further, they observed that the potent tumor driver (Il-11) was not necessarily a good competitor, which was measured by the clonal frequency in a given tumor. To illustrate, *FOXL3* overexpression did not enhance tumor growth but the clonal frequency war exceptionally high, which clearly emphasizes that clonal interactions can influence tumorigenesis and metastasis formation. Hence, tumor drivers enhance proliferation of all cells but yet can be outcompeted by different non-driver clones (Marusyk et al. 2014). Phenotypic heterogeneity and clonal interactions might therefore represent an underestimated mechanism of tumor formation and evolution.

3.5.1.3 Heterogeneity in melanoma

It has been shown that $BRAF^{V600E}$-mutated melanoma cells coexist with $BRAF^{wt}$ cells within a particular tumor (Yancovitz et al. 2012). Therefore, treatment with BRAF inhibitors might be ineffective since $BRAF^{wt}$ cells are drug-resistant. The BRAF mutational status is determined by a cobas test on DNA extracted from a single-needle biopsy, neglecting the entirety of the disease (Hachey & Boiko 2016). Phenotypic heterogeneity in melanoma also displays a major source of intratumor heterogeneity. ABCB5, CD271, ALDH1, CD133 or the histone demethylase JARID1B-positive melanoma populations have different biological features compared to the negative fractions, interspersing phenotypic diversity (Shannan et al. 2016). Further, tumor-associated antigens like gp-100 and MART-1 are heterogeneously expressed within a particular melanoma, possibly explaining a partial immune escape (Slingluff et al. 2000; Shannan et al. 2016). Hoek et al propose a dynamic *in vivo* "phenotype switch" model (Hoek et al. 2008). While early phase melanomas express a proliferative gene signature, a microenvironmentally-driven signal switch would, according their model, promote a more invasive phenotype as the tumor progresses

3.5.2. Tumor clonality

Supported by evidence, it is widely accepted that cancers derive from only one clone (monoclonal) (Weinberg 2006; Walsh et al. 1998; Sawada et al. 1994; Niho et al. 1998; Garcia et al. 2002; Nilbert et al. 1995). Those studies are mainly based on the analysis of tumors derived from female cancer patients heterozygous for certain X-chromosome-linked markers. In early embryogenesis, one of both X-chromosomes (inherited from the mother or from the father) remains genetically active while to other one forms an inactive Barr body. Since this process happens randomly, around 50% of all paternal and 50% of maternal chromosomes turn inactive, creating a genetic mosaic. In studies addressing tumor clonality, the haplotypes of X-chromosome-linked glucose-6-phosphate dehydrogenase (G6PD) have been examined. *G6PD* exists in two gene variants (Gd^A and Gd^B), encoding for slightly different enzymes. Clonality analysis can be conducted in females heterozygous for Gd^A/ Gd^B. In a monoclonal tumor, all cells carry either the Gd^A or Gd^B background while multiclonal tumors present with a mix of both clones (Figure 3.13.).

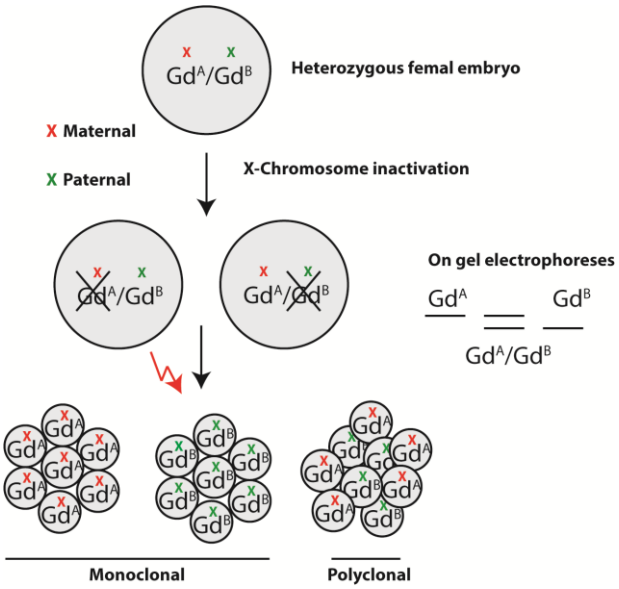

Figure 3.13. A method to address clonality in tumors. X-chromosome-linked *G6PD* exists as Gd^A or Gd^B gene variant. The X-Chromosome inactivation (black cross) happens randomly (50:50) in either the paternal (red) or the maternal (green) X-Chromosome. Therefore, women heterogeneous for *G6PD* either have the Gd^A or Gd^B gene variant in all somatic cells. In a hypothetical monoclonal tumor, only one form (Gd^A or Gd^B) is observed upon oncogenesis. On the other hand, a combination (Gd^A and Gd^B) is detected if multiple found clones established the tumor. Drawn by Simon Schäfer.

In 1965, Linder and Gartler analyzed 27 leiomyomas and surrounding myometrium (Linder & Gartler 1965). While normal myometrium tissue showed positivity for the forms Gd^A and Gd^B, the tumors only expressed one particular form, indicating a monoclonal tumor origin. Another study by

Fialkow et al. used the same method to study the clonality of three CML patients (Fialkow et al. 1967). Fibroblast samples from the patients revealed Gd^A and Gd^B bands while CML cells showed only the Gd^A variant, confirming the previous results. Nevertheless, other studies showed conflicting results. Using similar experimental setups, Smith et al, demonstrated that two out of five invasive cervical carcinomas had a multiclonal origin (Smith et al. 1971). Further, additional studies confirmed multiclonality for hereditary neurofibromas (Fialkow et al. 1971). In 1985, Bert Vogelstein developed a new method based on restriction fragment length polymorphisms (RFLP) (Vogelstein et al. 1985). The first endonuclease distinguished between the paternal and the maternal gene variant of the *HPRT* gene through RFLP and the second distinguishes the inactive and active X-Chromosome. In a monoclonal tumor, all cells should be active or inactive for the paternal/maternal gene variant. They observed monoclonality in three out of three analyzed human cancers.

Evidence supporting the multiclonal tumor model came from a study analyzing *ROSA26*/+ $Apc^{min/+}$ <=> +/+ $Apc^{min/+}$ chimera mice, which are prone to develop intestinal adenomas (Merritt et al. 1997). Although they observed that intestinal crypts were monoclonal, $Apc^{min/+}$-driven adenomas interestingly often presented as polyclonal structures (*ROSA26*-driven blue and +/+ white patches) (Figure 3.14.).

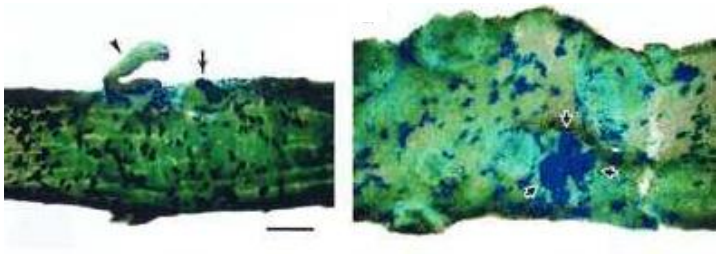

Figure 3.14. Polyclonality in *ROSA26*/+ $Apc^{min/+}$ <=> +/+ $Apc^{min/+}$ chimera. Whole mount X-Gal staining shows multiclonal intestinal adenomas, containing both blue and white components. Adapted from: (Merritt et al. 1997).

In another study, Kissberth and Sandgren developed chimeric mammary glands with an inherited predisposition for neoplasia (Kisseberth & Sandgren 2004). Mice overexpressing WAP-TGFα in the mammary epithelium develop carcinomas temporally preceded by hyperplastic alveolar nodules (HANs). The authors created WAP-TGFα/R26-hPAP <=> WAP-TGFα/hCK10 chimeric fat pads for transplantation, with hPAP and hCK10 as distinguishable markers. Interestingly, most of the HANs were polyclonal, supporting the data from (Merritt et al. 1997) and counteracting the single clone origin model. In summary, the question if tumors originate from one or multiple founder clones cannot be answered definitely and strongly depends on tumor type and experimental settings.

3.5.3. Lineage tracing using multi-color fluorescent reporter mice

Multicolor lineage tracing approaches can increase insights in the unresolved questions about clonal origins of tumors. In the year 2010, Snippert et al first designed a multicolor Cre-reporter mouse, informally called the "confetti mouse" (Figure 3.15.) (Snippert et al. 2010). TM-based Cre recombinase activation leads to excision of the loxP-flanked neomcycin roadblock and to random recombination of the four fluorescent colors GFP, YFP, RFP and CFP. GFP shows a nuclear expression pattern, RFP and YFP are cytoplasmic and CFP presents with a membrane-bound expression, enabling proper discrimination of the four fluorescent colors. The mouse is based on the Brainbow 2.1. mouse model by Livet and colleagues (Livet et al. 2007).

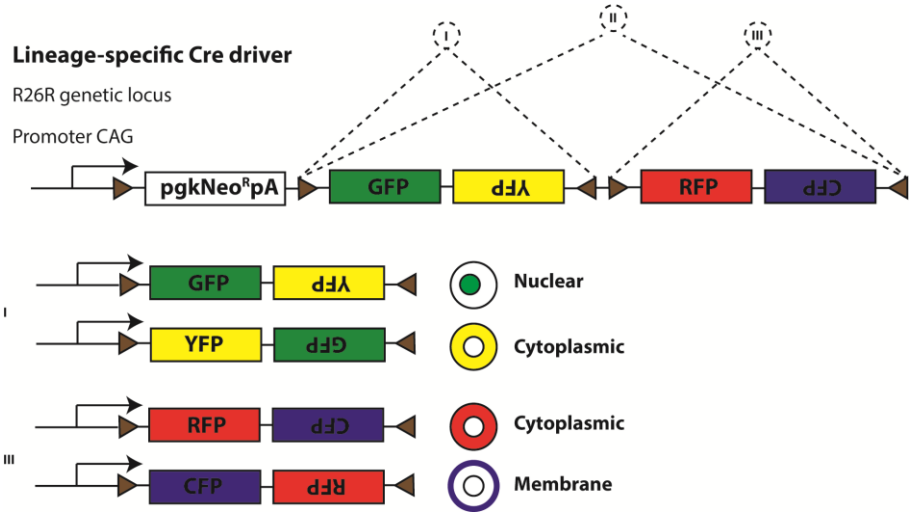

Figure 3.15. Confetti transgene. The R26R-confetti construct contains a CAG promoter, a loxP site-containing pgkNeo^{R}pA roadblock and a brainbow 2.1. cassette with two head to tail loxP sites. Lineage-specific Cre activation leads to inversion (reverse loxP) or excision ("same oriented" loxP) of the cassette and eventually to the random expression of one fluorescent color. Drawn by Simon Schäfer, Adapted from (Livet et al. 2007).

As an example, Snipert et al. used the confetti multicolor lineage tracing to characterize intestinal crypt homeostasis (Snippert et al. 2010). The authors labelled Lgr5^{High} intestinal stem cells and mapped the fate of the diverse colored clones. They observed that Lgr5^{High} cells persisted life-long but the crypts drifted towards monoclonality over time. Another group studied metastasis formation in an autochthonous model of pancreatic cancer by means of the confetti mouse (Maddipati & Stanger 2015). Although clonal selection occurred in the early phases of tumor progression in the *PDX::CreER KRAS^{G12D} p53$^{lox/lox}$* mouse model, most analyzed metastases were indeed polyclonal (polychrome). Hence, this multicolor lineage tracing mouse displays an elegant and potent model system to characterize, follow and map clonal evolution over time.

4. Results

4.1. My contributions to published articles

4.1.1. The roles of Sox10 and Sox9 in melanomagenesis

I helped unraveling the oncogenic role of Sox10 in melanoma formation (Shakhova et al. 2012). I performed shRNA-mediated *SOX10* KD experiments in human melanoma cells and was able to show that *SOX10* KD caused increased apoptosis and decreased proliferation. The cells were analyzed using either AnnexinV or Propidium Iodide assays and evaluated with the FACS ARIA III analyzer. Secondly, I contributed to the work showing the antagonistic role of Sox10 and Sox9 in melanomagenesis (Shakhova et al. 2015). I transfected human melanoma cells with a *SOX9* overexpression plasmid and observed a downregulation of SOX10 protein levels, which was quantified by Western Blot analysis.

Shakhova O., Zingg D., **Schaefer S.M.,** Hari L., Civenni G., Blunschi J., Claudinot, S., Okoniewski, M., Beermann, F., Mihic-Probst, D., Moch H., Wegner M., Dummer R., Barrandon Y., Cinelli P., Sommer L. *Nature Cell Biology Aug;14(8):882-90.*

Shakhova O., Cheng, P.F., Pravin J., Zingg D., **Schaefer S.M.**, Debbache, J., Haeusel, J., Matter, C., Guo T., Davis, S., Meltzer, P., Mihic-Probst, D., Moch, H., Wegner, M., Merlino G., Levesque, M.P., Dummer R., Santoro R., Cinelli P., Sommer L. *Plos Genetics 2014 Jan 28;11(1):e1004877.*

4.1.2. The roles of the epigenetic modifier EZH2 in melanomagenesis

I helped deciphering the role of the histone methyltransferase enhancer of zeste homolog 2 (EZH2) in melanoma formation (Zingg et al. 2015). I performed siRNA-mediated *EZH2* KD experiments in human melanoma cells and collected the RNA which was used for a microarray study.

Zingg, D., Debbache, J., **Schaefer, S.M.**, Tuncer, E., Frommel, S.C., Cheng P.F., Arenas-Ramirez, N., Haeusel J., Zhang, Y., Bonalli, M., McCabe M.T., Creasy, C.L., Levesque, M.P., Boyman O., Santoro R., Shakhova O., Dummer R., Sommer L. *Nature Communications 2015 Jan 22;6:6051*

4.2. The role of Sox2 in primary melanoma and metastasis formation

Previous studies have identified SOX2 as an oncogenic driver in human melanoma cells (see 3.4.9.). Those published studies are mostly based on shRNA-mediated *SOX2* KD experiments in human melanoma cells. Therefore, we decided to fully block *Sox2* function using different KO approaches, especially using a genetically engineered mouse model, in which metastatic melanoma spontaneously develops within an intact stromal environment. To address the potential relevance of Sox2 for human melanoma patients, we generated CRISPR-Cas9-mediated *SOX2* KO melanoma cells and analyzed patient data from TCGA. The goals for this project included:

1) The analysis and interpretation of SOX2 expression in human melanoma patients using RNA sequencing-based patient data from TCGA database.

2) The establishment and functional analysis of *SOX2* KO human melanoma cells using the CRISPR-Cas9 genome editing technology.

3) The investigation of Sox2 in melanoma and metastasis formation using a syngeneic melanoma mouse model, in which oncogenesis happens within an intact stromal environment.

Those illustrated results were recently accepted for publication:

Sox2 is dispensable for primary melanoma and metastasis formation

Schaefer, S.M., Segalada, C., Cheng, P.F., Bonalli M., Parfejevs V., Levesque M.P., Dummer R., Nicolis SK., Sommer L. *Oncogene, 2017, Apr.3, Epub ahead of print*

My contribution to this work was the following:

- Performed experiments
    - Mouse breedings, Tamoxifen injections, tissue collection
    - Cutting and immunostainings of paraffin-embedded tissue sections
    - Cell culture, protein isolation and Western Blot
    - RNA isolation and RT-qPCR
- Analyzed data
    - Quantifications of stainings
    - Quantifications of primary melanoma and metastases

4.2.1. SOX2 expression is not linked to patient survival

First, we compared TCGA-based (http://cancergenome.nih.gov/) SOX2 RNA expression in human melanomas with those of other cancers and plotted the three cancers with the lowest (acute myeloid leukemia (AML), diffuse large B-cell lymphoma (DLBC), chromophobe renal cell carcinoma (chRCC) and the highest SOX2 expression (lung squamous cell carcinoma (SCC), glioblastoma multiforme (GBM), lower grad (diffuse) gliomas). Further, we analyzed SOX2 expression in frequently diagnosed cancers (colorectal (CRC), breast, lung adenomas). We observed low SOX2 expression in cutaneous melanoma compared to the cancers highly expressing the transcription factor (Figure 4.1.a). Next, we investigated if Sox2 expression was changed based on the different sites of the biopsy (primary tumor, skin metastasis, lymph node metastases, distant metastases). We did not detect any difference in SOX2 expression comparing the different biopsy sites (Figure 4.1.b). Breslow depth, which is defined as the total vertical height of the tumor, is one major important prognostic predictor of death from melanoma (Buttner et al. 1995). Therefore, we plotted SOX2 expression from human primary melanomas to the Breslow thickness (Figure 4.1.c). We did not detect a significant correlation between expression and thickness. Next, we detected a large variation of SOX2 expression between 420 different human melanomas and established a SOX2 high (top 20%) and a SOX2 low (bottom 20%) group (Figure 4.1.d).

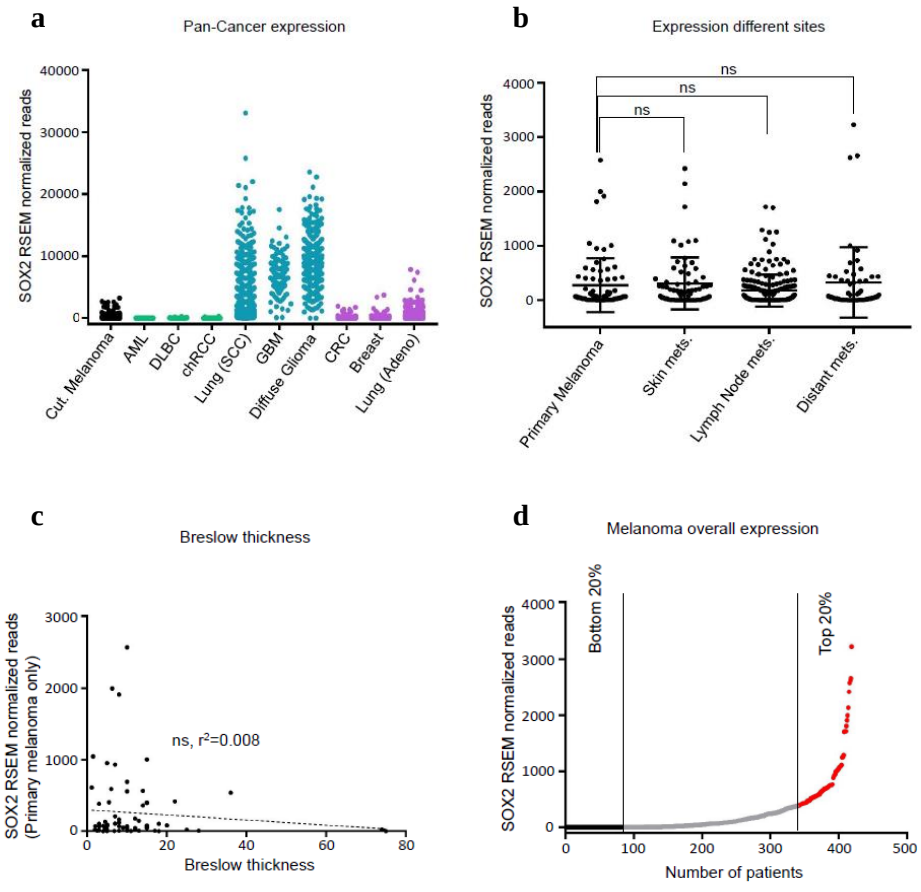

Figure 4.1. SOX2 is heterogeneously expressed in melanoma and does not correlate with Breslow thickness. (a) Comparison of RNA-seq-based SOX2 expression between cutaneous melanoma (black, n=471 patients, mean of SOX2 RSEM normalized reads (mean)=220.4), SOX2 low expressing tumors (green: AML, n=170, mean=0.3; DLBC, n=48, mean=15.54; chRCC, n=66, mean=8.5), high expressing (blue: Lung SCC, n=500, mean=4309; GBM, n=166, mean=6734; Glioma, n=530, mean=9200), and most frequently diagnosed tumors (violet: CRC, n=375, mean= 80.27; Breast, n=1097, mean=47; Lung adeno, n=516, mean=482) based on cBioPortal and TCGA data. **(b)** Comparison of SOX2 expression in primary melanoma (n=80, mean of SOX2 RSEM normalized reads (mean)=276.1), skin metastasis (n=71, mean=305), lymph node metastasis (n=208, mean=175), and distant metastasis (n=56, mean=326.3). 1-way ANOVA analysis shows slight but significant increase in SOX2 expression from lymph node to skin metastases (p=0.03) and from lymph node to distant metastases (p=0.02). SOX2 expression levels do not significantly (ns) differ otherwise between the different locations (p>0.05 for all indicated comparisons). Data is presented as mean ± s.d. **(c)** SOX2 expression from primary melanomas (n=72) do not correlate with Breslow thickness (r^2 = 0.008, Pearson r test). **(d)** Overall SOX2 expression in primary melanoma and metastasis (all patients: n=420; bottom 20%: n=80, mean=0.8; top 20%: n=80, mean=911).

Next, we analyzed if SOX2 expression correlates with patients survival. As mentioned above, we established SOX2 high (top 20%, 80 patients, mean expression 0.8 RSEM normalized reads) and a SOX2 low (bottom 20%, 80 patients, mean expression 911 RSEM normalized reads) group. Interestingly, the overall patient survival did not correlate with SOX2 expression levels (Figure 4.2a). Exclusively taking biopsies from metastases into account, the survival still did not correlate with SOX2 expression levels with a sample size of 67 patients (Figure 4.2b).

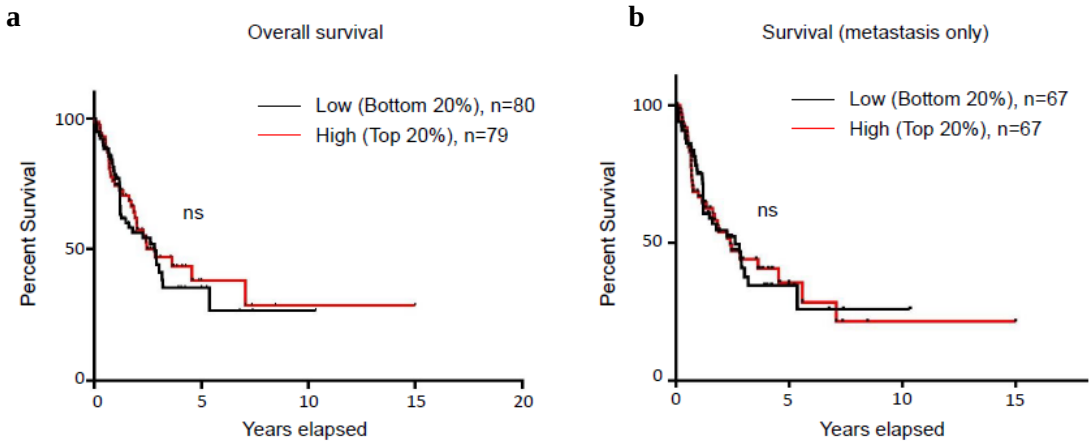

Figure 4.2. SOX2 expression is not linked to patient survival. (a) Kaplan-Meier curve comparing overall survival of melanoma patients (stage I-IV) with respect to SOX2 transcript levels based on TCGA (bottom 20%, n=80; top 20%, n=79). P-value=0.64 was calculated with log-rank (Mantel-Cox) test. **(b)** Kaplan-

Meier curve comparing survival of melanoma patients with metastases (stage II-IV) with respect to SOX2 transcript levels based on TCGA (bottom 20%, n=67; top 20%, n=67). P-value=0.98 was calculated with log-rank (Mantel-Cox) test. All TCGA data were analyzed with R (The R Foundation for Statistical Computing).

4.2.2. SOX2 KO does not influence tumor growth of human melanoma cells in vivo

We analyzed 3 publically available and 3 patient-derived human melanoma cultures for SOX2 protein expression. The only melanoma culture strongly expressing SOX2 was the patient-derived and *NRas*^{Q61L}-mutated M050829 "cell line". On the other hand, we observed a very weak expression in the cell lines A375 and Sk-Mel-28 and absent expression in M070302, MM159423 and WM83 (Figure 4.3.a). In collaboration with Dr. Mario Bonalli and Corina Segalada, we established two *SOX2* KO clones using the CRISPR-Cas9 genome editing technology (Figure 4.3.b). We performed a Western Blot analysis to demonstrate the loss of SOX2 protein in the two CRISPR clones. To identify a potential functional impact of *SOX2* loss, we subcutaneously injected 150000 cells of each conditions into Foxn1$^{nu/nu}$ female mice (n=4 for each condition) and followed tumor growth weekly over 8 consecutive weeks (Figure 4.3.c). Consistent with the data from the TCGA, we did not measure a significant difference in tumor growth between the control and the *SOX2* KO condition.

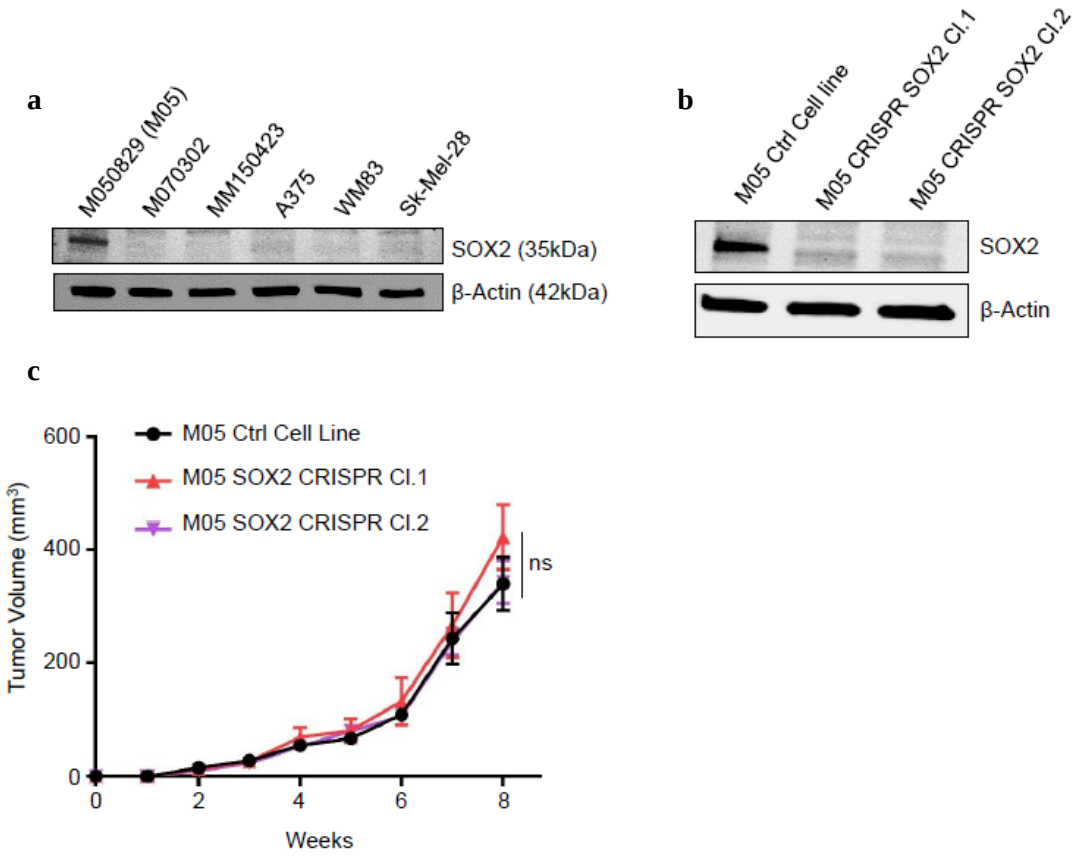

Figure 4.3. *SOX2* KO does not influence tumor growth of human melanoma cells *in vivo*. (a) The cell lines M050829 and M070302 have been characterized before (Zipser et al. 2011, Civenni et al. 2011). MM150423 was generated at the Department of Dermatology of the University Hospital Zurich and approved by the ethical committee of the Canton of Zurich, Switzerland. SOX2 protein expression of the human melanoma cell lines was analyzed by Western Blot **(b)** Western Blot analysis of SOX2 protein levels in M050829 control cell line, *SOX2*-CRISPR clone 1 (Cl.1) and *SOX2*-CRISPR clone 2 (Cl.2). Following sgRNA sequence was used for CRISPR Cl 1&2: 5'-GGCCCGCAGCAAACTTCGGGGGG-3' with a quality score of 87 according to http://crispr.mit.edu. **(c)** 2 month-old Foxn1$^{nu/nu}$ female mice were subcutaneously engrafted with 150'000 control (black curve), *SOX2* CRISPR Cl.1 (red curve), or *SOX2* CRISPR Cl.2 (violet curve) cells (M050829) (n=4 for each condition, non-blinded). Tumor volume was measured weekly with a caliper and calculated as follows: $V=2/3 \times \pi \times ((a+b)/4))^3$, where a (mm) was the length and b (mm) was the width of the tumor. 1-way ANOVA analysis shows no significant difference between control cells and the two SOX2-CRISPR clones (control vs. CRISPR Cl.1: p=0.47; control vs. CRISPR Cl.2: p=0.99).

Next, we immunostained paraffin-embedded tumor sections with a SOX2-specific antibody to confirm the *SOX2* loss. As expected, we observed a heterogeneous and nuclear SOX2 expression pattern in the control tumors. Next, we co-stained the control tumors with SOX2 and SOX10, which is a well-established melanoma marker (Shakhova et al. 2012). We exclusively observed SOX2/SOX10 double-positive cells, confirming that the SOX2-positive cells were indeed melanoma cells (Figure 4.4.a). In contrast, both *SOX2* KO clones showed nuclear SOX10 but absent SOX2 expression, confirming the CRISPR-Cas-mediated gene KO previously demonstrated by Western Blot analysis. Further, we did not observe major changes in the tumor morphology which was illustrated with a hematoxylin and eosin (H&E) staining (Figure 4.4.b).

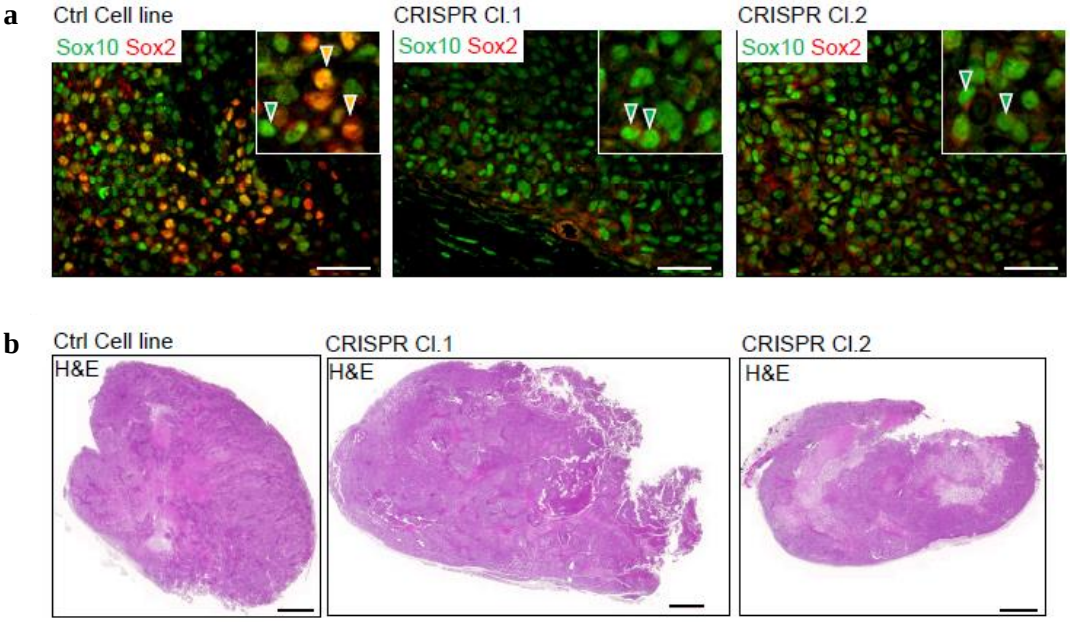

Figure 4.4. SOX2 KO does not cause major changes in tumor morphology. (a) Co- Immunostaining of SOX2 and SOX10 on paraffin-embedded control, SOX2-CRISPR Cl.1 and SOX2-CRISPR Cl.2 tumors (scale bars=50um). **(b)** Hematoxylin and eosin (H&E) staining showing the morphology of xenografted control, SOX2-CRISPR Cl.1 and SOX2-CRISPR Cl.2 cells (scale bars=1000um).

SOX2 plays a crucial role in maintaining a pluripotent cell state in the inner cell mass of the embryo (see 3.2.1.). Since the *SOX2* KO did not affect tumor initiation and growth, we asked if *SOX2* loss affects the grade of differentiation, according its role in ESCs. Hence, we performed an immunstaining for MITF, the master transcription factor in melanocyte development. We detected nuclear MITF expression in the control and the both *SOX2* KO tumors (Figure 4.5.a). To quantify those results, we isolated RNA directly from the tumors and performed a quantitative real time PCR (RT-qPCR) using *MITF*-specific primers. Since we did not observe a significant difference in MITF expression comparing the control and the two *SOX2* KO clones, we tested the expression of the two additional melanocyte differentiation markers DCT and melanoma antigen recognized by T-cells 1 (MLANA). We did not observe differences in RNA expression comparing the control and the *SOX2* KO condition, concluding that cell differentiation was not affected by *SOX2* KO (Figure 4.5.b).

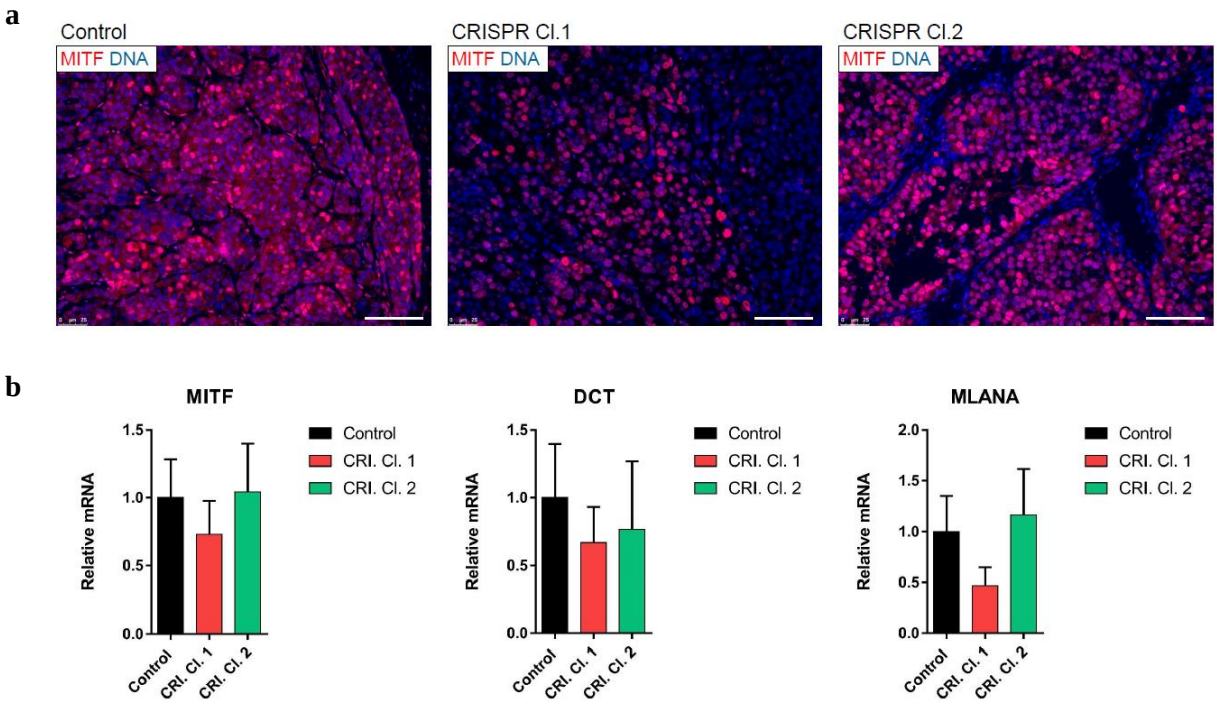

Figure 4.5. SOX2 KO does not affect tumor differentiation. (a) Immunostaining of MITF on paraffin-embedded control, *SOX2*-CRISPR Cl.1 and *SOX2*-CRISPR Cl.2 tumors (scale bars=50um). **(b)** RT-qPCR for *MITF*, *DCT* and *MLANA* from control (black), *SOX2*-CRISPR Cl.1 (red) and *SOX2*-CRISPR Cl.2 (green) RNA directly isolated from the different tumors (n=3, for each condition) . All p-values were > 0.05 and calculated with ANOVA and multiple comparison analysis.

4.2.3. Sox2 is expressed in murine melanoma but not critical for survival time

First, we monitored expression of Sox2 during disease progression in wildtype and *Tyr::N-Ras*^{Q61K} *Ink4a*$^{-/-}$ mice developing melanoma. In normal postnatal mouse skin, Sox2 was expressed in a subset of dermal papillae, consistent with previous findings in mouse and human (Rendl et al. 2005; Ryan R Driskell et al. 2009b). Further, we did not detect Sox2 expression in differentiated Sox10-positive melanocytes located in hair follicle bulbs. It has been shown that approximately 50% of human melanomas, but only a minority of nevi, express SOX2 (Laga et al. 2010; Laga et al. 2011; Santini et al. 2014; Girouard et al. 2012). Likewise, Sox2 was only expressed in a small subset of Sox10-positive hyperplasia cells of *Tyr::NRas*^{Q61K} *Ink4a*$^{-/-}$ mice (mean 3.2%), whereas a higher percentage of cells expressed the transcription factor in primary tumors (mean 7.9%). The percentage of Sox2/Sox10 double positive cells further increased in lymph node metastases (mean 11.2%) (Figure 4.6.).

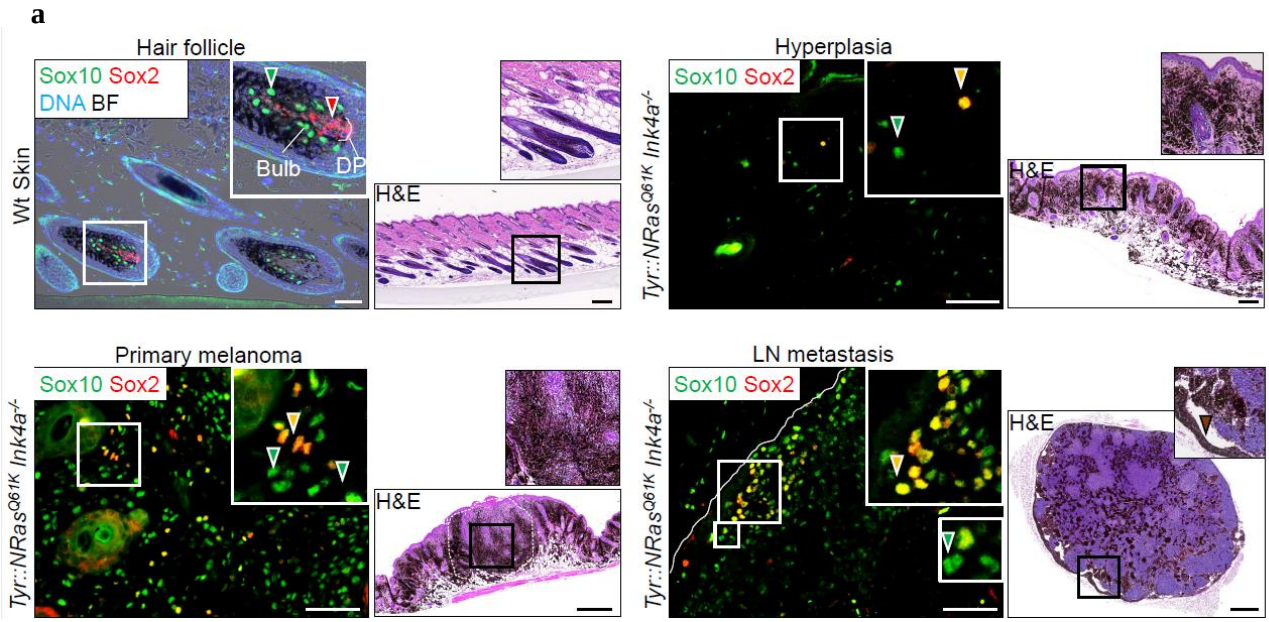

b

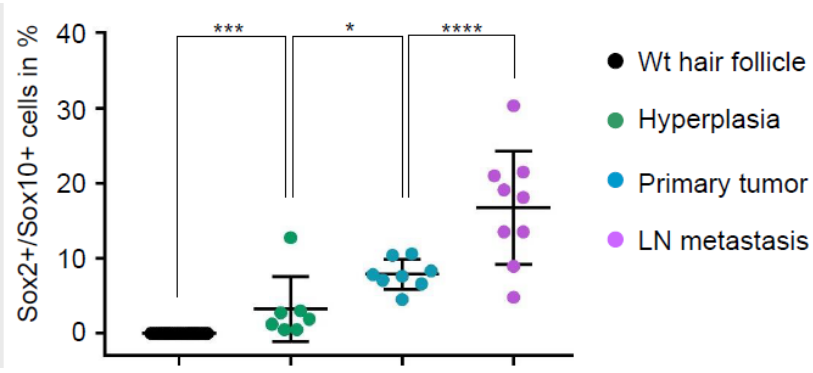

Figure 4.6. Sox2 is expressed in *Tyr::NRas^{Q61K} Ink$^{-/-}$*-driven mouse melanoma and upregulated during disease progression. (a) Immunostaining on trunk skin sections of wt mice for Sox2 and Sox10. Green arrowhead shows Sox10-positive hair follicle bulb melanocytes. Red arrowhead points at Sox2-positive dermal papilla (DP) cells (scale bar=50um). Hematoxylin and eosin (H&E) staining shows the morphology of hair follicles in wt skin (scale bar=200um). Immunolabeling of *Tyr::NRas^{Q61K} Ink$^{-/-}$*-driven hyperplasia (6 month of age) shows Sox10/Sox2 double-positive cells (orange arrowhead) as well as Sox10 single positive cells (green arrowhead) (scale bar=50um). H&E staining shows interfollicular ectopic pigmentation (scale bar=200um). Primary melanomas present with a bump-like morphology on H&E staining with adjacent hyperplasia (scale bar=500um). Orange arrowhead shows Sox10/Sox2 double-positive cells and green arrowheads point to Sox10 single-positive melanoma cells (scale bar=50um). Lymph nodes are mainly infiltrated by metastatic melanoma cells in the border regions (H&E, scale bar=500um). Orange arrowhead marks Sox10/Sox2 double-positive cells while green arrowhead points to cells positive for Sox10 only (scale bar=50um). **(b)** 0% of Sox10-positive melanocytes were also Sox2-positive in wt postnatal murine skin (n=50). On average, 3.2% of hyperplastic cells showed Sox10/Sox2 double expression (n=7, total count 3975 cells). In primary melanomas, 7.8% of all Sox10 positive cells also expressed Sox2 (n=8, total count 3393 cells). Lymph node metastases showed on average 16.7% Sox10/Sox2 double positivity (n=9, total count: 5110 cells). Data is presented as mean ± s.e.m. P-Values were calculated with ANOVA test (hair follicle vs hyperplasia: $p = 0.0005$; hyperplasia vs primary tumor: $p = 0.02$; primary tumor vs lymph node metastasis: $p \leq 0.001$. *$p \leq 0.05$, ***$p \leq 0.001$, ****$p \leq 0.0001$.

Based on this expression pattern, Sox2 might promote primary melanoma and metastasis formation. Therefore, we conditionally deleted *Sox2* (*Sox2$^{lox/lox}$* (Favaro et al. 2009)) in the melanocytic lineage (Tyr::Cre^{ERT2} (Bosenberg et al. 2006)) in a genetic mouse melanoma model previously described (Ackermann, et al. 2005; Zingg et al. 2015; Shakhova et al. 2012). The Cre-reporter allele (*R26::LacZ* (Soriano 1999)) was used to fate map the recombined cells *in vivo*. TM was applied by intraperitoneal (IP) injection to 1 month-old animals for recombination. Hence, *Sox2* was deleted in a genetic *Tyr::N-Ras^{Q61K} Ink4a$^{-/-}$ Tyr::Cre^{ERT2} Sox2$^{lox/lox}$ R26R::LacZ* mouse melanoma model. As control, we used *Tyr::N-Ras^{Q61K} Ink4a$^{-/-}$ Sox2$^{lox/lox}$ R26R::LacZ* mice, lacking the *Cre* transgene. The experimental and the control group were injected on five consecutive days with TM and monitored for melanoma and metastasis formation (Figure 4.7.)

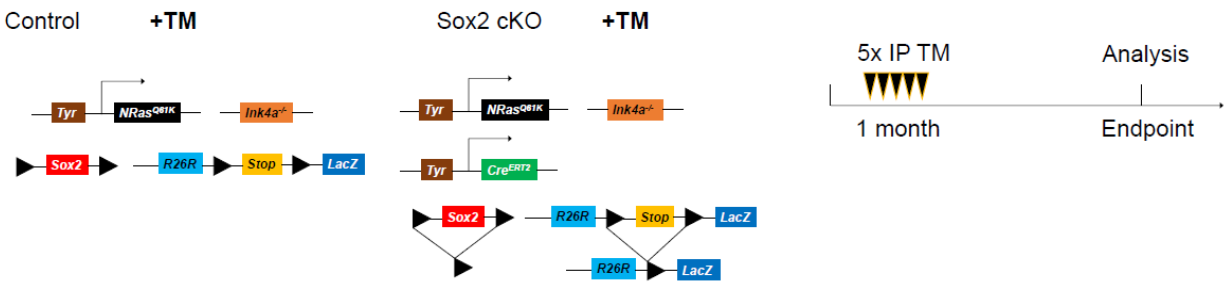

Figure 4.7. Genotypes and strategy used to analyze the effect of conditional Sox2 deletion in melanoma formation. TM=Tamoxifen. Experimental condition: *Tyr::N-Ras^{Q61K} Ink4a$^{-/-}$ Tyr::Cre^{ERT2} Sox2$^{lox/lox}$ R26R::LacZ.* Control condition: *Tyr::N-Ras^{Q61K} Ink4a$^{-/-}$ Sox2$^{lox/lox}$ R26R::LacZ.* For both condition TM (10mg/ml, 200ul per day) was applied on five consecutive days as IP injection.

To confirm *Sox2* ablation, we co-stained three different hyperplasias for *R26R::LacZ*-mediated β-Galactosidase (β-Gal) and Sox2 expression. While in *Sox2* conditional knockout (cKO) mice, Sox2 expression was never found in β-Gal-positive cells, the transcription factor was expressed in a subset of non-recombined, β-Gal-negative cells (Figure 4.8.a). Surprisingly, we did not observe a change in melanoma-specific survival between the *Sox2* cKO and the control group (median survival control: 147 days, median survival *Sox2* cKO: 154 days) (Figure 4.8.b).

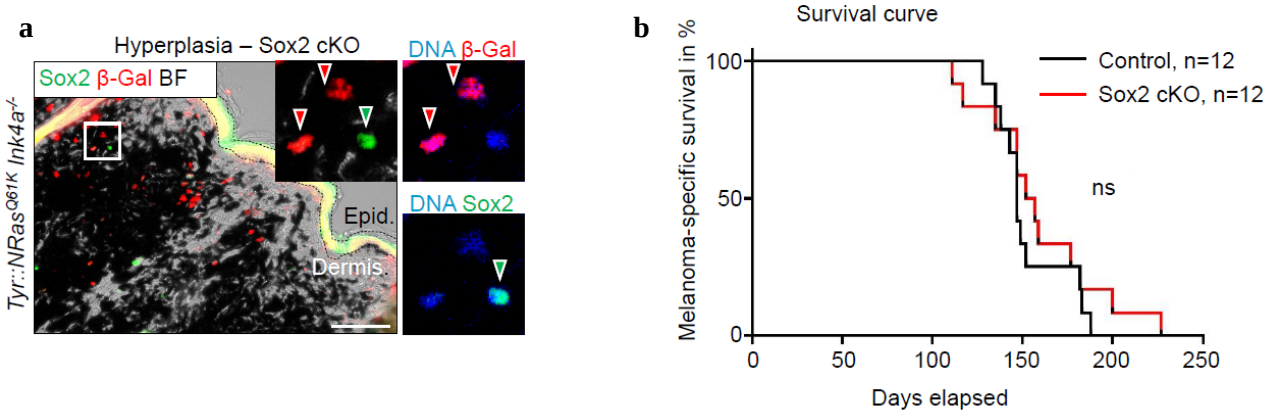

Figure 4.8 Sox2 cKO does not influence the melanoma-specific survival. (a) Immunostaining of β-Gal developed with TSA^{TM} plus Cy3 amplification kit and Sox2 in *Tyr::NRas^{Q61K} Ink4a$^{-/-}$*-driven hyperplasia. All cells expressing β-Gal (red arrowheads) lack Sox2 expression. The green arrowhead marks a Sox2-expressing pigmented cell and is β-Gal-negative (scale bar=50um). 3 different recombined hyperplasias and 3 melanomas were analyzed; no β-Gal/Sox2-positive cells were detected (not shown). **(b)** Kaplan-Meier curve comparing melanoma-specific survival after conditional *Sox2* ablation (Mantel-Cox test, p=0.96, unpaired t-test). 3-8 month-old male and female mice with mixed genetic background were used. The sample size was not predetermined by statistical methods.

4.2.4. Sox2 is dispensable for primary tumor and metastasis formation

Tyr::NRas^{Q61K} *Ink4a*$^{-/-}$ mice reliably develop skin melanoma within 6 months of age and often present with metastases in lymph nodes, lungs and liver (Ackermann et al. 2005; Shakhova et al. 2012). Of note, both control as well as the *Sox2* cKO mice developed a macroscopically visible hyperplasia and primary melanomas (Figure 4.9.a). Histological analysis of control and *Sox2* cKO melanomas did not reveal overt changes in the morphological appearance of tumors (Figure 4.9.a, b). Moreover, quantification of total skin tumor numbers failed to discriminate between the two groups (Figure 4.9.c). Since in *Tyr::NRas*^{Q61K} *Ink4a*$^{-/-}$ mice, TM-induced *Tyr::Cre*^{ERT2} – mediated recombination efficiency does usually not reach 100% of all melanocytic cells, primary melanoma in *Sox2* cKO mice might arise from non-recombined cells. To exclude this possibility, we determined the overall recombination rate (β-Gal-positive/Sox10-positive cells) in hyperplastic skin and in primary tumors of *Sox2* cKO mice, in which *Tyr::Cre*^{ERT2} had been activated at 1 month of age (Figure 4.9.d). Importantly, the percentage of recombination in skin tumors (49.0%; n=8) was not significantly altered when compared to hyperplastic lesions (50.4%; n=5) (Figure 4.9.d and Figure 4.10.a, b). Thus, loss of Sox2 neither favored nor prevented contribution of melanocytic cells to growing primary melanoma, demonstrating that Sox2 is dispensable for melanoma formation in the *Tyr::NRas*^{Q61K} *Ink4a*$^{-/-}$ mouse melanoma model.

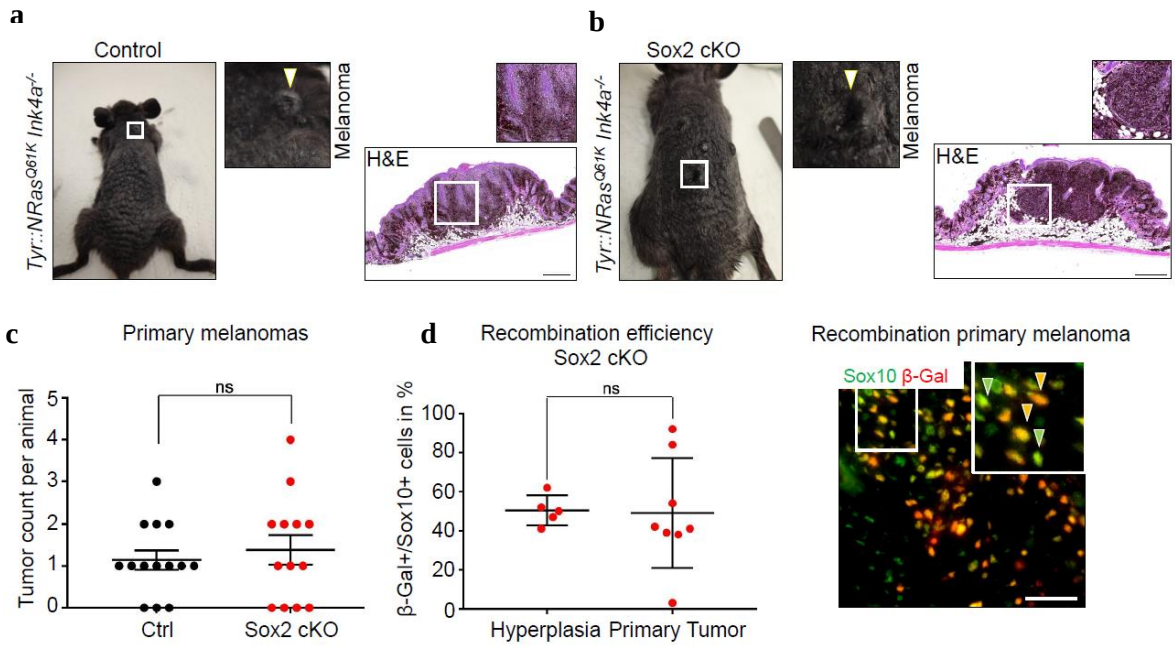

Figure 4.9 Sox2 is dispensable for tumor growth and metastasis formation. (a) Macroscopic picture shows the shaved back skin of a control mouse at 4.5 month of age. The white arrowhead marks a primary melanoma, which was further analyzed by H&E staining (scale bar=500um). **(b)** Macroscopic picture shows the shaved back skin of a *Sox2* cKO mouse at 4.5 month of age. The white arrowhead marks a primary melanoma further analyzed by H&E staining (scale bar=500um). **(c)** Total number of primary melanomas

control: n=14, *Sox2* cKO: n=13, p=0.56, unpaired t-test). Data is presented as mean ± s.e.m. **(d)** Comparison of recombination efficiency in hyperplasia and primary tumors. 50.4% of β-Gal/Sox10 double positive cells were counted in hyperplasia (n=5, total count: 3995 cells) and 49.1% in primary tumors (n=8, total count: 6400 cells, p=0.92, unpaired t-test). Animals: 4.5-8 month of age, males and females, mixed background. Data is presented as mean ± s.e.m. Representative picture of primary melanoma immunostained for β-Gal and Sox10 (green arrowheads: Sox10-positive cells, orange arrowheads: β-Gal/Sox2 double-positive cells) Scale bar=50um.

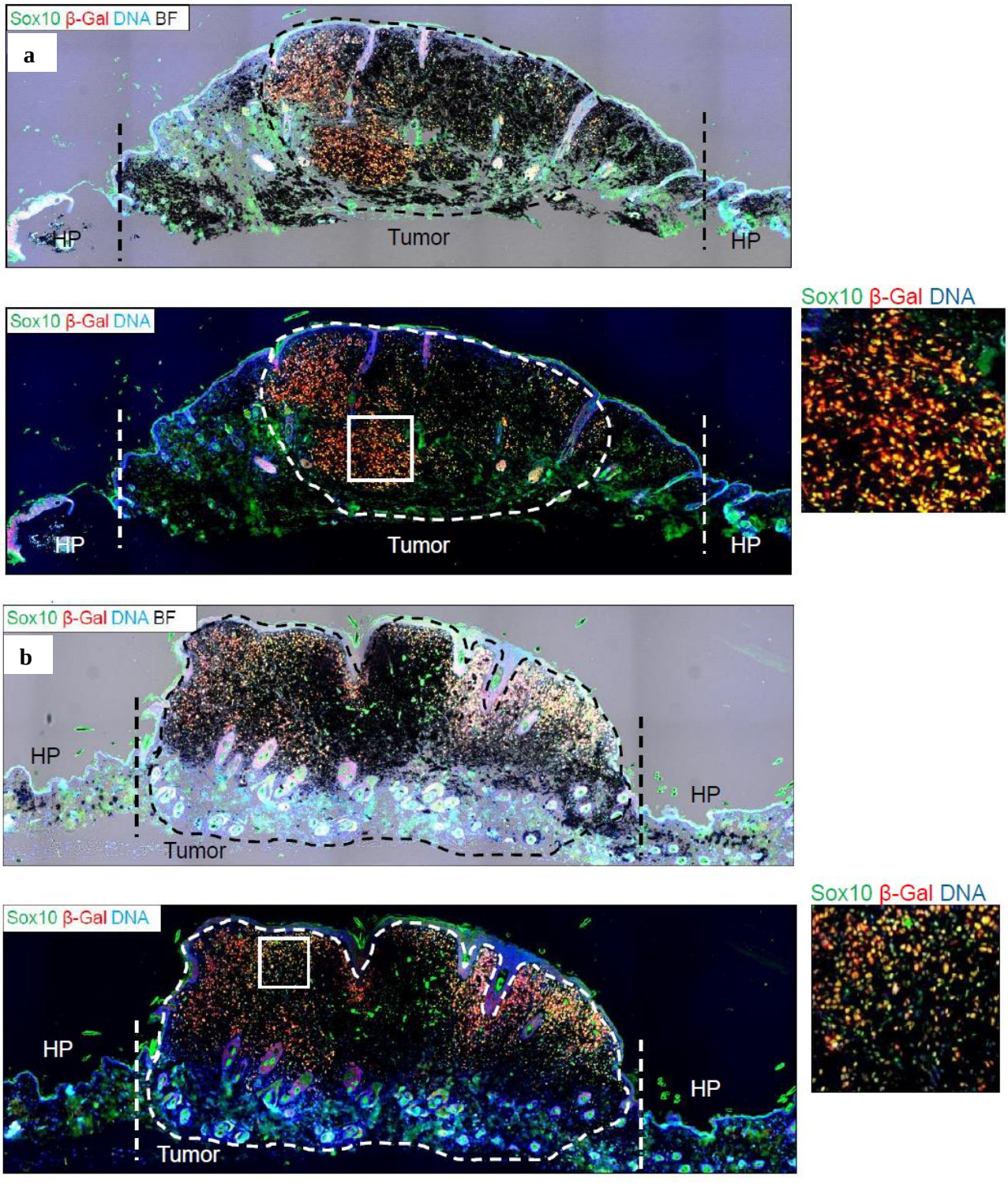

Figure 4.10 Recombined β-Gal-positive/Sox10-positive melanomas. (a) First example of a β-Gal-positive/Sox10-positive melanoma (Sox2 cKO). HP=Hyperplasia, BF=Brightfield **(b)** Second example of a β-Gal-positive/Sox10-positive melanoma (Sox2 cKO). HP=Hyperplasia, BF=Brightfield.

It has been reported that Sox2 promotes invasiveness in cultured human melanoma cells (Girouard et al. 2012). Therefore, we also analyzed whether deletion of *Sox2* in melanoma cells affects distant metastasis formation *in vivo*. However, lung and liver metastases were readily detectable in control as well as *Sox2* cKO animals (Figure 4.11 a, b, d, e) and the total count of lung and liver metastases was not significantly altered upon *Sox2* deletion (Figure 4.11. c and f). Further, we stained lung metastases for β-Gal and Sox10 to quantify the recombination frequency of the metastasized melanoma cells. Again, when comparing the recombination frequency in hyperplastic lesions to that in lung metastases (mean 52.3%), we could not find any evidence for a positive or negative selection of *Sox2* cKO cells during formation of distant metastases (Figure 4g and h). Hence, melanocyte-specific *Sox2* ablation does not affect the capacity of melanoma cells to engage in metastasis formation.

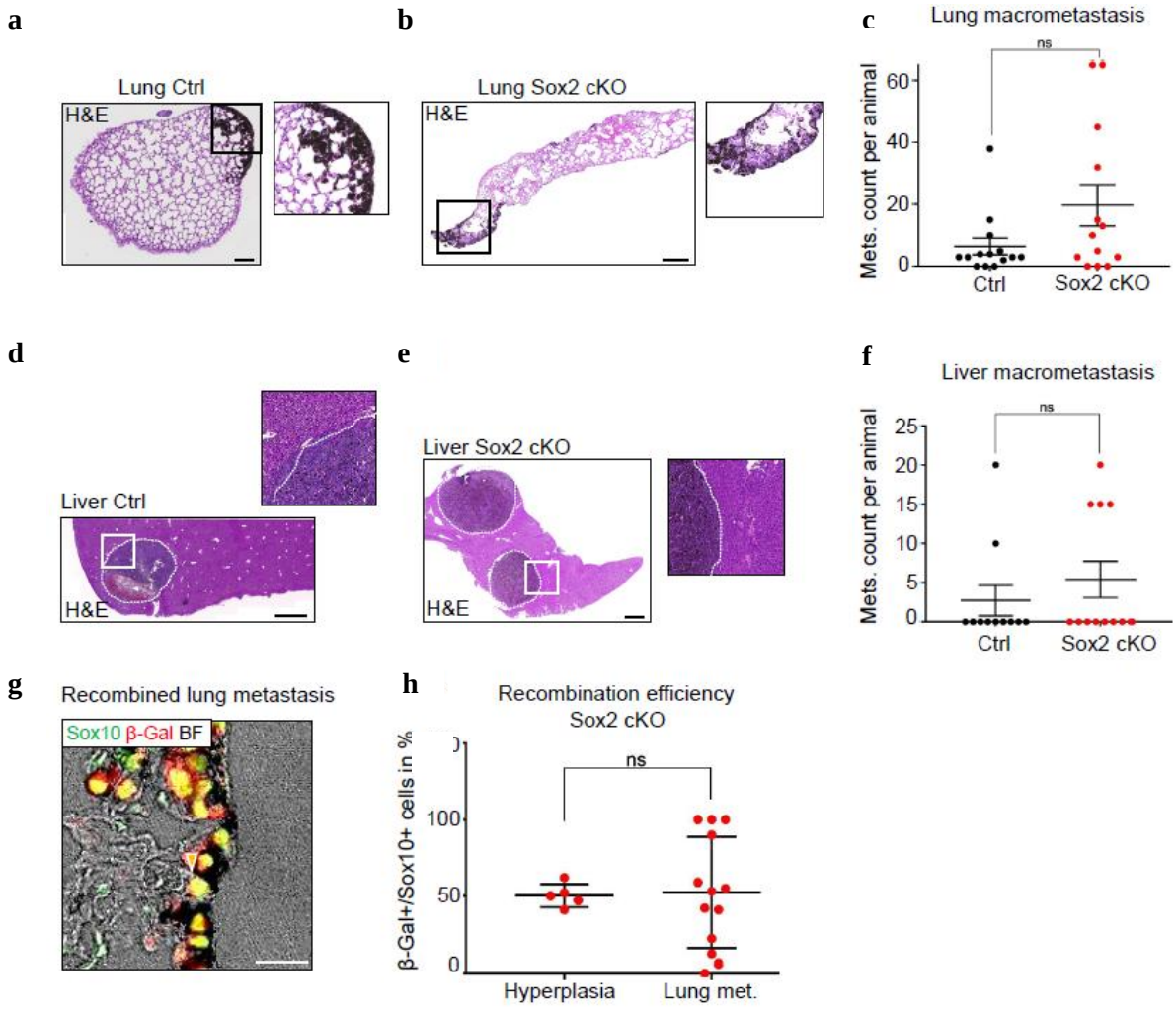

Figure 4.11. Sox2 is dispensable for metastasis formation. (a) H&E staining shows lung tissue from a control animal with a pigmented melanoma metastasis (scale bar=100um). **(b)** H&E staining shows lung tissue from a *Sox2* cKO animal with a pigmented melanoma metastasis (scale bar=200um)**. (c)** Total number of lung metastases (control: n=14, *Sox2* cKO: n=13, p=0.07, unpaired t-test). **(d)** H&E staining shows liver tissue from a *Sox2 cKO* animal with pigmented melanoma metastasis (scale bar=500um). **(e)** H&E staining shows liver tissue from a *Sox2* cKO animal with pigmented melanoma metastasis (scale bar=500um). **(f)** Total number of liver metastases (control: n=11, *Sox2* cKO: n=12, p=0.39, unpaired t-test). **(g)** Representative picture of melanoma lung metastasis immunostained for β-Gal and Sox10 (orange arrowhead: β-Gal/Sox10-double positive cell (scale bar, 20um). **(h)** Comparison of recombination efficiency in hyperplasia and lung metastases. 50.4% of β-Gal/Sox10-double positive cells observed in hyperplasia (n=5, total count 3995 cells) and 52.3% in lung metastases (n=13, total count: 438 cells, p=0.91, unpaired t-test). Data are presented as mean ± s.e.m.

In conclusion, our work suggests that the transcription factor SOX2 is not required for melanoma formation and progression. Although TMA studies have previously confirmed SOX2 expression in a subset of human melanomas (Laga et al. 2010; Laga et al. 2011), our analysis of TCGA data did not reveal any correlation between SOX2 levels and disease outcome. Similarly, despite its increasing expression in a fraction of melanoma cells during disease progression, Sox2 was dispensable for tumorigenesis and metastasis in a genetically engineered melanoma mouse model. The lack of phenotype in our study might be due to other Sox family members, in particular the SOX2-related factor SOX3, compensating for the absence of SOX2 (Miyagi et al. 2008). However, such compensation was not observed and we could not find evidence for SOX3 expression, neither in human *SOX2* KO cells nor in murine tumors (Figure 4.12a, b and c).

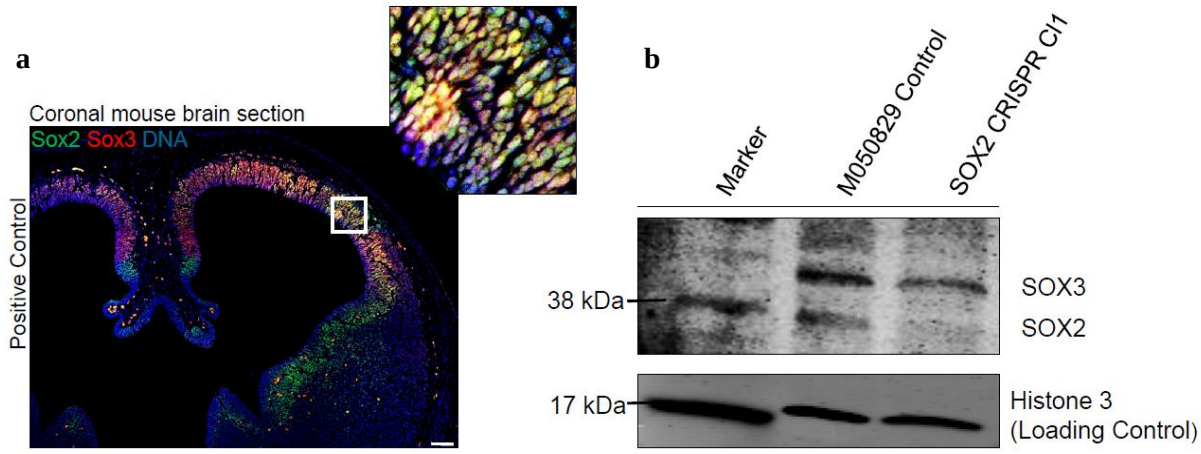

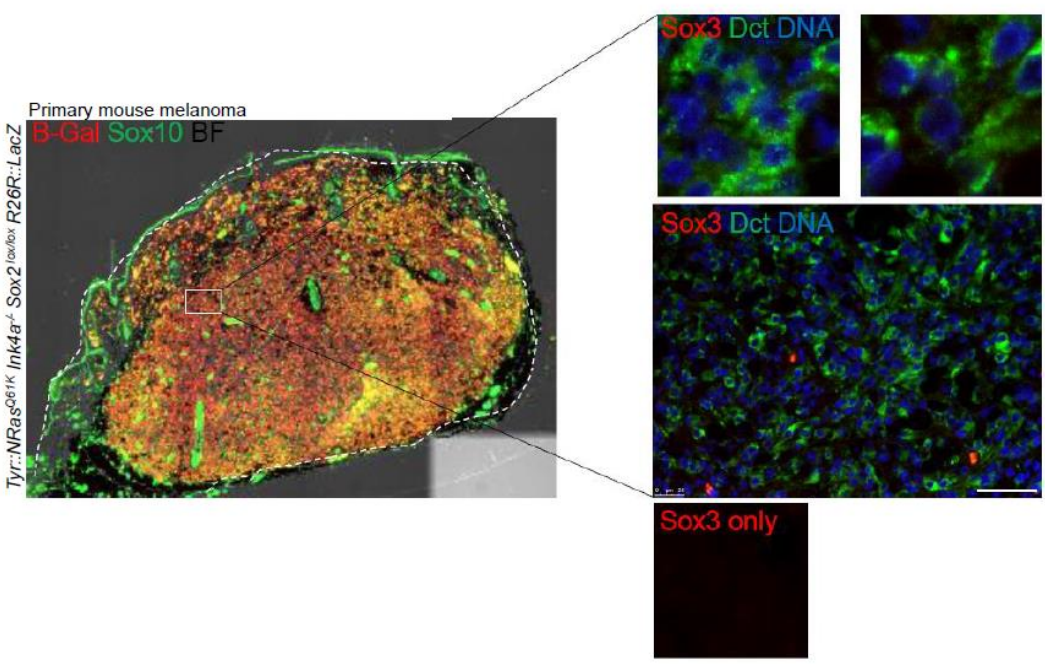

Figure 4.12 SOX3 is not upregulated in SOX2 KO melanoma cells and mice. (a) A coronal mouse brain section from an E12.5 embryo was used as positive control for the tested Sox3 antibody. Sox2/Sox3 double-positive cells were detected in the cortex (scale bar=100um). **(b)** Western blot analysis of the protein lysate from M050829 human melanoma cells (control) and M050829 SOX2 CRISPR cells (SOX2 CRISPR Cl.1). While no SOX2 protein was detected in the SOX2 CRISPR cells (bandsize: 35kDa), the SOX3 band was detected at 42kDa. The SOX3 protein was not upregulated but rather downregulated in the SOX2 KO condition. **(c)** Immunostaining of β-Gal and SOX10 show a highly recombined *Tyr::Cre^{ERT2} Tyr::NRas^{Q61K} Ink4a$^{-/-}$ Sox2$^{lox/lox}$ R26R::LacZ*-driven mouse melanoma (*Sox2 cKO*). The melanoma cells expressed the melanocytic marker Dct but no Sox3 protein was detected (scale bar=50um).

Unlike the transcription factor Sox10, however, Sox2 is not expressed in migratory NCSCs and, at early stages of development, actually suppresses neural crest induction and formation of NCSCs from neural plate cells (Wakamatsu et al. 2004). Thus, the lack of a tumorigenic function of Sox2 described in the present study is consistent with the distinct stem cell program active in NCSCs and, conceivably, during melanoma formation.

4.3 A multicolor lineage tracing approach to address clonality in primary mouse melanomas and metastases

If tumors arise from one (mono) or several (multi) clones remains a fundamental and highly debated question in cancer biology. In general, the idea that tumors have a monoclonal origin remains the dominant thinking in the field (Weinberg 2006). This view is mainly based on studies analyzing cancers derived from female patients which are heterozygous for X chromosome-linked markers like G6PD (see 3.5.2.). Although most of those studies demonstrate monoclonality in a variety of human cancers, multiclonal adenomas have been observed in mice. Hence, we decided to shed more light on this controversial issue. We therefore made use of a TM-based multicolor lineage tracing strategy to stochastically label premalignant melanocytes with four different fluorescent colors (RFP, YFP, GFP, CFP) in the *Tyr::Cre^{ERT2} Tyr::NRas^{Q61K} Ink4a$^{-/-}$ R26R::Confetti* mouse melanoma model (see 3.5.3). Subsequent analysis of the color compositions of mouse tumors allowed us to draw conclusions about the clonality of those melanomas. The goals for this project included:

1) Addressing if primary mouse melanomas originate from one or several clones.

2) A possible characterization of the distinct (different colored) intratumor clones.

3) Addressing if lymph node and distant metastases originate from one or several clones.

The following data has not been published yet and was carried out by following people:

A multicolor lineage tracing approach to address clonality in primary mouse melanomas and metastases

Schaefer, S.M., Baggiolini A., Segalada, C., Sommer L.

My contribution to this work was the following:

- Performed experiments
    - Mouse breedings, Tamoxifen injections, tissue collection
    - Cutting and immunostaings of cryo-embedded tissue sections
- Analyzed data
    - Quantification of colors (tumors and metastases)

4.3.1. The majority of Tyr::NRas^{Q61K} Ink4a$^{-/-}$-driven mouse melanomas are multiclonal

To test the hypothesis if melanoma arise from one or several clones, we bred transgenic mice carrying the *R26R::Confetti* allele to *Tyr::Cre^{ERT2} Tyr::NRas^{Q61K} Ink4a$^{-/-}$* mice to obtain *Tyr::Cre^{ERT2} Tyr::NRas^{Q61K} Ink4a$^{-/-}$ R26R::Confetti* animals (Figure 4.13.a). TM was administered either to one-month-old mice by intraperitoneal (IP) injections and to postnatal one to three day-old animals by intragastric (IG) injections (Figure 4.13.b) (Pitulescu et al. 2010). The additional strategy of early recombination was chosen since the oncogenic *Tyr::NRas^{Q61K}* and *Ink4a$^{-/-}$* transgenes are constitutively active throughout development and adulthood. Hence, induction of recombination at one month could cause missleading results. A multicolored tumor could originate from only one clone because, although unlikely, we labelled two or more dividing and already oncogenic cells derived from the same parental founder clone. According literature (see 3.5.3), we expected the cellular localization of RFP and YFP to be cytoplasmic, a nuclear GFP and a membrane-located CFP.

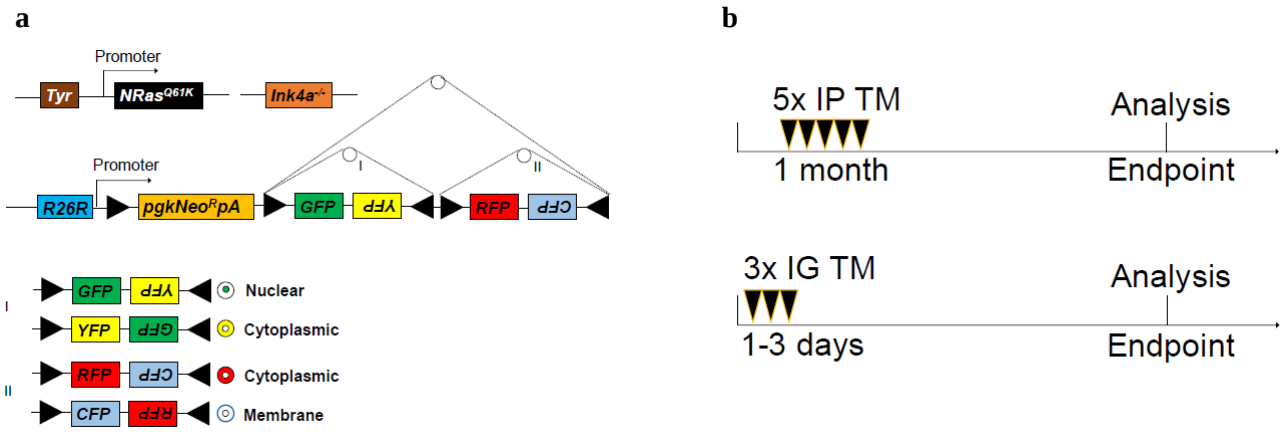

Figure 4.13. Mouse genotypes and experimental strategies to address clonality in mouse melanoma. (a) Transgenic *Tyr::Cre^{ERT2} Tyr::NRas^{Q61K} Ink4a$^{-/-}$ R26R::Confetti* mice were used to address clonality in melanoma. Upon TM-based removal of the floxed pgkNeo^{R}pA roadblock, one of the four fluorescent colors is expressed (cellular location: RFP and YFP=cytoplasmic, GFP=nuclear, CFP=membrane). **(b)** TM was applied to one-month-old animals (IP injection, 5 consecutive days) or to one to three day-old animals (IG injection, 3 consecutive days).

Since we used animals heterozygous and homozygous for the *R26R::Confetti* allele, not only four but ten different color combinations were possible, dependent on the given genotype (Figure 4.14.). Additionally, we counted uncolored (unrecombined) Dct-positive melanoma cells as an extra clone(s).

Astonishingly, we observed polyclonality in the vast majority (80%) of all analyzed primary mouse melanomas (n=14, 1 month injection; n=1, early injection). No evidence for mulitclonality was

observed in 3/15 (20%) tumors. (Figure 4.15.) Nevertheless, those unicolored tumors could potentially also be derived from two or more clones, namely if multiple same-colored clones formed one melanoma.

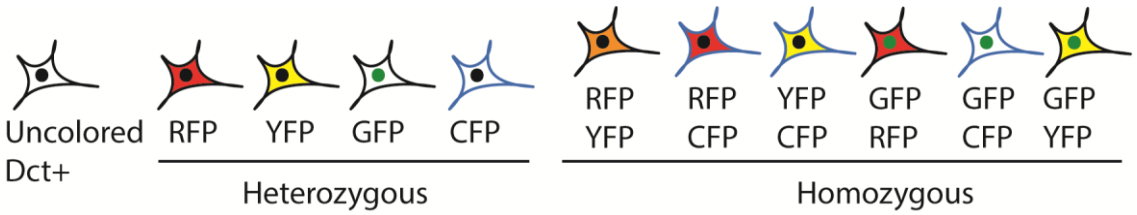

Figure 4.14 Scheme of different color combinations. Since the TM-based recombination efficiency never reaches 100%, some premalignant melanoma cells (Dct+) stay uncolored/untraced. Four different color combinations are possible for mice heterozygous for the *R26R::Confetti* allele. Ten different color combinations are possible for mice homozygous for the *R26R::Confetti* allele. Drawn by Simon Schäfer, adapted from (Baggiolini et al. 2015).

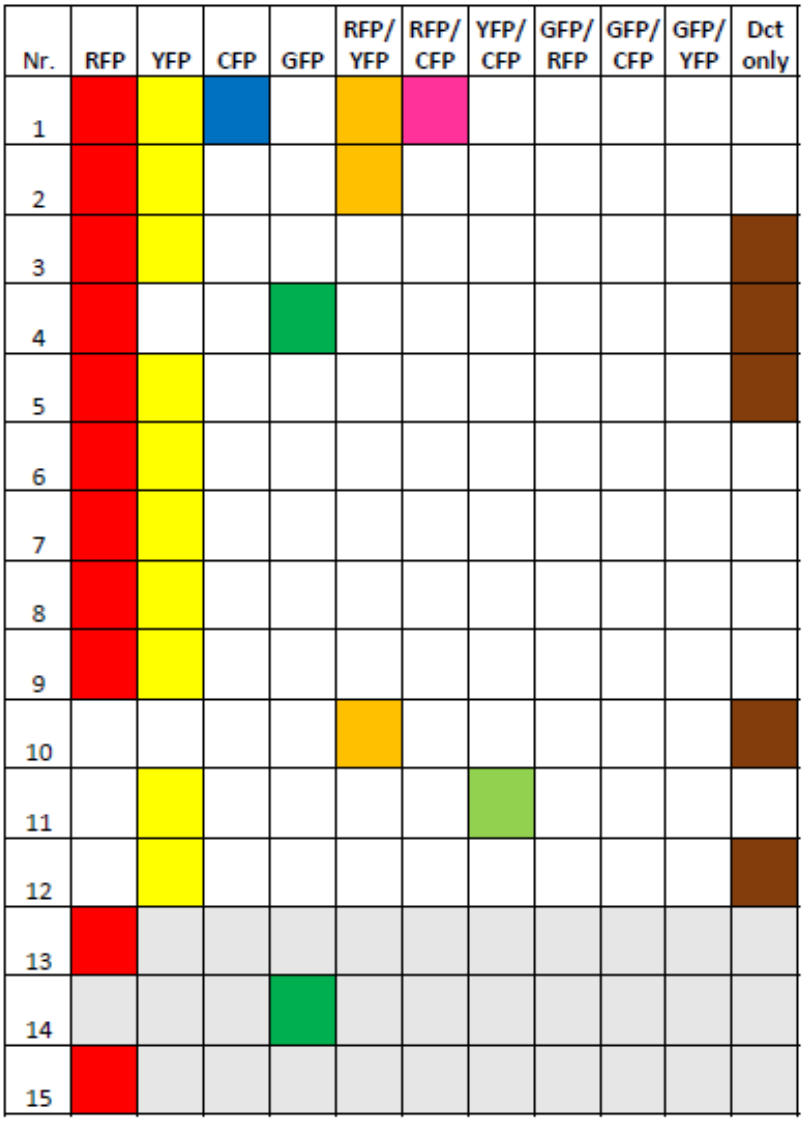

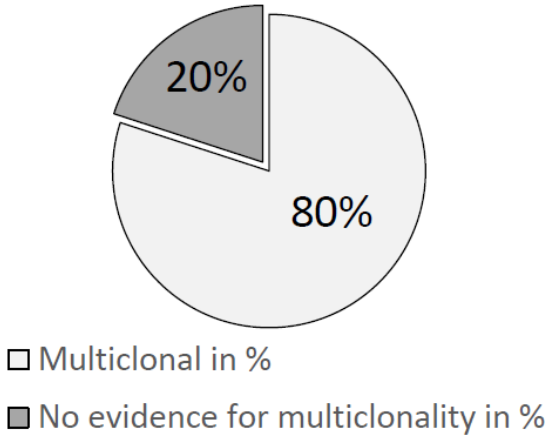

Figure 4.15. The majority of primary mouse melanomas are multiclonal. Multiclonality was observed in 12/15 (80%) of all analyzed mouse melanomas (tumors 1-12). No evidence for multiclonality was observed in 3/15 (20%) of the melanomas (tumors 13-15). Recombination was induced at postnatal day 1-3 for tumor Nr.12. For all other mice, recombination was induced at one month of age.

4.3.2. Examples of mulitclonal tumors

a

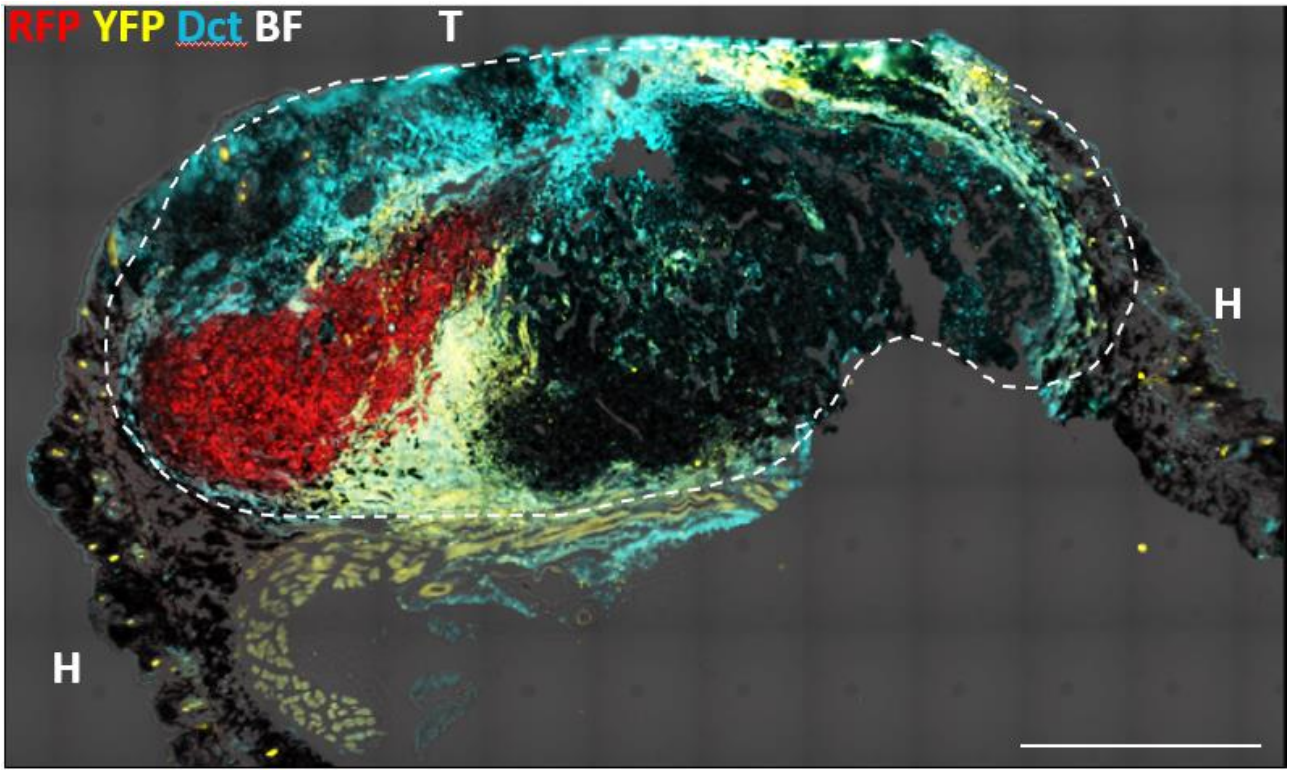

b

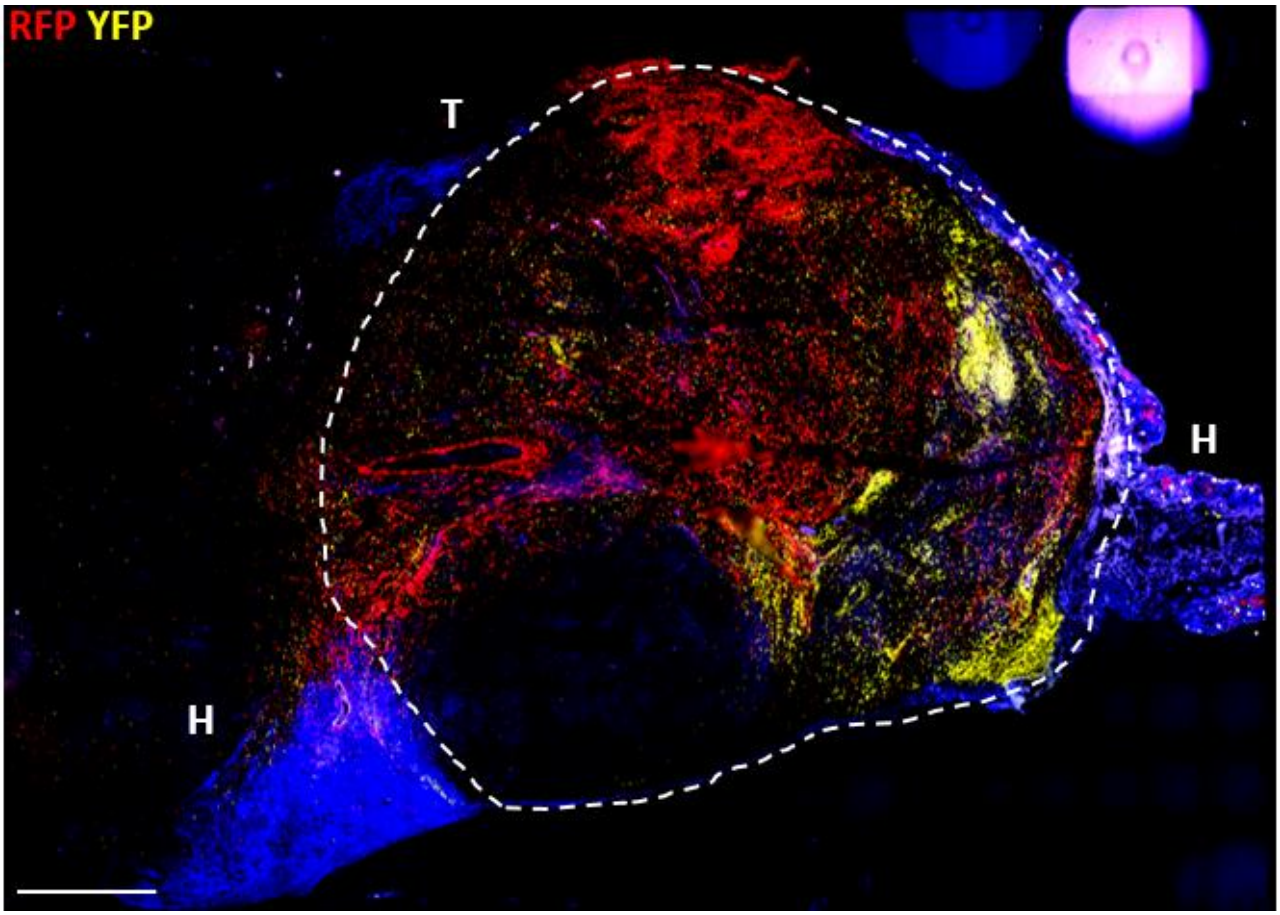

c

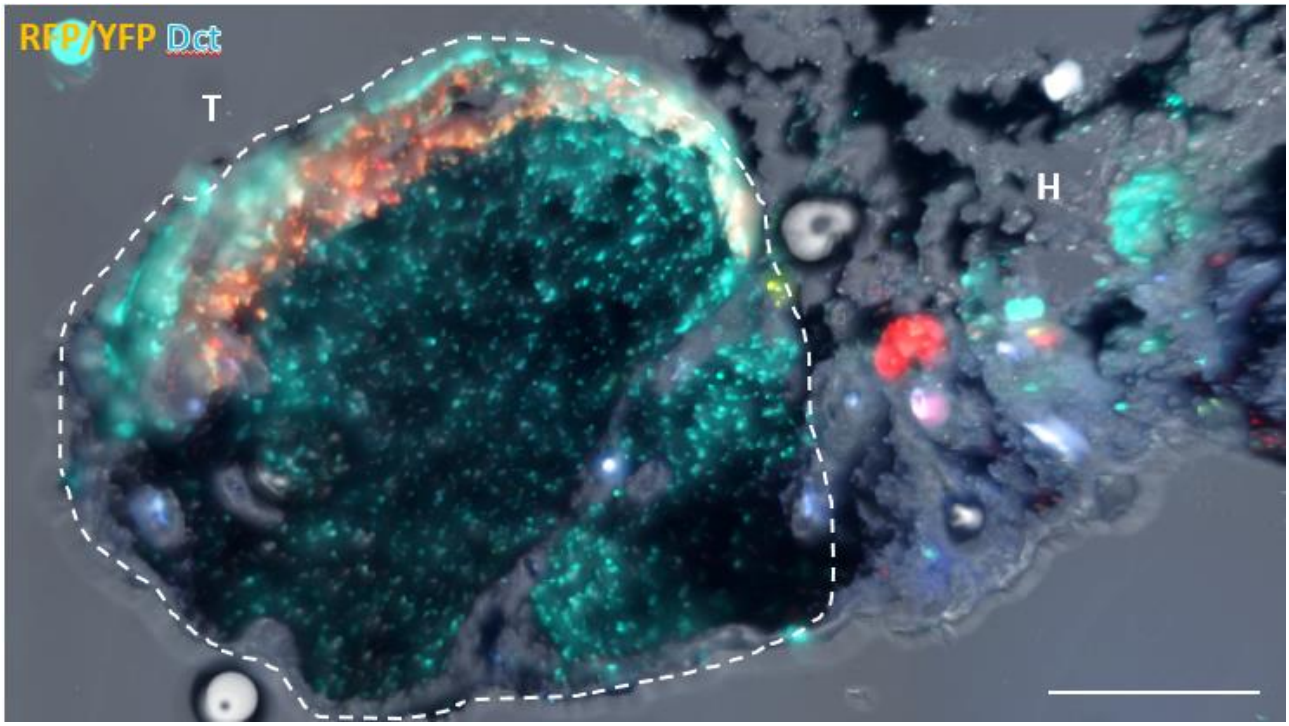

d

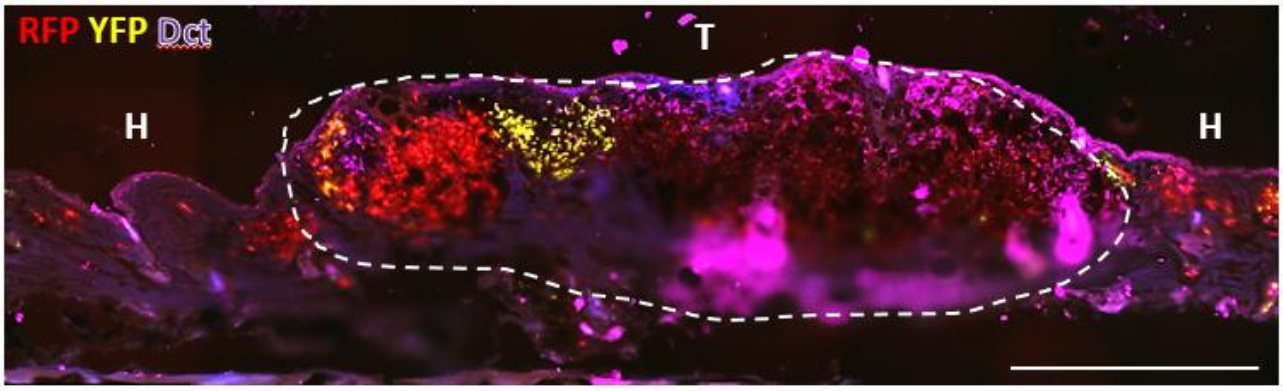

e

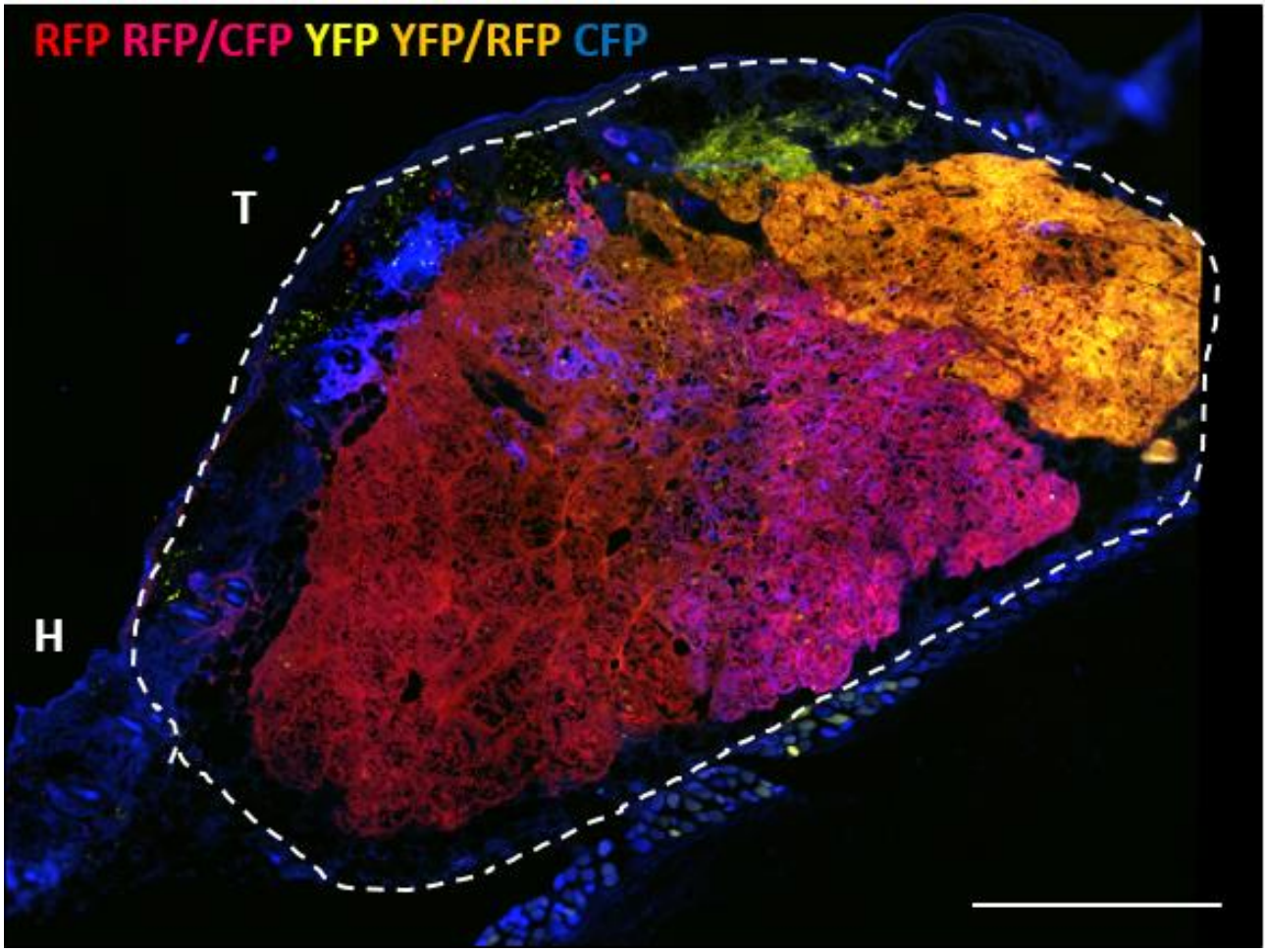

f

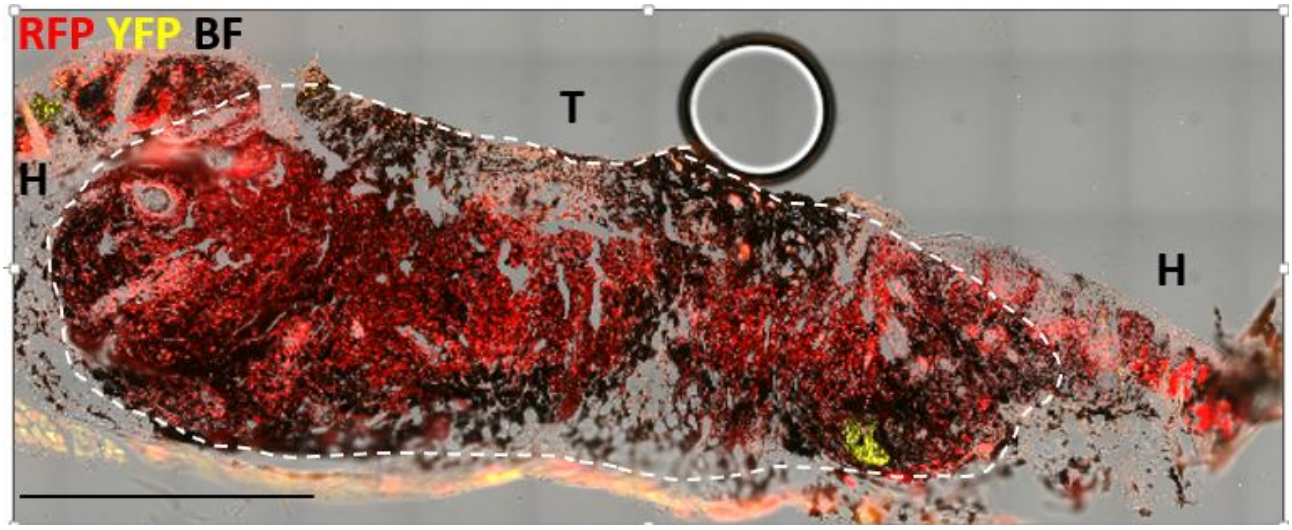

g

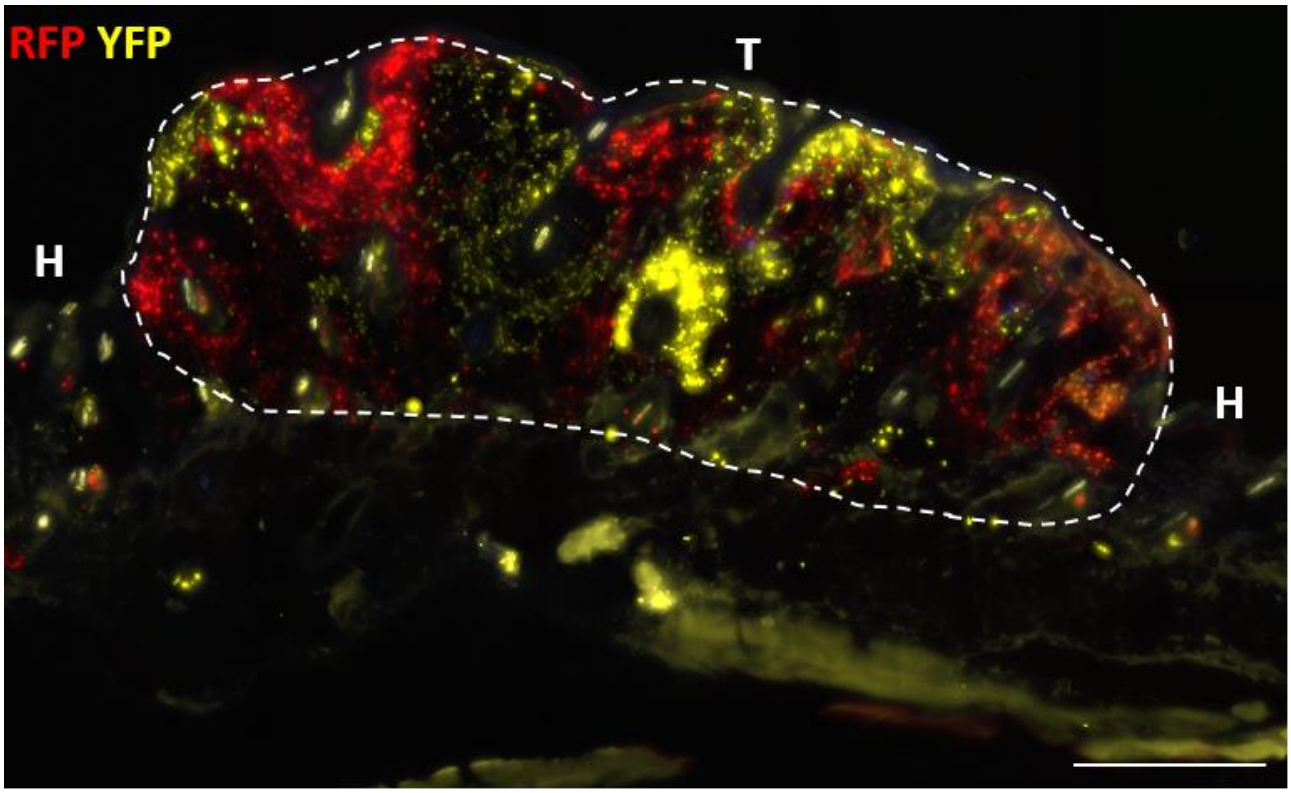

Figure 4.16. Examples of multiclonal melanomas. (a-g): For all presented tumors, recombination was induced when the mice were 1 month of age old. T=tumor, H=hyperplasia, BF=Brightfield. Scale bars: **(a,b,f)**=1000um; **(d,e)**=500um; **(c,g)**=300um.

4.3.3. Examples of tumors without evidence for multiclonality

a

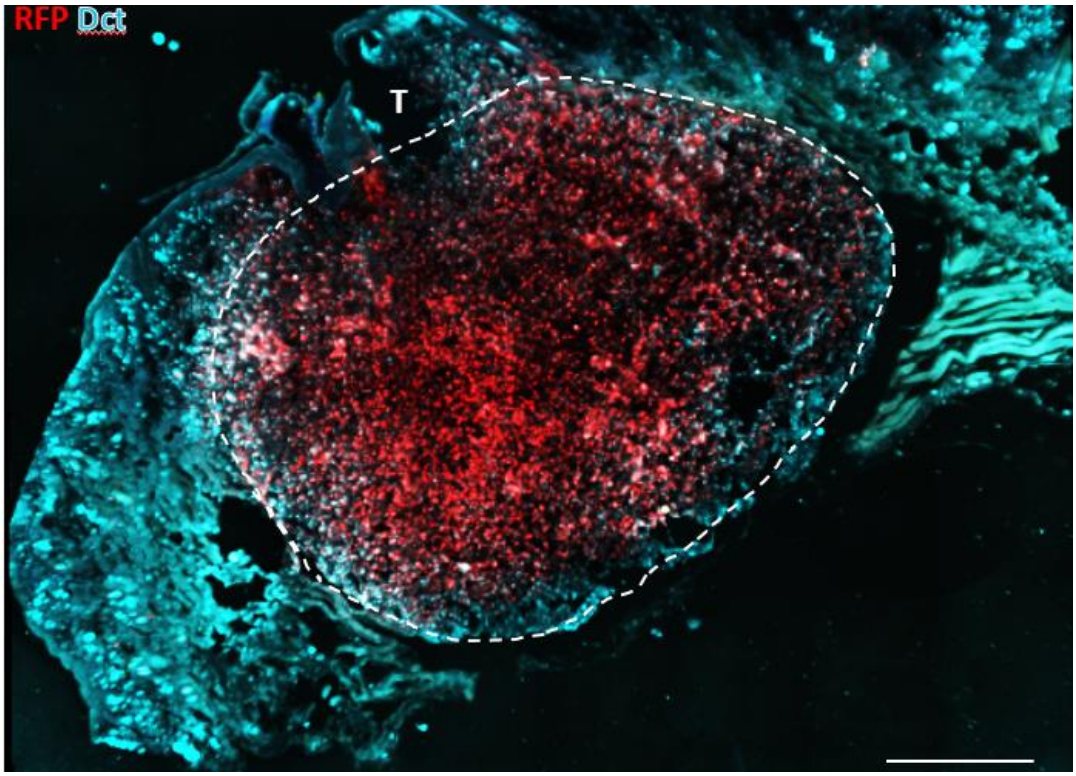

b

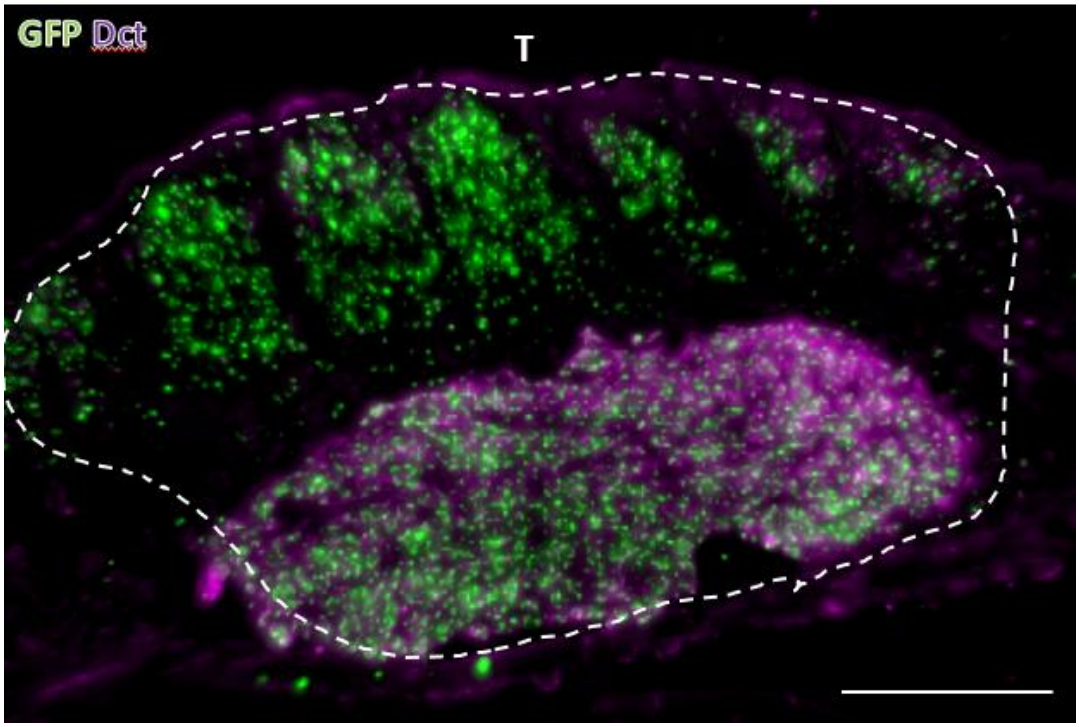

Figure 4.17. Examples of tumors without evidence for mulitclonality. (a-b) For both tumors, recombination was induced at 1 month of age. T=tumor. Scale bars **(a,b)**=500um.

4.3.4. Intratumor clones can be separated and re-initiate tumors upon injection into immunocompromized mice

The observed results raise the question if all intratumor colored clones are indeed tumorigenic. Possibly, some fluorescent cells could originate from the hyperplastic skin and be therefore non-tumorigenic. To address this question, we separated the different colored intratumor clones from the melanoma using FACS. One part of the tumor was taken for histological analysis while a single cell suspension was prepared of the second part. Consistently, we observed the same fluorescent colors using the FACS as we detected on the histological frozen sections. 24% of all recorded events were uncolored living single cells, 0.4% YFP-positive and 0.5% RFP-positive (500000 recorded events). After sorting, the RFP-positive clone, YFP-positive clone, uncolored clone and a 1:1:1 mix of each were subcutaneously injected into immunocompromized nude mice (Foxn1$^{nu/nu}$ female) (Figure 4.19.). All single-colored clones and the mix grew and expanded in the host mice, confirming the tumorigenicity of the distinct intratumor clones (Figure 4.20.). As a control, we isolated either Confetti or tdTomato-traced hyperplasia cells from 4 month old *Tyr::Cre^{ERT2} Tyr::NRas^{Q61K} Ink4a$^{-/-}$* mice. The injected premalignant melanoma cells did not grow upon injection for at least one year, enabling discrimination of tumorigenic from non-tumorigenic cells (Figure 4.18.).

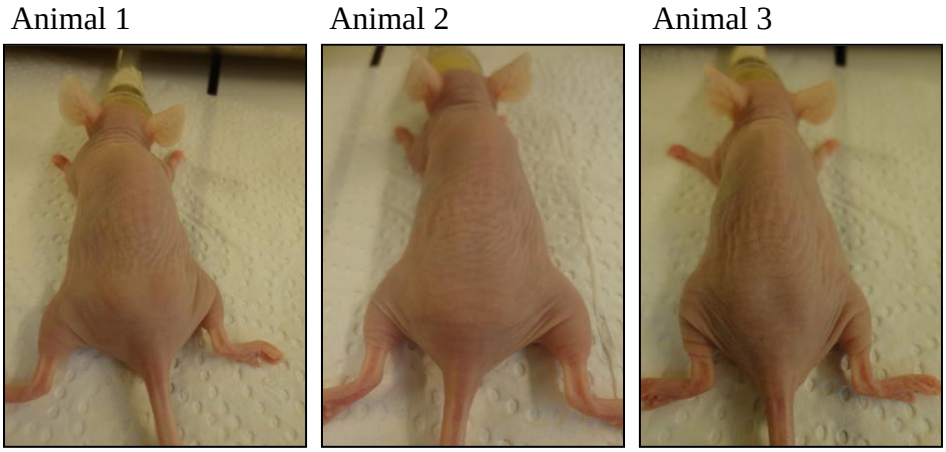

Figure 4.18. Hyperplasia cells do not form tumors upon injection into Foxn1$^{nu/nu}$ mice. Backskin of one-and-a-half-year-old Foxn1$^{nu/nu}$ mice injected with tdTomato-traced melanocytic hyperplasia cells, which were isolated from 4 month old *Tyr::Cre^{ERT2} Tyr::NRas^{Q61K} Ink4a$^{-/-}$* mice. No tumor formation was observed on a macroscopic level. The cells were injected into two-month-old Foxn1$^{nu/nu}$ mice.

Interestingly, the YFP-positive clone and the mix grew faster than the RFP-positive and the uncolored clone although the percentage of RFP-positive and YFP-positive cells was similar in the parental tumor (Figure 4.20.). Next, we sectioned the different xenograft tumors to confirm that their specific fluorescent color was preserved. As expected, we observed the same colors in the

sectioned xenografts as originally sorted and injected. Although we used mice carrying the melanocyte-specific *Tyr::Cre*^{ERT2} driver, we isolated the RNA of cells originating from the different xenografts to confirm their melanocytic origin. All the clones expressed the melanocytic markers *Mitf* and *Sox10*, verifying the melanocytic nature of the cancer cells. Interestingly, the YFP-positive clone showed lower expression of the melanocyte differentiation markers *Silv, Oca2, Dct, Tyrp1* (Figure 4.21). Those results highlight that *Tyr::NRas*^{Q61K} *Ink4a*$^{-/-}$-driven mouse melanomas are highly heterogeneous, which might increase the "oncogenic fitness" of the cancer. To test this hypothesis, further functional assays need to be carried out to clarify the biological relevance of the observed intratumor heterogeneity.

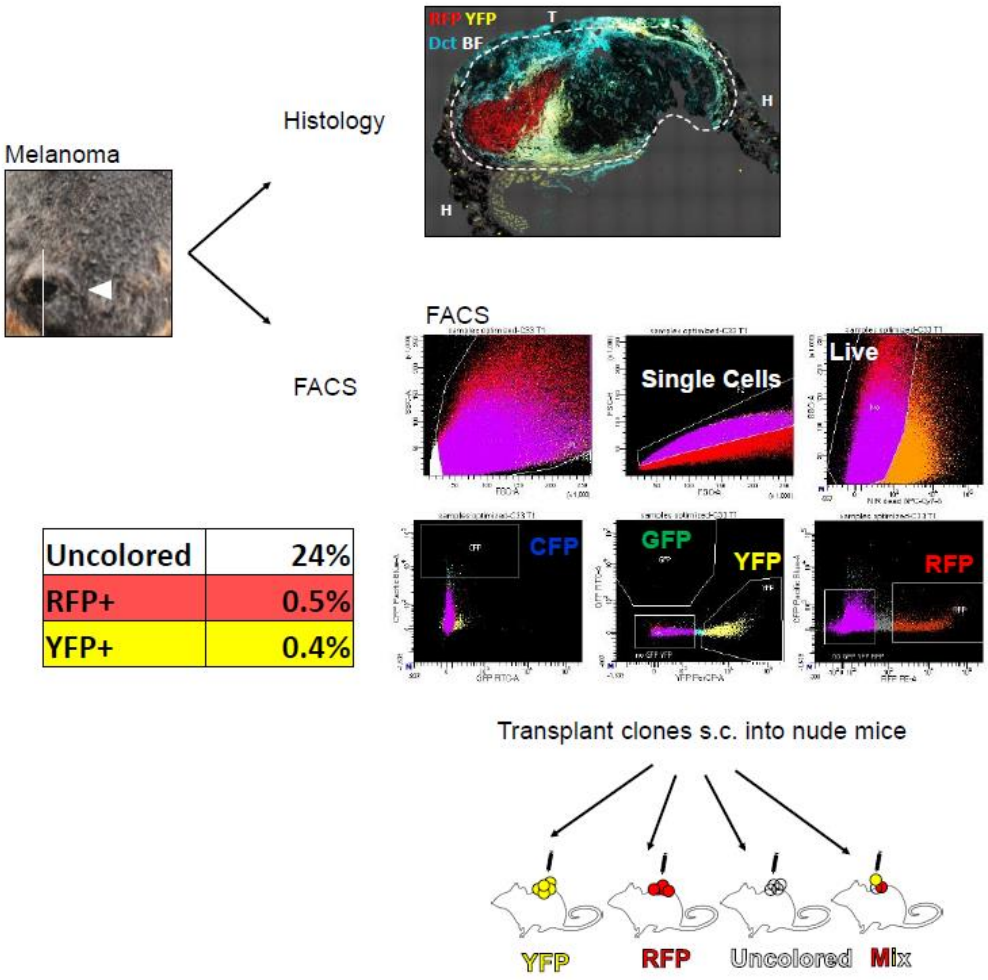

Figure 4.19. Intratumor clones can be isolated using FACS. A *Tyr::NRas*^{Q61K} *Ink4a*$^{-/-}$-driven mouse melanoma (n=1) was separated into two parts which were used for histological analysis and FACS. Out of 500000 recorded events, 24% were uncolored living single cells, 0.5% were RFP-positive and 0.4% YFP-positive. 45000 cells of each single-colored clone were subcutaneously injected into Foxn1$^{nu/nu}$ female mice. 15000 cells of each clone were combined for the mix (total 45000 cells).

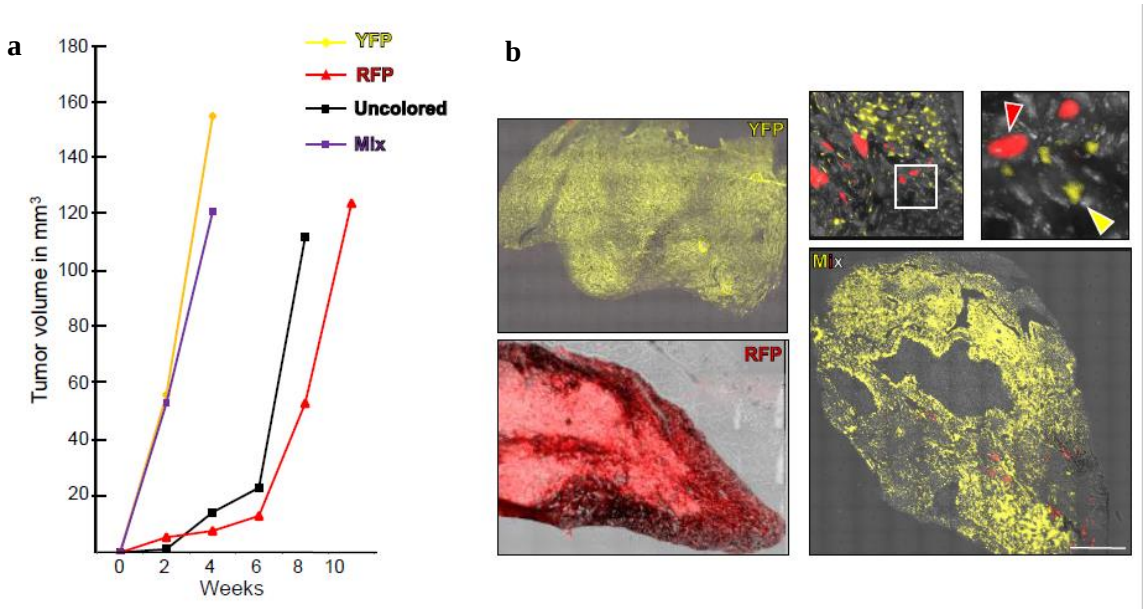

Figure 4.20. All color-sorted intratumor clones grew in nude recipient mice. (a) Growth curve of injected clones. **(b)** Color analysis of transplanted tumor clones/mix on cryo-embedded tissue. In the mixed xenograft, the red arrowhead points to an RFP-positive cell and the yellow arrowhead to a YFP-positive cell.

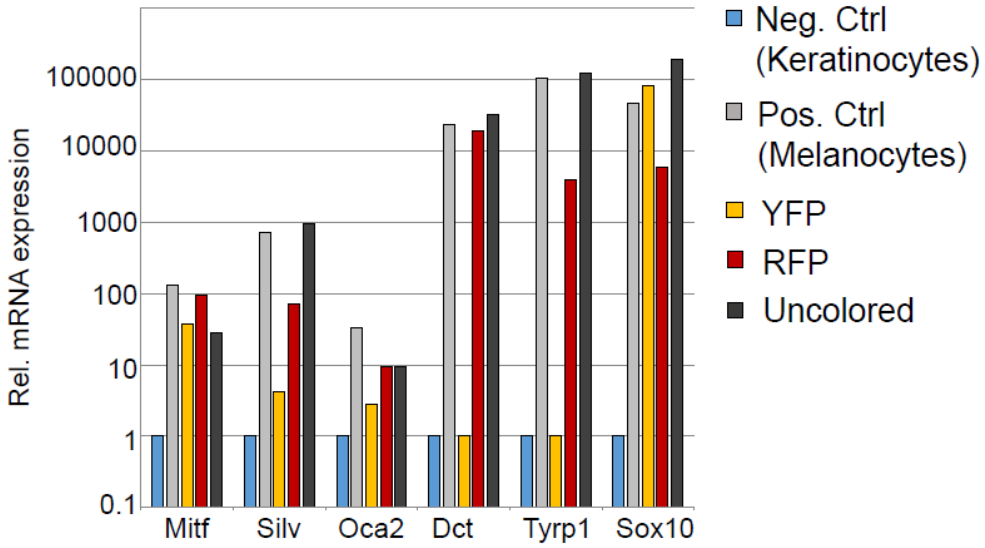

Figure 4.21. The transplanted intratumor clones are melanocytic/melanoma cells. RNA was isolated from cells (passage 2) derived from the different xenografts. RNA from mouse epithelial keratinocytes (XB2) was used as a negative control and RNA from melan-a melanocytes was used as a positive control. RT-qPCR for the melanocytic lineage genes *Mitf*, *Silv*, *Oca2*, *Dct*, *Tyrp1* and *Sox10*.

4.3.5. Multiple clones are able to infiltrate lymph nodes

To test if one or several clones are able to infiltrate lymph nodes, we analyzed the lymphatic organs of recombined *Tyr::Cre^{ERT2} Tyr::NRas^{Q61K} Ink4a$^{-/-}$ R26R::Confetti* mice. Multiple colors within a given lymph node would indicate that several clones, likely with different underlying (epi)-genetics, infiltrated the organ. On the other hand, unicolored lymph nodes would demonstrate that only one particular clone is capable of penetrating the lymphatic organs. One might speculate that this infiltrating "superclone" would harbor additional genetic mutations, epigenetic alterations or special microenvironmental conditions enabling the clone to escape the skin. Hence, we analyzed eight different lymph nodes from four animals, exclusively using the early recombination strategy described in Figure 4.13. Interestingly, we observed multiple colors in all analyzed lymph nodes (lymph nodes n=8; animals n=4), indicating polyclonal invasion (Figure 4.22, Figure 4.23.). Nevertheless, further experimental tests would need to be carried out to analyze if the different clones also harbor different genetic mutations. Additionally, we cannot speak with certainty about polyclonal metastasis formation but rather about polyclonal invasion. Staining for the proliferation marker Ki67 and re-transplantation assays of isolated colored cells would shed more light into those issues.

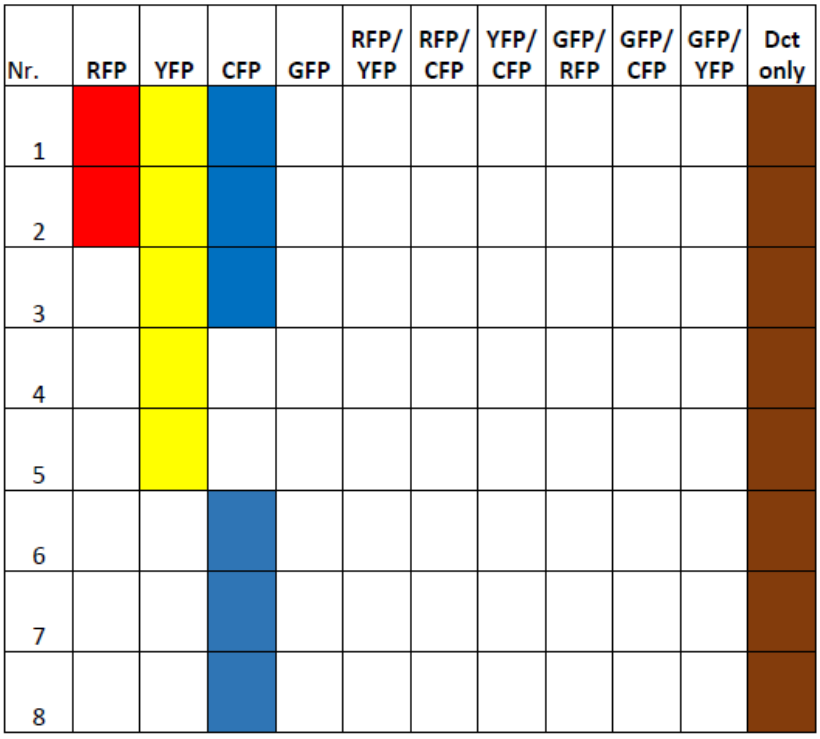

Figure 4.22. Multiple clones can infiltrate lymph nodes. Multiclonal lymph node infiltration was observed in 8/8 (100%) analyzed lymph nodes. Recombination was induced in one to three day old mice.

4.3.6. Examples of multiclonal lymph node infiltration

a

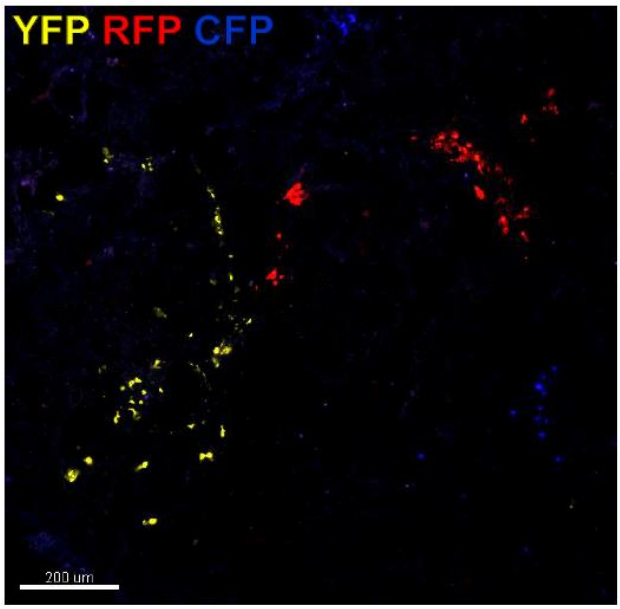

b

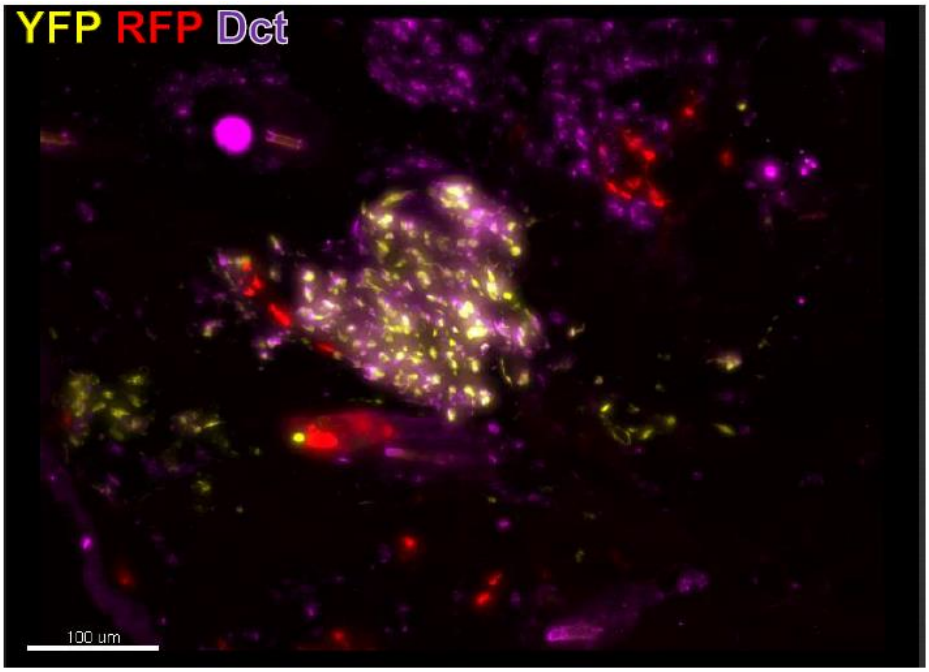

Figure 4.23. Examples of melanoma lymph node infiltration. Both animals were recombined at postnatal day one to three (early recombination). Scale bars **(a)**=100um; **(b)**=200um.

4.3.7. Evidence and examples for multiclonal distant metastases

Next, we analyzed the color distributions in distant metastases. Since the formation of distant metastases displays a rather infrequent event in the *Tyr::NRas*^{Q61K} *Ink4a*$^{-/-}$ mice with the given genetic background, the number of studied metastases was rather small (n=3). Nevertheless, first

evidence also shows multiclonal infiltration into distant organs. The strongest evidence supporting these results came from analyzed lung metastases. We observed Dct-positive/RFP-positive melanoma cells besides Dct-positive and uncolored cells within the very same lung lesions, strongly speaking for a multiclonal infiltration (Figure 4.24.). Interestingly, we also observed RFP-positive/Dct-negative cells within the lung metastasis. Given that all cells within the same metastasis derived from the same clone, some cells downregulated the melanocyte differentiation gene Dct, promoting phenotypic plasticity. As a second example, we observed uncolored, Dct-positive cells besides YFP-positive/Dct-positive cells, confirming polyclonal invasion.

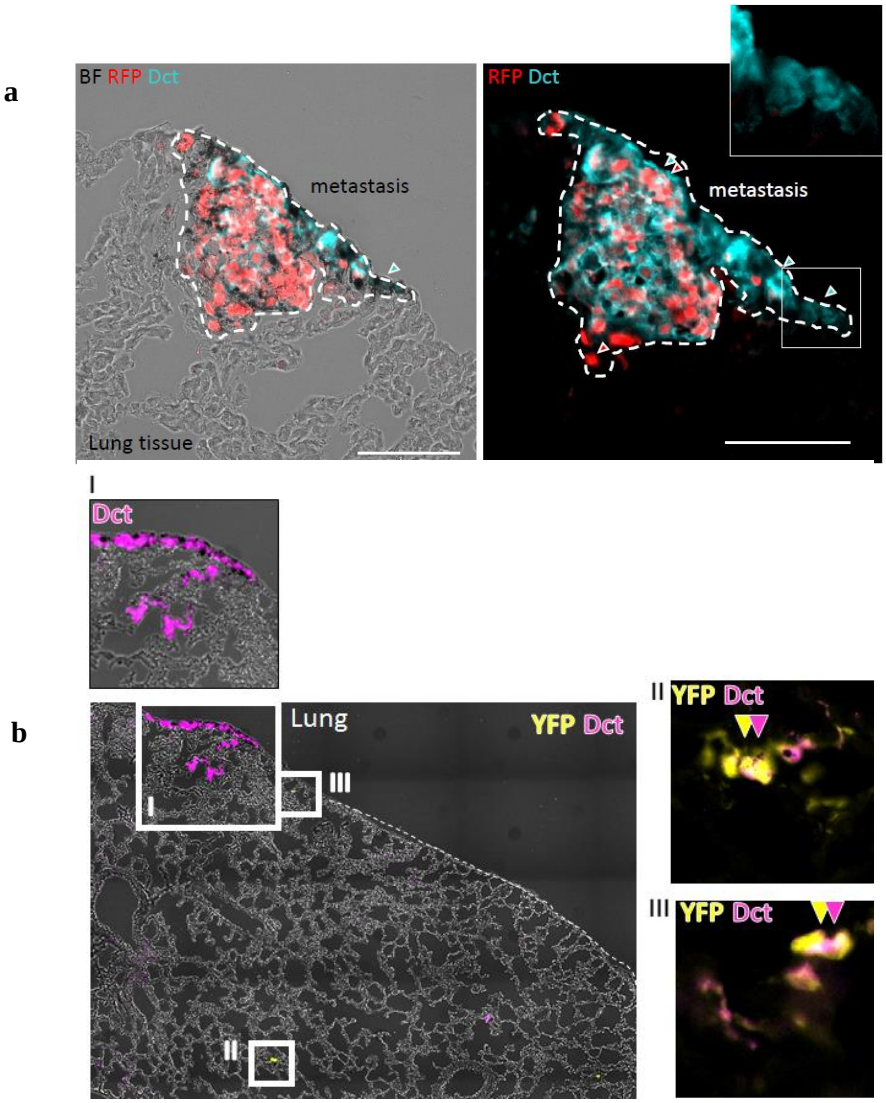

Figure 4.24. Examples of multiclonal lung infiltration. (a) Example of a pigmented distant lung metastasis with Dct-positive/RFP-positive (red/cyan double arrowhead) and Dct-positive uncolored (cyan. arrowhead only) melanoma cells. Red arrowhead points towards a RFP-positive and Dct-negative cell. Recombination was induced in one-month-old animals. BF=Brightfield. Scale bars=80um**. (b)** Example of pigmented distant lung metastasis with Dct-positive/YFP-positive (yellow/violet double arrowhead) and Dct-positive melanoma cells (violet). Recombination was induced in one-to-three day old animals.

5. Discussion

5.1. Sox2 is dispensable for primary melanoma and metastasis formation

Using different KO approaches, we observed that Sox2 was not required for melanoma formation and progression in human melanoma cell cultures and in a genetically modified mouse model. In the following chapter, I speculate about possible explanations for the lack of phenotype. Further, I aim to clarify why our data might be contradictory to already published work.

5.1.1. Hypotheses explaining the lack of phenotype

5.1.1.1. Reactivation of developmental gene programs during tumor formation

Often, striking similarities are found between tumorigenesis and basic developmental processes, especially in terms of migration and invasion, gene expression and protein profiles, signaling pathways, cell differentiation and mechanisms of immune escape (Vogelstein & Kinzler 2004; Xie & Abbruzzese 2003; Wilczynski 2006; Ma et al. 2009; Ma et al. 2010; Wang 2009). Sox10, which is expressed throughout eNCSC development has a potent oncogenic role in melanoma formation and serves as prime example linking developmental and tumorigenic processes (Shakhova 2014; Shakhova et al. 2012). Further, it has been shown that the NCSC marker CD271 ($P75^{NTR}$) is upregulated in melanoma patients and expressed in a highly tumorigenic melanoma stem cell population (Boiko et al. 2010; Civenni, et al. 2011). The epigenetic modifier EZH2 is required for NCSC-derived cartilage and bone formation and controls melanoma growth and metastasis through silencing of distinct tumors suppressors (Zingg et al 2015; Schwarz et al. 2014). Further unpublished work from the Sommer lab links additional transcription factors which are highly expressed in multipotent NCSC to melanoma development and progression (Varum et al, unpublished).

Sox2 is highly expressed in the inner cell mass of the embryo and crucial for the maintenance of a multipotent cell state (see 3.2.1) (Avilion et al. 2003). An interesting study by Cimadamore demonstrated that Sox2 expression is downregulated in migratory NCSC but re-expressed in neurogenic dorsal root ganglion (DRG)-like clusters (Cimadamore et al. 2011). Consistent with those results, another paper showed that forced Sox2 expression blocks EMT and inhibits NCSC delamination (Wakamatsu et al. 2004). Further, downregulation of Sox2 in Schwann cell precursors (SCP) permits the differentiation of SCP and NCSC into the melanocytic lineage (Adameyko et al. 2012).

Assuming that tumor formation depends on the reactivation of developmental gene networks and Sox2 is downregulated in delaminating NCSC and not required for the formation of the melanocytic lineage, it could partly explain why Sox2 was not required for melanoma formation and progression *in vivo*.

5.1.1.2. Sox2 expression in melanocytes and melanoma

We did not detect Sox2 expression in differentiated Sox10-positive melanocytes located in mouse hair follicle bulbs, which is consistent with already published data (Schaefer et al. 2017; R. R. Driskell et al. 2009). Further, normal human epidermal melanocytes showed absent Sox2 levels measured by RT-q PCR (Santini et al. 2014). In agreement, co-Immunostaining of SOX2 and SOX10 in human skin revealed and exclusive expression pattern (Laga et al. 2010). Using patient-based RNA-seq data from TCGA, Sox2 expression is rather low or even absent in many melanoma patients (Figure 4.1.d). Those results are consistent with Sox2 expression in human melanoma cells analyzed by RT-q PCR (Santini et al. 2014). In our study, Sox2 was expressed in a very small subset of Sox10-positive mouse melanoma cells (Schaefer et al. 2017). In summary, Sox2 is not expressed in the melanocytic lineage but upregulated in a subset of human and mouse melanomas. Nevertheless, I would like to highlight that the vast majority of all human melanoma patients showed either absent or very low Sox2 expression.

In sharp contrast, other tumors highly expressing Sox2 (Figure 4.1.a) depend more on the transcription factor. For example, studies have shown that high Sox2 expression is strongly associated with tumor aggressiveness in glioblastoma (Garros-Regulez et al. 2016; Ben-Porath et al. 2008). Further, shRNA-mediated *Sox2* silencing impaired proliferation and tumor initiation potential of glioblastoma stem cells (Ikushima et al. 2009; Gangemi et al. 2009). Lung squamous cell carcinomas (LSCC) displays another example of a tumor highly expressing Sox2. An interesting study by Ferone and colleagues showed that Sox2 expression, in combination with *Cdkn2ab* and *Pten* loss in mouse tracheobronchial basal cells, resulted in LSCC formation (Ferone et al. 2016). Hence, we speculate that the lack of phenotype could be explained by the low expression pattern in most mouse and human melanomas. Additionally, Sox2 is not expressed in the melanocytic lineage and not required for the survival of the lineage.

5.1.1.3 Xenografts vs genetically engineered mouse models (GEMM)

Although we performed *SOX2* KO in human melanoma cells with subsequent transplantations, the main findings and conclusions of our study are based on the *Tyr::NRas*^{Q61K} *Ink4a*$^{-/-}$ mouse model. GEMM are usually fully immunocompetent allowing the study of cancer development in a

relatively realistic context (Jung 2014). Further, the melanomas develop in an intact stroma, allowing investigations of the cancer cells in their microenvironment (Jung 2014). In contrast, cancer cells are subcutaneously injected into immunodeficient mice in the xenograft model. It was shown that mice deficient for various components of the immune system displayed increased tumor formation compared to their immunocompetent counterparts in a carcinogen-induced tumor model (Hanahan & Weinberg 2011). Hence, cancer immune surveillance displays a crucial protection mechanism inhibiting tumorigenesis (Kim et al. 2007). Assuming that a given gene plays an essential role during immune escape, an immunodeficient xenograft model might not be the optimal model system. Moreover, it was shown that the immune system is able to target Sox2, possibly explaining the lack of phenotype in the mentioned studies using the xenograft models (Dhodapkar et al. 2013).

5.1.2. Discrepancies between our data and published work – Possible explanations

While CRISPR-Cas9-mediated *SOX2* KO did not lead to reduced growth upon xenotransplantation in our study, other groups obtained different results using similar models. Further, we did not observe changes in metastasis formation comparing control and *Sox2* cKO mice while other groups linked high Sox2 expression to invasion. In the following chapter, I discuss differences which might explain some observed discrepancies.

5.1.2.1. Different gene silencing methods - off target effects using shRNA

Literature shows that Sox2 is crucial for melanoma initiation, promotes tumor growth and enhances invasiveness (Laga et al. 2010; Girouard et al. 2012; Santini et al. 2014) (see 4.4.9.). In those studies, *Sox2* silencing was achieved by transfecting (infecting) human melanoma cells with DNA-based transcriptional templates expressing a shRNA (Gu et al. 2012). The shRNA, which is processed into siRNA, leads to stable and long term gene silencing (McCaffrey et al. 2002; Brummelkamp 2002; Gu et al. 2012). In the year 2003, Jackson and colleagues performed gene expression profiling to characterize the specificity of siRNA-mediated gene silencing (Jackson et al. 2003). The authors found direct silencing of non-targeted genes containing as few as eleven contiguous nucleotides of identity (Jackson et al. 2003). Another paper showed that commonly used shRNA constructs can induce an interferon response, which leads to activation or silencing of off-targets (Bridge et al. 2003). Sox1, Sox2 and Sox3 belong to the SoxB1 gene family and show 80% sequence similarity (Zhang 2014). It has been shown that the genes of the SoxB1 gene family are able to compensate for the loss of another family members (Miyagi et al. 2008; Kan et al. 2007; Graham et al. 2003; Ekonomou et al. 2005; Archer et al. 2011). Hence, we speculate that a *SOX2*-

specific shRNA constructs might have off-gene effects, maybe additionally targeting other members of the Sox gene family and therefore preventing possible compensations. Although we did not detect an upregulation of Sox3 in a highly recombined *Sox2* cKO tumor, possible compensatory mechanisms with other members of the Sox gene family are thoroughly conceivable. In our study, we made use of the CRISPR-Cas9 genome editing strategy. To minimize potential off-target effects, we determined the sequence of the single guide (sg) RNA with the online tool crispr.mit.edu, which predicts the faithfulness of on-target activity computed as 100%. According the tool, all computed values above 50% should be considered targeting sequences. The guide sequence we chose targeting Sox2 reached a score of 87. Nevertheless, it has been shown that the CRISPR-Cas9 technology is also not freed from off-target effects (Fu et al. 2013; Hsu et al. 2013; Pattanayak et al. 2013). Nonetheless, the different gene silencing methods used in our study and in other studies might explain some of the observed discrepancies.

5.1.2.2. Different mutation status of patient-derived melanoma cells

In one study, shRNA-mediated *SOX2* silencing in A2058 melanoma cells caused reduced tumor growth upon xenotransplantation (Laga et al. 2010). These melanoma cells carry the $BRAF^{V600E}$ mutation and show loss of the tumor suppressor *PTEN*. Growth suppression was also observed in the study by Santini and colleagues, which used the patient-derived cell cultures SSM2c and M26c (Santini et al. 2014). Unfortunately, the authors did not provide information about possible mutations occurring in those cells. In sharp contrast, the patient-derived and many times passaged human melanoma cells we used for our *SOX2* KO study (M050829) harbor a $NRAS^{Q61L}$ mutation. It has been shown that *NRAS*-mutated melanomas tend to be thicker and present with higher rates of mitosis compared to $BRAF^{V600E}$-mutated melanomas (Devitt et al. 2011). Hence, although both oncogenic mutations enhance Ras/Raf/MAPK signaling, mutations in different proteins might change how the cells react on *SOX2* loss.

5.1.2.3. Different models used to address invasion and metastasis formation – In vitro invasion vs GEMM

Girouard and colleagues demonstrated that SOX2 contributes to melanoma cell invasion (Girouard et al. 2012). The authors observed preferential SOX2 expression in cells that interfaced and infiltrated dermal stroma. Further, shRNA-mediated *SOX2* KD caused significantly reduced invasion *in vitro*, which was measured in matrigel invasion assays. In sharp contrast, we observed similar numbers of distant lung and liver metastases in control and *Sox2* cKO animals. Although measuring invasion *in vitro* might reflect a relatively simple and low-cost method, there are certain

disadvantages coming with this technique. First, the conditions *in vitro* poorly recapitulate the complex environment observed *in vivo*. For example, it was shown that tumor-associated stromal cells, which are completely absent in the invasion assay in vitro, play crucial roles in cancer cell invasion (Hanahan & Coussens 2012). Second, *in vitro* invasion assays are based on serum-starved cells migrating through matrigel toward high FBS-containing medium (chemotaxis). Those artificial conditions might not represent the situation *in vivo.* Third, matrigel, which resembles extracellular matrix (ECM), is not a well-defined mix and produces a source of variability and does only partially recapitulate the physiological conditions. Fourth, the assay only quantifies the cell-intrinsic invasion potential but not growth in distant organs (metastasis formation), which reflects the critical factor for melanoma patient survival (www.cancer.org, American Cancer Society, 2016). In the *Tyr::NRas*^{Q61K} *Ink4a*$^{-/-}$ GEMM, invasion and metastasis formation occurs in an intact microenvironment, representing a more physiological model. The differences in the used model systems could potentially explain the observed discrepancies regarding invasion and metastasis formation.

In summary, published data is partly contradictory to our data. Different gene silencing methods, cell lines harboring distinct genetic mutations and experimental models might explain the observed differences. Further, Sox2 absence in delaminating NCSCs, the melanocytic lineage and low expression in many melanoma patients might indicate why Sox2 was dispensable for melanoma formation. We therefore favor the hypothesis that the upregulation of Sox2 expression observed in some melanoma patients might rather reflect a bystander effect than having profound oncogenic implications.

5.2. A multicolor lineage tracing approach to address clonality in primary mouse melanomas and metastases

5.2.1. Limitations of the study

5.2.1.1. Time of recombination

Since the TM-based recombination efficiency was rather low by injecting one-to-tree day old animals, many tumors were uncolored and could therefore not be used for the statistical analysis. Hence, most obtained data stems from mice recombined at one month of age. The transgene *Tyr::NRas^{Q61K}* is active throughout embryonic development from embryonic day E10.5 on. Although no visible lesions were present on the skin of one-month-old *Tyr::NRas^{Q61K} Ink4a$^{-/-}$* mice, melanocytic cells could therefore already be tumorigenic at the time of recombination. Consequently, dividing cancer cells could be labeled with different colors although they would originate from the same parental founder clone. Multiple colors observed in tumors would therefore not reflect true polyclonality but rather recombination of already tumorigenic cells (Figure 5.1.).
Increasing the recombination efficiency of early injected animals would be a helpful strategy. Using a higher TM concentration or injecting over a longer period of time could potentially increases the number of recombined cells. Nevertheless, the exact time of oncogenesis is not known and tumorigenesis could theoretically already occur during developmental stages. Hence, recombining at postnatal day three might already be too late. As counter-argument, sorted hyperplastic melanocytes from four-month-old *Tyr::NRas^{Q61K} Ink4a$^{-/-}$* mice did not grow upon injection into immunocompromised mice, strongly favoring the hypothesis that the onset of tumorigenesis occurs after the point of TM administration.

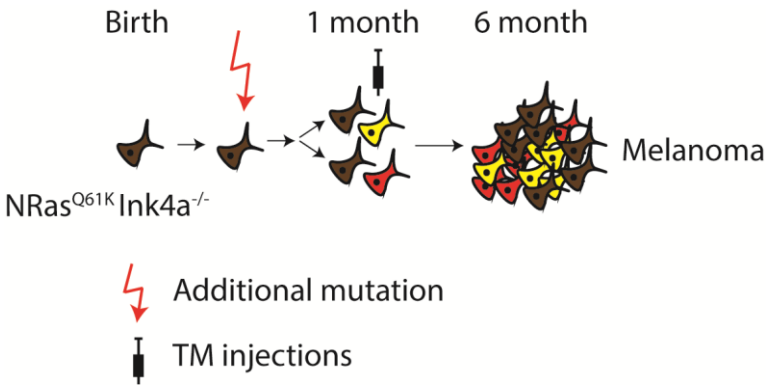

Figure 5.1. Late TM administrations might falsify the results. Early oncogenic mutations (red blizzard) occurring in addition to the *Tyr::NRas^{Q61K} Ink4a$^{-/-}$* genotype could cause an early onset of tumorigenesis. Hence, oncogenic cells could be labeled with different colors although they originate from the same parental

founder clone. The subsequent analyzed melanomas would be quantified as polyclonal though the cells stem from a common founder. Drawn by Simon Schäfer.

5.2.1.2. All melanocytes carry the *Tyr::NRas*^{Q61K} transgene and a homozygous *Ink4a* deficiency.

The majority of all analyzed tumors were polyclonal. Those results might not or only partially reflect melanoma formation in human patients. Since all melanocytes present with constitutively active Ras/Raf/Erk signaling and an *Ink4a* deficiency, one might speculate that possible tumorigenic recruitments and cellular co-operations might be facilitated due to the premalignant state of all neighboring melanocytes (Figure 5.2.). This hypothesis is supported by a study using *ROSA26*/+ *Apc*$^{min/+}$ <=> +/+ *Apc*$^{min/+}$ chimera mice (Merritt et al. 1997). Those mice lack one copy of the *Apc* tumor suppressor gene in all cells and are therefore prone to develop intestinal adenomas. Interestingly, the authors observed that polyclonal tumors occurred rather frequently, supporting the hypothesis that co-operations or recruitment might be facilitated by the premalignant state of neighboring cells. Since 80% of all human melanomas arise *de novo* and not from preexisting benign nevi harboring *BRAF*^{V600E} mutations, one might speculate that the situation in the mouse might only partially reflect the situation in human melanoma patients (Togawa et al. 2010).

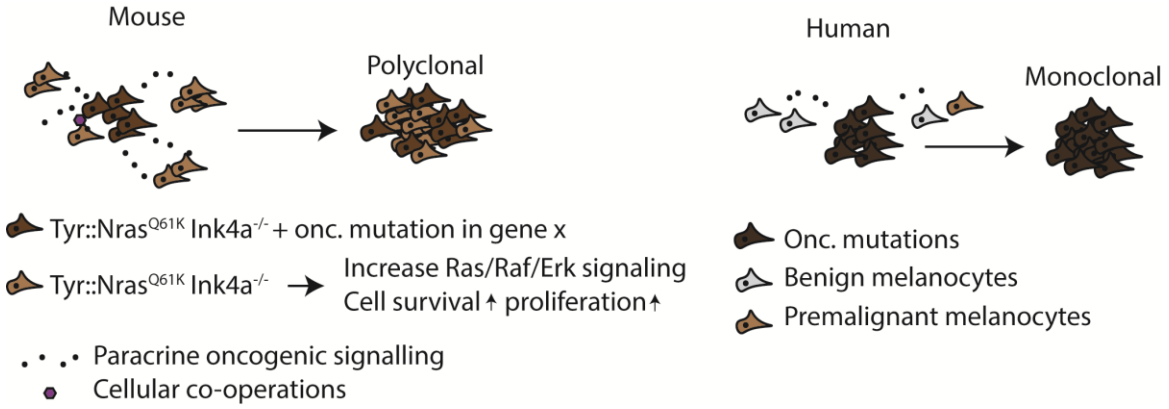

Figure 5.2 Specified mutations in all premalignant mouse melanocytes might change the clonality outcome. All melanocytes in the mouse carry the *Tyr::NRas*^{Q61K} transgene and a homozygous *Ink4a* deficiency, which leads to increased cellular survival and proliferation. Those premalignant melanocytes can be transformed into aggressive cancer cells upon additional oncogenic alterations. Since the cells are already in a premalignant state, oncogenic signaling might be sufficient for transformation. In sharp contrast, benign melanocytes of human melanoma patients do not carry predefined mutations and might be therefore more difficult to transform through oncogenic signaling or cellular co-operations. Nevertheless, one might speculate that signaling might transform benign melanocytes into premalignant melanocytes, following the proposed model of a stepwise tumorigenesis (Vogelstein & Kinzler 1993). Drawn by Simon Schäfer.

5.2.1.3. Collision of independently derived tumors and the discrimination of tumor and hyperplasia.

The observed polyclonality within a given melanoma could originate from random collision between independently derived monoclonal tumors (Andrew T Thliveris et al. 2013) (Figure 5.3). If multiple tumors would arise in anatomical proximity, they could intermingle and appear morphologically as one big melanoma although there was no recruitment or clonal interaction. One possible approach addressing this question is the quantification of the total tumor number on the back skin. A low number of tumors per animal would clearly point against the collision model. However, we would need to establish a mathematical model which relates the event frequency of overall tumor formation with the probability of multiple independent tumor collisions.

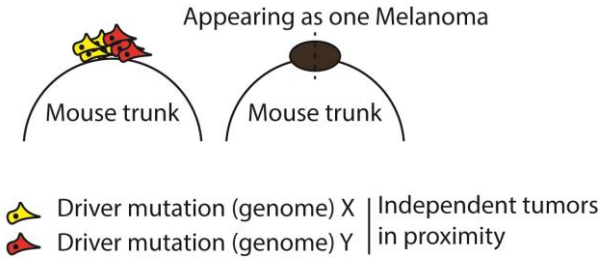

Figure 5.3. Collision of independently derived tumors might falsify the results. If two or multiple different colored tumors independently originate in anatomical proximity, they appear as one polyclonal tumor and might therefore falsify the quantified results. Drawn by Simon Schäfer

Figure 5.4. Example of five different *Tyr::NRas^{Q61K} Ink4a$^{-/-}$* back skins at the moment of euthanasia. Red arrowhead= hyperplasia, yellow arrowhead=tumors.

From morphological analysis, melanoma formation was a rather low frequency event (Figure 5.4.). Although we did not perform any mathematical validation, we speculate that the “collision of

independently derived tumors" hypothesis may be rejected due to the low number of tumors present on the skin of the mice.

Hyperplastic skin merged with tumor cells might display another possible pitfall of the study (Figure 5.5.). Although tumors would appear polyclonal, not all individual clones would be fully tumorigenic. Serving as a practical example, tumor 4.16 f could represent such a situation (Figure 4.16).

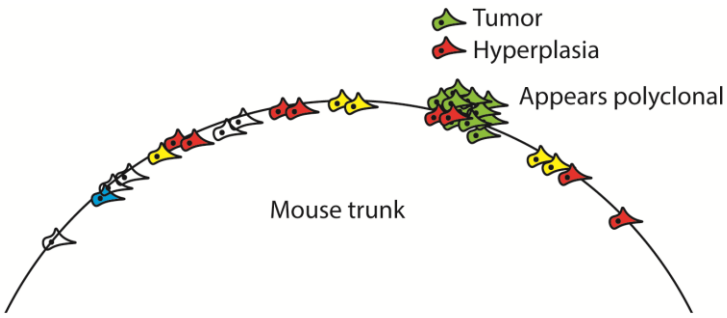

Figure 5.5. Hyperplastic skin merged with tumor cells might falsify the results. Colored premalignant melanocytes (hyperplasia) are located in the hair follicles and the interfollicular dermis. Hence, they could become surrounded by fast proliferating tumor cells. In the analysis, those tumors would be quantified as polyclonal although one clone would not be tumorigenic. Drawn by Simon Schäfer

One strong argument speaking against this potential pitfall is the performed FACS experiment shown in 4.19. All intratumor clones grew upon xenotransplantation, confirming their tumorigenicity. On the other hand, traced hyperplastic cells isolated from four-month-old *Tyr::NRas*^{Q61K} *Ink4a*$^{-/-}$ mice did not grow upon transplantation into immunocompromised mice, discriminating tumorigenic from non-tumorigenic cells. However, we only analyzed the growth of FACS-sorted intratumor clones originating from one melanoma and the numbers should be therefore increased.

Immunostraining for Ki67, a cellular marker for proliferation and active during all phases of the cell cycle, would portray another possibility discriminating malignant tumor cells from hyperplastic cells. The existence of slow proliferating/quiescent tumor cells, which have been described in several cancers, remain the biggest challenge using this approach (Francescangeli et al. 2012; Gao et al. 2010; Pece et al. 2010; Roesch et al. 2010). From my point of view, FACS-based clonal separations and subsequent injections into immunocompromised mice might portray the most promising approach to discriminate hyperplasia from tumor cells.

5.2.3. Possible mechanisms of cancer cell cooperation and recruitment

Interactions among multiple progenitor cells might display a possible explanation for the observed polyclonality (A. T. Thliveris et al. 2013). Thliveris and colleagues analyzed if polyclonal intestinal adenomas arose from cellular cooperations of juxtaposed initiated progenitors or if the tumors were rather caused by recruitment (for example through paracrine signaling) of an initiated progenitor (Figure 3.6.). In the section 3.5.2., I described the experiment by Merrit and colleagues demonstrating the existence of polyclonal intestinal adenocarcinomas using *ROSA26*/+ $Apc^{min/+}$ <=> +/+ $Apc^{min/+}$ chimera mice (Merritt et al. 1997). Based on those experiments, Thliveris and colleagues developed a system in which one genetic lineage of the $Apc^{min/+}$ <=> $Apc^{1638N/+}$ *ROSA26*/+ chimera mice was highly resistant to spontaneous tumorigenesis (A. T. Thliveris et al. 2013). If cellular cooperation of juxtaposed cells would be the predominant mechanism of recruitment, the number of polyclonal tumors would be very low since the number of initiated progenitors in the resistant lineage is low. On the other hand, the percentage of polyclonal tumors would be much higher if polyclonality would be established through recruitment (no close proximity between the initiated cells needed). Since the authors found that the actual number of polyclonal tumors corresponded to the numbers calculated for the "recruitment theory", they suggested that polyclonal intestinal adenomas rather originate by recruitment. However, it must be pointed out the blue and the white initiated progenitors were already tumorigenic. In the *Tyr::*$NRas^{Q61K}$ $Ink4a^{-/-}$ mice, additional genetic alterations are required for a full oncogenic transformation.

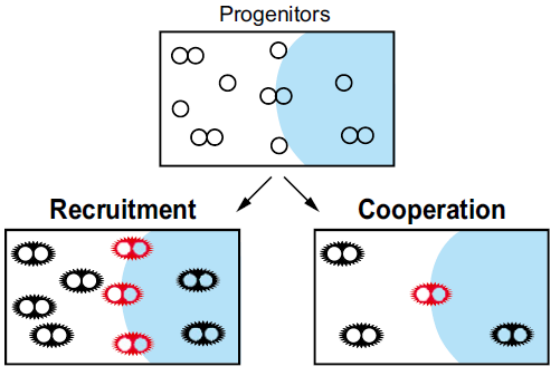

Figure 5.6. Recruitment and cellular cooperation of juxtaposed progenitors. $Apc^{min/+}$ <=> $Apc^{1638N/+}$ *ROSA26*/+ chimera mice were generated, with the white $Apc^{min/+}$ lineage as intestinal adenoma permissive (white) and the $Apc^{1638N/+}$ *ROSA26*/+ resistant (blue) genetic lineage. Hence, multiple white but only a few blue initiated progenitors were found. The number of polyclonal tumors should be higher in the recruitment hypothesis, since no proximal cellular interactions are needed. In contrast, the number of polyclonal tumors should be low if cells need to be juxtaposed (cooperation). The actual number of polyclonal tumors

corresponded with the numbers calculated for the "recruitment theory", suggesting that polyclonal intestinal adenomas rather originate by recruitment. Adapted from: (A. T. Thliveris et al. 2013).

5.2.4. Wnt ligands as possible "recruitment/initiator" molecules

A recent study in lung adenocarcinomas elegantly demonstrated that porcupine (PORCN)-positive cells produced several Wnt ligands (Wnt producer, Wnt5a, Wnt7a,b) while Lgr5-positive cells responded (Wnt responders) with increased tumor propagation ability to the paracrine signaling (Tammela et al. 2017). Another interesting study showing the importance of Wnt signaling made use of the MMTV-Wnt1 breast cancer mouse model (Cleary et al. 2014). Those mouse tumors are composed of comingling basal and luminal tumor cell subtypes derived from a common bipotent progenitor. While the luminal cells secreted canonical Wnt ligands, growth of basal cells was dependent on that particular signaling by the other compartment, highlighting the importance of oncogenic signaling. Another study by Koo and colleagues showed that paracrine Wnt secretion was an essential driver of $RZ^{-/-}$ tumor growth (RZ: transmembrane E3 ligases removing surface Wnt recpetors) (Koo et al. 2015). Unpublished data from the Sommer lab further shows that upregulation of certain Wnt ligands transforms *Tyr::NRas*^{Q61K} *Ink4a*$^{-/-}$-derived hyperplasia cells into MM cells. Hence, one might speculate that paracrine Wnt-ligand secretion might be an important mechanism potentially mediating oncogenic recruitment. Blocking ligand production and secretion, for example through the Porcupine inhibitor Lgk974, would therefore portray a possible option arresting oncogenic signaling (Zimmerli et al. 2017).

To test this hypothesis, we could conditionally ablate different Wnt ligands in the *Tyr::NRas*^{Q61K} *Ink4a*$^{-/-}$ *Tyr::Cre*^{ERT2} *R26R::Confetti* mouse model, in which the number of polyclonal tumors should be significantly reduced. Treating mice with Porcupine inhibitor Lgk974 would illustrate another possibility blocking Wnt ligand secretion.

Another approach facing this issue is combining fluorescent hyperplastic cells with elsewise colored Wnt ligand overexpressing tumor cells. Only tumors cells should grow in the control condition (no Wnt ligand overexpression), resulting in monocolored tumors. However, Wnt ligand overexpressing tumor cells could potentially recruit hyperplastic cells causing bicolored tumors. FACS-based sorting and subsequently reinjection into Foxn1$^{nu/nu}$ mice would show if the recruited clone is per se tumorigenic. One could answer additional questions by inefficiently overexpressing Wnt ligands in hyperplasia cells. A monocolored tumor would indicate that overexpressing ligand X would be sufficient to transform the infected cells but not to recruit non-infected cells. On the other hand, a bicolored tumor would demonstrate that the overexpression of ligand X would be sufficient to recruit non infected cells.

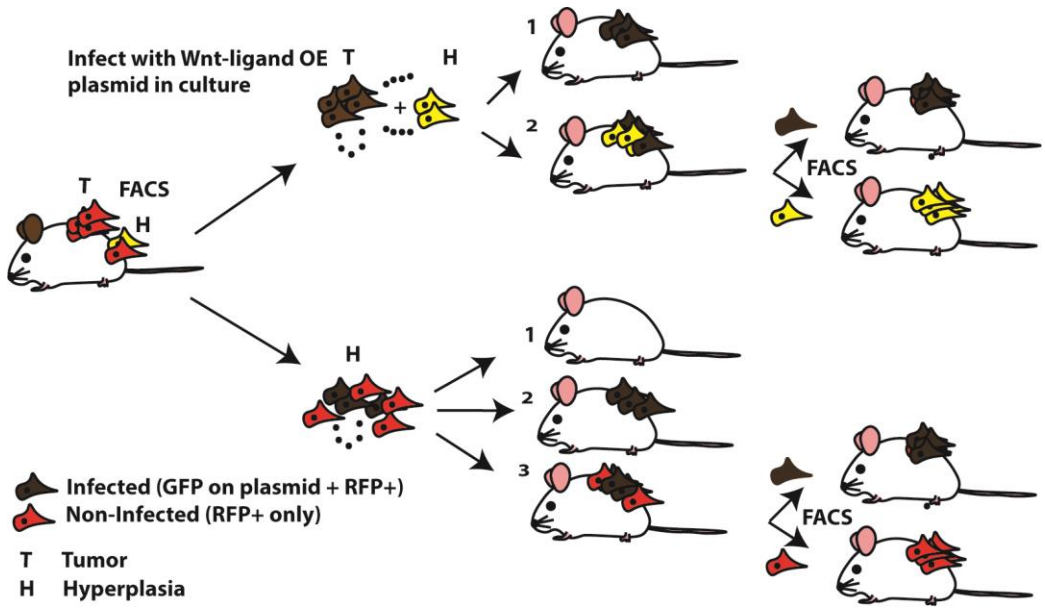

Figure 5.7. Experimental setup to investigate the role of paracrine signaling in cellular recruitment/initiation. Tumor (T) and hyperplasia (H) cells can be purified and isolated from recombined *Tyr::NRas^{Q61K} Ink4a$^{-/-}$ Tyr::Cre^{ERT2} R26R::Confetti* animal using FACS. Several experiments could be carried out using either tumorigenic or hyperplastic cells. Tumor cells overexpressing certain ligands can potentially recruit and initiate hyperplasia cells causing bicolored tumors (upper panel). By inefficiently overexpressing ligands in a subset hyperplasia cells, one could test if the overexpression per se results in tumorigenicity and if the signaling would be sufficient to transform the non-infected cells (lower panel). Drawn by Simon Schäfer.

5.2.5. Biological relevance of polyclonal tumors

Although there are several limitations of the study, our data suggests that mouse melanomas can have a polyclonal origin. Since cancer development and progression might resemble an evolutionary process, we speculate that the observed polyclonality could bring a survival advantage for the developing cancer. As described in section 5.1.1.2., Marusyk and colleagues show that tumor driver clones are not necessarily good competitors (Marusyk et al. 2014). Although the study was not based on genetically distinct subclones but on overexpression of factors, one might speculate about reciprocal benefits of driver clones initiating tumor growth of competitor clones. For example, the fast proliferating competitor clone could create a microenvironmental niche protecting and supporting the driver clone. On the other hand, the driver clone (in the Marusyk study overexpressing Il-11) might stimulate the growth of competitor clones, creating a temporary win-to-win situation for all involved subclones of the developing cancer. Over time, additional

oncogenic mutations or epigenetic alteration in the genome of the competitor clone might cause independency from driver clone.

Hence, although evolution is based on competition between individuals, which should favor selfish behavior, cooperation has been observed on many levels of biological organizations (Nowak 2006). For example, cells cooperate with other cells in a multicellular organism and animals cooperate with animals from the same or even from genetically distinct species. A cooperator is defined by paying a cost for another individual to receive a benefit. On the other hand, a defector has no cost but also does not benefit other individuals (Nowak 2006). In mixed populations, the defector has an advantage over the cooperator. Hence, the community drifts towards a population only composed of defectors. Astonishingly however, a population with only cooperators has the highest fitness while a population of defectors has the lowest.

An elegant study by Cleary and colleagues showed that *Wnt1*-induction the breast epithelium stem cells caused cancer with features of the basal and luminal lineage (Cleary et al. 2014). Intriguingly, many tumors contained more than one clone. Basal cells often harbored mutations in the *HRas* gene in a subset of breast tumors and while luminal cells carried the wildtype gene copy. Interestingly, neither of the clones (basal or luminal) was able to initiate tumors upon transplantation, while the combination of both clones was highly tumorigenic, suggesting clonal dependency. The authors argue that paracrine interactions between *HRas*-mutant basal cells and *Wnt-1* producing luminal cells, on which the basal cells depend, is potently driving oncogenesis (Polyak & Marusyk 2014).

Hence, blocking those cellular interactions might portray a promising approach preventing tumor formation, or, at least, reducing early intratumor heterogeneity. Therefore, identification and characterization of oncogenic paracrine signaling might represent an inevitable step to suppress tumor formation *in vivo*.

5.2.6. Biological relevance of polyclonal metastases

A recently published large cohort study analyzing 1934 melanoma patients demonstrated no survival difference between melanoma-positive lymph node dissection vs ultrasonography observation (Faries et al. 2017). Nevertheless, the histological status of sentinel lymph nodes displays a highly significant prognostic factor for melanoma patients, highlighting the importance of studying dissemination from the skin to the lymph node (Wagner et al. 2003).

Multiple clones (colors) were present in all analyzed lymph nodes. Due to those observations, we assume that several clones, presumably with different underlying (epi)-genetics, are able to leave the locally growing cancer to infiltrate distinct organs. Thus, one might speculate that invasion and subsequent local metastasis formation might represent a rather frequent event, at least in the studied

mouse model. However, we cannot discriminate if the melanoma cells disseminated as clusters or as single cells which started to proliferate in the lymphatic organs. As described above (see 5.1.1.2), multiregional sequencing revealed that branched evolution is a commonly observed phenomenon in primary tumors. Hence, the observed results in the lymph nodes might reflect the situation present in primary tumors, where clones with different genetic mutations co-exists besides each other.

As described as biological relevance for primary tumors, reciprocal and beneficial cooperation mechanisms could potentially increase the fitness of the clones also in host organs. Further, maintaining genetic diversity might serve as protection mechanism against various external influences like lack of oxygen, immune surveillance or human-induced therapy. Evolution seems therefore to favor genetic diversity over clonal dominancy in cancer progression.

Further, we collected small evidence that also distant metastases can be derived from multiple clones. Strikingly, we observed RFP/Dct-positive cells next to Dct-positive cells within the same lung metastasis. Using this lineage tracing model however, we are not able to tell if the cancer cells disseminated from primary tumors, hyperplastic cells or other metastatic sites. Further, we cannot draw conclusions if the tumor cells disseminated as single cells or in clusters. Interestingly, only a subset of RFP-positive metastatic melanoma cells expressed the melanocyte differentiation marker Dct describing intraclonal phenotypic heterogeneity (assuming that the RFP-positive cells originated from one clone).

Cancer initiation, growth, invasion and metastasis formation presumably not only represents mutation-induced clonal growth but rather reflects a complex interplay between probably genetically distinct clones resembling an ecosystem of communicating species.

6. Materials and Methods

6.1. In vitro experiments

6.1.1. Protein isolation and Western Blotting

Cells were lysed in RIPA buffer (Thermo Fisher, 89900) containing 100x Halt™ phosphatase and protease inhibitor (Thermo Fisher, 87786) cocktail and incubated for 30min on ice. Protein concentration was determined with Pierce™ BCA protein assay kit. Absorbance measurements were conducted with the DTX800 multimode detector (Beckman Coulter). SDS-page was carried out on 4-20% Mini-PROTEAN TGX gels (Bio Rad, 456-1094). For the SDS-page, 10x running buffer (Tris/Glycine/SDS) (Bio Rad, 1610732) was purchased. Transfer was performed in wet chambers at 100V for 60min with 10x transfer buffer (Tris/Glycine) (Bio Rad, 1610734) (1l:200ul MeOH, 100ml transfer buffer, 700ml ddH_2O). Nitrocellulose membranes and filter papers were purchased from Bio Rad (Bio Rad, 1620234). Membrane was blocked for 1h at room temperature (RT) in Odyssey blocking buffer (LI-COR Biosciences, 927-40000). Primary antibodies were applied in Odyssey blocking buffer overnight at 4°C and visualized using secondary antibodies in Odyssey blocking buffer for 1h at RT. After removal of primary and secondary antibodies, the membrane was washed 3x for 5min with PBS/0.1% Tween 20 (Sigma, P9416). Blots were scanned and quantified with the Odyssey imaging system. Following antibodies were used:

Table 1. Primary antibodies used for Western Blot.

Antigen	*Specificity*	*Company*	*Serial number*	*Dilutions*
Sox2	human	Santa Cruz Bio	sc-17320	1:200
B-Actin	human / mouse	Sigma Aldrich	A5316	1:10000
Sox3	human	Abcam	ab104248	1:200
Histone H3	human / mouse	Cell Signaling	3638	1:1000

Table 2. Secondary antibodies used for Western Blot.

Fluorophore	*Specificity*	*Company*	*Serial number*	*Dilutions*
IRDye-800CW	mouse	LI-COR Bioscience	926-32212	1:10000
IRDye-680LT	rabbit	LI-COR Bioscience	926-68023	1:10000

6.1.2. RNA isolation and RT-qPCR

RNA isolation from cells was carried out with the RNeasy Mini Kit (Qiagen, 74104) and the RNase-free DNase set (79254, Qiagen). The isolation was conducted according to the

manufacturer's guidelines. The NanoDrop™ (Thermo Fisher) was used for quality control and quantification of the isolated RNA. 750ng to 1ug isolated RNA was used for reverse transcriptase reaction using Maxima First Strand cDNA Synthesis Kit (Thermo Scientific, K1641). Next, the cDNA was treated with RNase H (Thermo Scientific, EN0202) according the manufacturer's recommendations. RT-qPCR was performed using the LightCycler 480 (Roche) system with SYBR Green I Master (Roche, 4707516001) in technical triplicates. The following human and mouse primer sequences (table 3 & 4) were used. The human RT-qPCR have been previously described (Shakhova et al. 2012).

Table 3. Mouse RT-qPCR primers.

Gene	*Forward Sequence*	*Reverse Sequence*
Sox10	GAAGAAGGCTCCCCCATGTC	GCTCTGTCTTTGGGGTGGTT
Mitf	CCCCAAGTCAAATGATCCAG	GCAACTTCCGGATGTAGTCC
Silv	GGGGATGCATTTGAGCTGAC	CTGGCACCCTGGTGATGAAA
Dct	CCTGAATGGGACCAATGCCT	AGGCATCTGTGGAAGGGTTG
Oca2	TGTTGGAGAACAGACTGCCC	ATGATGCCAAGGCTGAGACC
Tyrp1	GTACTTGGGAGGTCGTCACC	GTCCCTCAGGTGTTCCATCG
Usf1	CAGGGCTCAGAGGCACTACT	GCTCCCTCCCTGCAATACTT

Table 4. Human RT-qPCR primers.

Gene	*Forward Sequence*	*Reverse Sequence*
MITF	CGAGCTCATGGACTTTCCCTTA	CTTGATGATCCGATTCACCAAA
DCT	CCAATGATCCCATTTTTGTG	AGGCATCTGCAGGAGGATTA
MLANA	GCTCATCGGCTGTTGGTATT	TTCTTGTGGGCATCTTCTTG
USF1	TACTACCCAGGGCTCAGAGG	TCCCTGCAGTACTTCTTGTGG

6.1.3. Cell cultures

All human and mouse melanoma cells were cultured in RPMI-1640 medium containing 10% FCS (Life Technologies, 16140), 4mM L-Glutamine (Life Technologies, 25030), Penicillin-Sterptomycin (Life Technologies, 15070) and Fungizone Antimycotic (Life Technologies, 15290) as specified (Zipser et al. 2011). The cell lines M050829 and M070302 have been characterized before (Zipser et al. 2011; Civenni et al. 2011). MM150423 was generated at the Department of Dermatology of the University Hospital Zurich and approved by the ethical committee of the Canton of Zurich, Switzerland. Written informed consent was obtained from all subjects and approved by the local institutional review boards (EK647 and EK800). A375, SK-MEL-28 and

WM83 were purchased from ATCC. XB2 and melan-a cell lines were previously described (Bennett et al. 1987).

6.1.4. CRISPR/Cas9-mediated *SOX2* KO

The CRISPR/Cas9-mediated SOX2 KO M050829 clones were performed in a collaboration with Dr. Mario Bonalli (LASC Zürich) and MSc. Corina Segalada (University of Basel). The online tool (http://crispr.mit.edu/) was used to determine the sgRNA sequence: 5'-GGCCCGCAGCAAACTTCGGGGGG-3' (quality score of 87) to target the only Sox2 exon. Double stranded oligonucleotides were then ligated into the sgRNA expressing MLM3636 vector (addgene, 43860). Electroporation of 10ug MLM3636 (sgRNA) and 10ug pCAG-T7-Cas9-P2A-EGFP (kindly provided by Dr. Pawel Pelczar, USZ) was used to transfect M050829. Three days after transfection, EGFP-positive cells were seeded as single cells in 96-well plates using the BD FACSAria™ III 5L (BD Biosciences). AmpliTaq Gold PCR 360 was used to amplify the regions encompassing the sgRNA target sequence. The amplified DNA was send for sanger-sequencing (Microsynth). The KO was confirmed by Western Blot analysis (see Figure 2.3.) using a SOX2-specific antibody.

6.2. In silico analyses

6.2.1. TCGA analysis

The RNAseq and clinical datasets for skin cutaneous melanoma, acute myeloid leukemia (AML), diffuse large b cell lymphoma (DLBL), chromophobe renal cell carcinoma (chRCC), lung squamous cell carcinoma (lung SCC), glioblastoma multiforme (GBM), glioma, colorectal cancer (CRC), breast cancer and lung adenomas were downloaded from cBioPortal (Cerami et al. 2012; Gao et al. 2013). The raw data was plotted with GraphPad prism. Clinical TCGA datasets (survival and Breslow thickness) were provided by Dr. Phil Cheng (University hospital Zurich). All TCGA data were analyzed with R (The R Foundation for Statistical Computing) and plotted with GraphPad prism.

6.2.2. Statistical analysis

P-values for comparison of two groups were calculated with unpaired Students t-test in GraphPad prism. For all statistical tests, $p \leq 0.05$ was considered significant. $p \leq 0.001$. *$p \leq 0.05$, ***$p \leq 0.001$, ****$p \leq 0.0001$. P-values of Kaplan-Meier survival curves were calculated with the Log-rank (Mantel-Cox) test. P-values for comparison of multiple groups were calculated with analysis

of variance (ANOVA) and multiple comparison. The applied statistical tests are indicated for each experiment in the figure legends.

6.3. In vivo experiments

6.3.1. Mouse strains and genotyping

The following transgenic and KO mice were used in my studies (table 4):

Table 4. Transgenic and KO mice used in my studies.

Transgenic/KO mice	*Described in*
Tyr::NRas^{Q61K} Ink4a$^{-/-}$	(Ackermann 2005; Shakhova et al. 2012a; Schaefer et al. 2017)
Tyr::Cre^{ERT2}	(Bosenberg et al. 2006; Harris & Pavan 2013)
R26R::LacZ	(Soriano 1999)
Sox2$^{lox/lox}$	(Favaro et al. 2009)
R26R::Confetti	(Snippert et al. 2010)

The *Tyr::NRas^{Q61K} Ink4a$^{-/-}$ Tyr::Cre^{ERT2} R26R::LacZ Sox2$^{lox/lox}$* and *Tyr::NRas^{Q61K} Ink4a$^{-/-}$ Tyr::Cre^{ERT2} R26R::Confetti* animals carried a mixed genetic background. *Sox2$^{lox/lox}$* mice were kindly provided by Prof. Dr. Silvia Nicolis (University of Milano Bicocca). All other above listed mouse strains were maintained in the lab of Prof. Dr. Lukas Sommer. Both, male and female animals, which were born with expected ratio of Mendelian inheritance, were used for experiments. Mice were subjected to TM at one month or at postnatal day one, depending on the experimental conditions. The transgenic mice developed melanomas after 4-8 month and were frequently monitored. The animals were sacrificed according predetermined criteria/adverse clinical symptoms: Hunch back, multiple skin melanomas (Ø > 5mm), weight loss (Δm > 15%), poor health condition. Toe clipping was used to obtain biopsies for DNA isolation. PCR (Kapa Biosystems, KK1024) using gene specific primers (see table 5) was used for genotyping. 2-month-old athymic nude *Foxn1$^{nu/nu}$* were purchased from Envigo. Tumor volume was measured weekly with a caliper and calculated as follows: $V=2/3 \times \pi \times ((a+b)/4))^3$, where a (mm) was the length and b (mm) was the width of the tumor. All animal experiments have been approved by the veterinary authorities of Canton Zurich, Switzerland and were performed in accordance with the Swiss law.

Table 5. Mouse genotyping primers

Gene/allele	*Forward sequence*	*Reverse sequence*
Cre	CTATCCAGCAACATTTGGGCCAGC	CCAGGTTACGGATATAGTTCATGAC
LacZ	GGTCGGCTTACGGCGGTGATTT	AGCGGCGTCAGCATTGTTTTT
Sox2$^{lox/lox}$	AGGCTGAGTCGGGTCAATTA	CAGTCCAAGCTAGGCAGGTT
Confetti	CCAGATGACTACCTATCCTC	GAATTAATTCCGGTATAACTTCG
Ink4a	**P1:** GTGATCCCTCTACTTTTTCTTCTGACTT	**P2:** CGGAACGCAAATATCGCAC
	P3: GAGACTAGTGAGACGTGCTACTTCCA	

Ras$^{Q61K/+}$ and *Ras*$^{+/+}$ mice were morphologically discriminated by the tail and paws hyperpigmentation present in *Ras*$^{Q61K/+}$ animals.

6.3.2. Tamoxifen administration

TM powder (Sigma-Aldrich, T5648) was suspended in an EtOH:Oil mix (1:9) over night at RT as 10mg/ml concentration. After the animals reached one month of age, 2mg (200ul of the stock solution) TM was intraperitoneally injected daily over five consecutive days. This particular injection protocol has been described before in our lab (Shakhova et al. 2012). For the early injections (postnatal day 1-3), a TM stock solution of 1mg/ml concentration was prepared. 100ug TM was daily injected intragastrically over 3 consecutive days. This injection protocol has been described before (Pitulescu et al. 2010).

6.3.3. Histological analysis and immunofluorescence

For the project "Sox2 is dispensable for primary melanoma and metastasis formation" (see 2.2.), all mouse tissue samples were washed with Hank's balanced salt solution (HBSS) (Thermo Fisher Scientific) and fixed in Histofix (4% formaldehyde) (Carl Roth, p087.3) overnight at 4°C. The following day, the fixed tissue was washed with PBS and 70% EtOH and embedded in paraffin. After 5um thick sections were cut with a microtome, the following staining protocol was executed: The sections were deparaffinized (decreasing EtOH row) and heated up in a pressure cooker to achieve epitope retrieval. Next, the sections were subjected to blocking buffer (1% BSA in PBS and 0.05% Triton X-100) for 1h at RT. Subsequently, primary antibodies (table 6) were applied to the sections and incubated over night at 4°C. On the following day, the sections were washed with PBS, subjected to secondary antibodies (table 7) for 1h at RT and finally mounted with Hoechst (Sigma-Aldrich, 14533) -containing mounting solution (Dako, S3023). For β-Gal staining, the TSA Plus Cy3 Kit (1:100, NEL744001KT, PerkinElmer) was used for signal amplification.

Table 6. Primary antibodies

Antigen	*Specificity*	*Company*	*Number*	*Dilution*
Sox10	human	Santa Cruz Bio	sc-17342	1:100
Sox2	human/mouse	Abcam	ab15830	1:100
Dct	human/mouse	Santa Cruz Bio	sc-10451	1:250
B-Gal	mouse	Abcam	ab9361	1:1000
Sox3	human	Abcam	ab104248	1:200
Mitf	human/mouse	Dr. Julien Debbache	Cl. LH7	1:200

Table 7.1. Secondary antibodies

Antigen	*Specificity*	*Company*	*Number*	*Dilution*
Alexa488	goat	Jackson Immuno R.	705-545-147	1:400
Alexa488	rabbit	Jackson Immuno R.	711-545-152	1:400
Cy3	rabbit	Jackson Immuno R.	711-165-152	1:400
Alexa647	goat	Jackson Immuno R.	711-605-152	1:400
Biotin	chicken	Merck Millipore	AP194B	1:300

Table 7.2. Secondary antibodies

Antigen	*Specificity*	*Company*	*Number*	*Dilution*
HRP-Streptavidin		Jackson Immuno R.	016-030-084	1:300

For the project "A multicolor lineage tracing approach to address clonality in primary mouse melanomas and metastases" (see 2.3), tissue samples were washed in HBSS and fixed overnight at 4°C as described above. The following day, the samples were washed with PBS and subjected to a 30% sucrose/PBS solution over night at 4°C. On the next day, the samples were embedded in Tissue-Tek O.C.T.™ (BioLab, SKU4583) and frozen at -80°C. 12um cryosections were cut and stained for Dct (see above). The images were taken with a DMI6000B microscope (Leica) or an Axio Scan Z.1 slide scanner (Zeiss). Imaris (BITPLANE) and Photoshop CC (Adobe) were used for image processing. The counting tool from Photoshop CC was used for quantifications.

6.3.4. Quantification of skin melanomas and metastases

Skin melanomas were defined by two criteria. 1) The average size of the lesion was > 2mm and 2) The lesion was morphologically distinguishable from the hyperplastic adjacent skin (see Figure 3.4). After the mice were sacrificed, the total number of skin melanomas were counted for the statistical analysis. B-Gal stainings were established to check for recombination (Sox2 loss) in those tumors. Pigmented lesions within distant the organs (lung, liver) were quantified as melanoma metastasis. The lesions were stained for the melanocyte marker Sox10. Only lesion > 15 clustered

Sox10-positive cells were counted as melanoma metastasis, single Sox10-positive cells were excluded from statistics. Again, B-Gal stainings were used to check for recombination. Axillary and sciatic lymph nodes were excised for identification of the color distribution for the Confetti project.

6.3.5. Allografting of murine melanoma cells

Tumors from *Tyr::NRas^{Q61K} Ink4a$^{-/-}$ Tyr::Cre^{ERT2} R26R::Confetti* animals were dissociated into small pieces using scalpel and scissors. Next, the tissue pieces were digested using 0.25mg/ml Liberase DH Research Grade (Roche, 05401054001) in pure RPMI1640 (Life Technologies, 42401) for 45min at 37°C. Next, the cell suspension was treated with 0.2mg/ml DNase I (Roche, 10104159001) for 15min at 37°C. The single cell suspension was purified using a 40um cell strainer (Falcon™ cell strainers, 08-771-1). Next, FACS (BD FACSAria™ III 5L (BD Biosciences)) was used to separate the different intratumor colors. The FACS was performed by operators of the Flow Cytometry Facility at the University of Zurich and established by Dr. Florian Mair. The single cell suspension was used and engrafted into *Foxn$^{nu/nu}$* mice with matrigel (Corning, 356234) as a 1:1 (cell:matrigel) mix.

7. Curriculum vitae

SIMON MANUEL SCHÄFER

From Lucerne, Switzerland

Regensbergstrasse 79

8050 Zürich

+41 76 456 00 43

Simon.schaefer@uzh.ch

* 26.10.1988

Education

07/2012-today
University Zürich

PhD Thesis
Supervisor:
Prof. Dr. Lukas Sommer, Institute of Anatomy

Highlight: During my PhD, I analyzed the role of the stem cell factor Sox2 during the formation of black skin cancer (melanoma). By means of transgenic mice, cell culture experiments and novel biotechnologies (CRISPR-Cas9 system), I was able show that Sox2 was dispensable for the formation of primary melanoma and metastases.
I learned to plan, manage and execute my own project in an independent manner, leading to high impact scientific publications.

01/2011-01/2012
University Zürich

Master of Science in Biology, Neurosciences:
"Investigations into the role of Sox10in the normal and malignant melanocyte lineage"
Supervisor:
Prof. Dr. Lukas Sommer, Institute of Anatomy
Dr. Olga Shakhova, University Hospital Zurich
Dr. Daniel Zingg, Institute of Anatomy

Grade: 5.3 (1 lowest, 6 highest)

09/2007-08/2010
University Zürich

Bachelor of Science in Biology

08/2004-08/2007
High School Stadelhofen
Zürich

Matura, music profile

Key Skills and Competencies

Subject-specific	Laboratory skills (Immunohistochemistry, cell cultures, qRT-PCR, Western Blot, cloning, PCR, DNA and RNA isolation, cell transplantations)
Subject-specific	Mice handling (genotyping, weaning, injections, biopsy, breedings)
General	● Writing skills (scientific publications) ● Analysis and interpretation of complex data ● Experienced in oral presentations ● Teaching, guiding and supervision of students ● Teamplayer

Languages

German	Mother tongue
English	Fluent (oral and written)
French	Basics (oral and written)

Teaching

11/2014-11/2015 University Zürich	Supervision of a master thesis (Human Biology)
08/2013-09/2017 University Zürich	Tutor and co-examinator histology classes
11/2014-12/2014 University Zürich	Supervision of a matura thesis (Gymn. Beaulieu)
12/2015 Luzern Natural Museum	Advice and expertise for a stem cell exhibition

Journal Publications

2017	**Schaefer, S.M.,** Segalada, C., Cheng, P.F., Bonalli M., Parfejevs V., Levesque M.P., Dummer R., Nicolis SK., Sommer L. *Oncogene 2017 Apr 3; Epub*
2015	Zingg, D., Debbache, J., **Schaefer, S.M.**, Tuncer, E., Frommel, S.C., Cheng P.F., Arenas-Ramirez, N., Haeusel J., Zhang, Y., Bonalli, M., McCabe M.T., Creasy, C.L., Levesque, M.P.,

	Boyman O., Santoro R., Shakhova O., Dummer R., Sommer L. *Nature Communications 2015 Jan 22;6:6051.*
2014	Shakhova O., Cheng, P.F., Pravin J., Zingg D., **Schaefer S.M.**, Debbache, J., Haeusel, J., Matter, C., Guo T., Davis, S., Meltzer, P., Mihic-Probst, D., Moch, H., Wegner, M., Merlino G., Levesque, M.P., Dummer R., Santoro R., Cinelli P., Sommer L. *Plos Genetics 2014 Jan 28;11(1):e1004877.*
2012	Shakhova O., Zingg D., **Schaefer S.M.,** Hari L., Civenni G., Blunschi J., Claudinot, S., Okoniewski, M., Beermann, F., Mihic-Probst, D., Moch H., Wegner M., Dummer R., Barrandon Y., Cinelli P., Sommer L. *Nature Cell Biology Aug;14(8):882-90.*

Awards

2016 Davos	Excellent oral presentation at the 6th students retreat of the „Cancer Biology PhD program“

8. References

Ackermann, J. et al., 2005. Metastasizing Melanoma Formation Caused by Expression of Activated N-Ras Q61K on an INK4a-Deficient Background. *Cancer Res*, 65(10), pp.4005–11.

Adameyko, I. et al., 2012. Sox2 and Mitf cross-regulatory interactions consolidate progenitor and melanocyte lineages in the cranial neural crest. *Development*, 139(2), pp.397–410.

Agnarsdóttir, M. et al., 2010. SOX10 expression in superficial spreading and nodular malignant melanomas. *Melanoma research*, 20(6), pp.468–78.

Al-Hajj, M. et al., 2003. Prospective identification of tumorigenic breast cancer cells. *Proceedings of the National Academy of Sciences*, 100(7), pp.3983–3988.

Van Allen, E.M. et al., 2014. The genetic landscape of clinical resistance to RAF inhibition in metastatic melanoma. *Cancer Discovery*, 4(1), pp.94–109.

Alonso, L. & Fuchs, E., 2006. The hair cycle. *Journal of cell science*, 119(Pt 3), pp.391–393.

Andoniadou, C.L. et al., 2013. Sox2+ stem/progenitor cells in the adult mouse pituitary support organ homeostasis and have tumor-inducing potential. *Cell Stem Cell*, 13(4), pp.433–445.

Andor, N. et al., 2016. Pan-cancer analysis of the extent and consequences of intratumor heterogeneity. *Nature medicine*, 22(1), pp.105–13.

Aoki, H. et al., 2009. Two distinct types of mouse melanocyte : differential signaling requirement for the maintenance of non- cutaneous and dermal versus epidermal melanocytes. , 2521, pp.2511–2521.

Aoki, Y. et al., 2003. Sox10 regulates the development of neural crest-derived melanocytes in Xenopus. *Developmental Biology*, 259(1), pp.19–33.

Archer, T.C., Jin, J. & Casey, E.S., 2011. Interaction of Sox1, Sox2, Sox3 and Oct4 during primary neurogenesis. *Developmental Biology*, 350(2), pp.429–440.

Arnold, K. et al., 2011. Sox2 + adult stem and progenitor cells are important for tissue regeneration and survival of mice. *Cell Stem Cell*, 9(4), pp.317–329.

Avilion, A.A. et al., 2003. Multipotent cell lineages in early mouse development on SOX2 function. *Genes Dev.*, 17, pp.126–140.

Baggiolini, A. et al., 2015. Premigratory and migratory neural crest cells are multipotent in vivo. *Cell Stem Cell*, 16(3), pp.314–322.

Balch, C.M. et al., 2009. Final version of 2009 AJCC melanoma staging and classification. *Journal of Clinical Oncology*, 27(36), pp.6199–6206.

Bao, S., Wu, Q., McLendon, R.E., et al., 2006. Glioma stem cells promote radioresistance by preferential activation of the DNA damage response. *Nature*, 444(7120), pp.756–60.

Bao, S., Wu, Q., Sathornsumetee, S., et al., 2006. Stem cell-like glioma cells promote tumor angiogenesis through vascular endothelial growth factor. *Cancer Research*, 66(16), pp.7843–7848.

Beier, D. et al., 2007. CD133+ and CD133- glioblastoma-derived cancer stem cells show differential growth characteristics and molecular profiles. *Cancer Research*, 67(9), pp.4010–4015.

Ben-Porath, I. et al., 2008. An embryonic stem cell–like gene expression signature in poorly differentiated aggressive human tumors. *Nature Genetics*, 40(5), pp.499–507.

Bennett, D.C., Cooper, P.J. & Hart, I.R., 1987. A line of non-tumorigenic mouse melanocytes, syngeneic with the B16 melanoma and requiring a tumour promoter for growth. *International journal of cancer*, 39(3), pp.414–8.

Bergenmar, M. et al., 1998. Nodular histogenetic type -- the most significant factor for thick melanoma: implications

for prevention. *Melanoma research*, 8(5), pp.403–11.

Boiko, A.D. et al., 2010. Human melanoma-initiating cells express neural crest nerve growth factor receptor CD271. *Nature*, 466(7302), pp.133–137.

Bollag, G. et al., 2012. Vemurafenib: the first drug approved for BRAF-mutant cancer. *Nature Reviews Drug Discovery*, 11(11), pp.873–886.

Bondurand, N. et al., 1998. Expression of the SOX10 gene during human development. *FEBS letters*, 432(3), pp.168–72.

Bosenberg, M. et al., 2006. Characterization of melanocyte-specific inducible Cre recombinase transgenic mice. *Genesis (New York, N.Y. : 2000)*, 44(5), pp.262–7.

Boumahdi, S. et al., 2014. SOX2 controls tumour initiation and cancer stem-cell functions in squamous-cell carcinoma. *Nature*, 511(7508), pp.246–250.

Breitbart, Ma. et al., 1997. Ultraviolet light exposure, pigmentary traits and the development of melanocytic naevi and cutaneous melanoma. *Acta Derm Venerol*, 77, pp.374–378.

Bridge, A.J. et al., 2003. Induction of an interferon response by RNAi vectors in mammalian cells. *Nature genetics*, 34(3), pp.263–4.

Britsch, S., 2001. The transcription factor Sox10 is a key regulator of peripheral glial development. *Genes & Development*, 15(1), pp.66–78.

Bronner-Fraser, M. & Fraser, S., 1989. Developmental potential of avian trunk neural crest cells in situ. *Neuron*, 3(6), pp.755–766.

Brummelkamp, T.R., 2002. A System for Stable Expression of Short Interfering RNAs in Mammalian Cells. *Science*, 296(5567), pp.550–553.

Buganim, Y. et al., 2012. Single-cell expression analyses during cellular reprogramming reveal an early stochastic and a late hierarchic phase. *Cell*, 150(6), pp.1209–1222.

Buttner, P. et al., 1995. Primary cutaneous melanoma: Optimized cutoff points of tumor thickness and importance of Clark's level for prognostic classification. *Cancer*, 75(10), pp.2499–2506.

Campbell, P.J. et al., 2008. Subclonal phylogenetic structures in cancer revealed by ultra-deep sequencing. *Proceedings of the National Academy of Sciences*, 105(35), pp.13081–13086.

Cerami, E. et al., 2012. The cBio Cancer Genomics Portal: An open platform for exploring multidimensional cancer genomics data. *Cancer Discovery*, 2(5), pp.401–404.

Cesarini, V. et al., 2017. Sox2 is not required for melanomagenesis, melanoma growth and melanoma metastasis in vivo. *Oncogene*.

Chalovich, J.M. & Eisenberg, E., 2009. Generation of human induced pluripotent stem cells in the absence of Sox2. *Stem Cells*, 257(5), pp.2432–2437.

Chan, M.P., Chan, M.M. & Tahan, S.R., 2010. Melanocytic nevi in pregnancy: Histologic features and Ki-67 proliferation index. *Journal of Cutaneous Pathology*, 37(8), pp.843–851.

Chapman, P.B. et al., 2011. Improved survival with vemurafenib in melanoma with BRAF V600E mutation. *The New England journal of medicine*, 364(26), pp.2507–16.

Cheli, Y. et al., 2010. Fifteen-year quest for microphthalmia-associated transcription factor target genes. *Pigment Cell and Melanoma Research*, 23(1), pp.27–40.

Cheli, Y. et al., 2012. Hypoxia and MITF control metastatic behaviour in mouse and human melanoma cells. *Oncogene*, 31(19), pp.2461–2470.

Chen, Y. et al., 2008. The molecular mechanism governing the oncogenic potential of SOX2 in breast cancer. *Journal*

of Biological Chemistry, 283(26), pp.17969–17978.

Cheng, P.F. et al., 2015. Methylation-dependent SOX9 expression mediates invasion in human melanoma cells and is a negative prognostic factor in advanced melanoma. *Genome biology*, 16(4), p.42.

Cichorek, M., Wachulska, M. & Stasiewicz, A., 2013. Heterogeneity of neural crest-derived melanocytes. *Central European Journal of Biology*, 8(4), pp.315–330.

Cichowski, K. & Jacks, T., 2001. NF1 tumor suppressor gene function: narrowing the GAP. *Cell*, 104(4), pp.593–604.

Cimadamore, F. et al., 2011. Article Human ESC-Derived Neural Crest Model Reveals a Key Role for SOX2 in Sensory Neurogenesis. *Stem Cell*, 8(5), pp.538–551.

Civenni, G. et al., 2011. Human CD271-Positive Melanoma Stem Cells Associated with Metastasis Establish Tumor Heterogeneity and Long-term Growth. *Cancer Research*, 71(8), pp.3098–3109.

Clarke, M.F. et al., 2006. Cancer stem cells - Perspectives on current status and future directions: AACR workshop on cancer stem cells. *Cancer Research*, 66(19), pp.9339–9344.

Cleary, A.S. et al., 2014. Tumour cell heterogeneity maintained by cooperating subclones in Wnt-driven mammary cancers. *Nature*, 508(7494), pp.113–117.

Cohen, C. et al., 2002. Mitogen-actived protein kinase activation is an early event in melanoma progression. *Clinical cancer research : an official journal of the American Association for Cancer Research*, 8(12), pp.3728–33.

Corominas-Faja, B. et al., 2013. Nuclear reprogramming of luminal-like breast cancer cells generates Sox2-overexpressing cancer stem-like cellular states harboring transcriptional activation of the mTOR pathway. *Cell Cycle*, 12(18), pp.3109–3124.

Costin, G.-E. & Hearing, V.J., 2007. Human skin pigmentation: melanocytes modulate skin color in response to stress. *FASEB journal : official publication of the Federation of American Societies for Experimental Biology*, 21(4), pp.976–94.

Crane, J.F. & Trainor, P.A., 2006. Neural crest stem and progenitor cells. *Annual review of cell and developmental biology*, 22, pp.267–86.

Cronin, J.C. et al., 2013. SOX10 ablation arrests cell cycle, induces senescence, and suppresses melanomagenesis. *Cancer research*, 73(18), pp.5709–18.

Cui, R. et al., 2007. Central Role of p53 in the Suntan Response and Pathologic Hyperpigmentation. *Cell*, 128(5), pp.853–864.

Dankort, D. et al., 2009. Braf(V600E) cooperates with Pten loss to induce metastatic melanoma. *Nature genetics*, 41(5), pp.544–52.

Darwin, C., 1859. On the Origin of Species by Means of Natural Selection, Or, The Preservation of Favoured Races in the Struggle for Life.

Davies, H. et al., 2002. Mutations of the BRAF gene in human cancer. *Nature*, 417(6892), pp.949–954.

Devitt, B. et al., 2011. Clinical outcome and pathological features associated with NRAS mutation in cutaneous melanoma. *Pigment Cell & Melanoma Research*, 24(4), pp.666–672.

Dhillon, A.S. et al., 2007. MAP kinase signalling pathways in cancer. *Oncogene*, 26(22), pp.3279–90.

Dhodapkar, K.M. et al., 2013. SOX2-specific adaptive immunity and response to immunotherapy in non-small cell lung cancer. *OncoImmunology*, 2(7), p.e25205.

Ding, L. et al., 2012. Clonal evolution in relapsed acute myeloid leukaemia revealed by whole-genome sequencing. *Nature*, 481(7382), pp.506–510.

Driskell, R.R. et al., 2009. Sox2-positive dermal papilla cells specify hair follicle type in mammalian epidermis. *Development*, 136(16), pp.2815–2823.

Ekonomou, A. et al., 2005. Neuronal migration and ventral subtype identity in the telencephalon depend on SOX1. *PLoS Biology*, 3(6), pp.1111–1122.

Elder, D.E., 2016. Melanoma progression. *Pathology*, 48(2), pp.147–154.

Ellis, P. et al., 2004. SOX2, a persistent marker for multipotential neural stem cells derived from embryonic stem cells, the embryo or the adult. *Developmental Neuroscience*, 26(2–4), pp.148–165.

Erdei, E. & Torres, S.M., 2010. A new understanding in the epidemiology of melanoma. *Expert review of anticancer therapy*, 10(11), pp.1811–23.

Erickson, C. a & Goins, T.L., 1995. Avian neural crest cells can migrate in the dorsolateral path only if they are specified as melanocytes. *Development*, 121(3), pp.915–24.

Evans, M.J. & Kaufman, M.H., 1981. Establishment in culture of pluripotential cells from mouse embryos. *Nature*.

Falabella, R., 2009. Vitiligo and the melanocyte reservoir. *Indian Journal of Dermatology*, 54(4), pp.313–318.

Fang, L. et al., 2014. A methylation-phosphorylation switch determines Sox2 stability and function in ESC maintenance or differentiation. *Molecular Cell*, 55(4), pp.537–551.

Fang, X. et al., 2010. ChIP-seq and Functional Analysis of the SOX2 Gene in Colorectal Cancers. *OMICS: A Journal of Integrative Biology*, 14(4), pp.369–384.

Faries, M.B. et al., 2017. Completion Dissection or Observation for Sentinel-Node Metastasis in Melanoma. *New England Journal of Medicine*, 376(23), pp.2211–2222.

Favaro, R. et al., 2009. Hippocampal development and neural stem cell maintenance require Sox2-dependent regulation of Shh. *Nature neuroscience*, 12(10), pp.1248–1256.

Ferone, G. et al., 2016. SOX2 Is the Determining Oncogenic Switch in Promoting Lung Squamous Cell Carcinoma from Different Cells of Origin. *Cancer Cell*, 30(4), pp.519–532.

Fialkow, P.J. et al., 1971. Multiple cell origin of hereditary neurofibromas. *The New England journal of medicine*, 284(6), pp.298–300.

Fialkow, P.J., Gartler, S.M. & Yoshida, A., 1967. Clonal origin of chronic myelocytic leukemia in man. *Proceedings of the National Academy of Sciences of the United States of America*, 58(4), pp.1468–71.

Fidler, I. & Hart, I., 1982. Biological diversity in metastatic neoplasms: origins and implications. *Science*, 217(4564), pp.998–1003.

Foulkes, W.D. et al., 1997. The CDKN2A (p16) gene and human cancer. *Molecular Medicine*, 3(1), pp.5–20.

Francescangeli, F. et al., 2012. Proliferation State and Polo-Like Kinase1 Dependence of Tumorigenic Colon Cancer Cells. *STEM CELLS*, 30(9), pp.1819–1830.

Frank, N.Y., 2005. ABCB5-Mediated Doxorubicin Transport and Chemoresistance in Human Malignant Melanoma. *Cancer Research*, 65(10), pp.4320–4333.

Fu, Y. et al., 2013. High-frequency off-target mutagenesis induced by CRISPR-Cas nucleases in human cells. *Nature Biotechnology*, 31(9), pp.822–826.

Fujii, H. et al., 2000. Frequent genetic heterogeneity in the clonal evolution of gynecological carcinosarcoma and its influence on phenotypic diversity. *Cancer research*, 60(1), pp.114–20.

Gaggioli, C. & Sahai, E., 2007. Melanoma invasion ? current knowledge and future directions. *Pigment Cell Research*, 20(3), pp.161–172.

Gajewski, T.F., Schreiber, H. & Fu, Y.-X., 2013. Innate and adaptive immune cells in the tumor microenvironment. *Nature Immunology*, 14(10), pp.1014–1022.

Gandini, S., Sera, F., Cattaruzza, M.S., Pasquini, P., Picconi, O., et al., 2005. Meta-analysis of risk factors for cutaneous melanoma: II. Sun exposure. *European Journal of Cancer*, 41(1), pp.45–60.

Gandini, S., Sera, F., Cattaruzza, M.S., Pasquini, P., Zanetti, R., et al., 2005. Meta-analysis of risk factors for cutaneous melanoma: III. Family history, actinic damage and phenotypic factors. *European Journal of Cancer*, 41(14), pp.2040–2059.

Gangemi, R.M.R. et al., 2009. SOX2 Silencing in Glioblastoma Tumor-Initiating Cells Causes Stop of Proliferation and Loss of Tumorigenicity. *Stem Cells*, 27(1), pp.40–48.

Gao, J. et al., 2013. Integrative Analysis of Complex Cancer Genomics and Clinical Profiles Using the cBioPortal. *Science Signaling*, 6(269), p.pl1-pl1.

Gao, M. et al., 2010. CD24+ cells from hierarchically organized ovarian cancer are enriched in cancer stem cells. *Oncogene*, 29(18), pp.2672–2680.

Garcia, S.B., Novelli, M. & Wright, N.A., 2002. The clonal origin and clonal evolution of epithelial tumours. *International Journal of Experimental Pathology*, 81(2), pp.89–116.

Garraway, L.A. et al., 2005. Integrative genomic analyses identify MITF as a lineage survival oncogene amplified in malignant melanoma. *Nature*, 436(7047), pp.117–22.

Garros-Regulez, L. et al., 2016. Targeting SOX2 as a Therapeutic Strategy in Glioblastoma. *Frontiers in Oncology*, 6.

Gerlinger, M. et al., 2012. Intratumor Heterogeneity and Branched Evolution Revealed by Multiregion Sequencing. *New England Journal of Medicine*, 366(10), pp.883–892.

Gershenwald, J.E. et al., 1998. Patterns of recurrence following a negative sentinel lymph node biopsy in 243 patients with stage I or II melanoma. *Journal of clinical oncology : official journal of the American Society of Clinical Oncology*, 16(6), pp.2253–60.

Gibney, G.T. & Smalley, K.S.M., 2013. An unholy alliance: cooperation between BRAF and NF1 in melanoma development and BRAF inhibitor resistance. *Cancer discovery*, 3(3), pp.260–3.

Girouard, S.D. et al., 2012. SOX2 contributes to melanoma cell invasion. *Laboratory Investigation*, 92(3), pp.362–370.

González-García, I., Solé, R. V & Costa, J., 2002. Metapopulation dynamics and spatial heterogeneity in cancer. *Proceedings of the National Academy of Sciences of the United States of America*, 99(20), pp.13085–9. Graham, V. et al., 2003. SOX2 functions to maintain neural progenitor identity. *Neuron*, 39(5), pp.749–65.

Gray-Schopfer, V., Wellbrock, C. & Marais, R., 2007. Melanoma biology and new targeted therapy. *Nature*, 445(7130), pp.851–857.

Greaves, M. & Maley, C.C., 2012. Clonal evolution in cancer. *Nature*, 481(7381), pp.306–313.

Grob, J.J. et al., 1990. Count of benign melanocytic nevi as a major indicator of risk for nonfamilial nodular and superficial spreading melanoma. *Cancer*, 66(2), pp.387–395.

Gu, S. et al., 2012. The Loop Position of shRNAs and Pre-miRNAs Is Critical for the Accuracy of Dicer Processing In Vivo. *Cell*, 151(4), pp.900–911.

Guldberg, P. et al., 1997. Disruption of the MMAC1/PTEN gene by deletion or mutation is a frequent event in malignant melanoma. *Cancer research*, 57(17), pp.3660–3.

Guzman, M.L. et al., 2005. Plenary paper The sesquiterpene lactone parthenolide induces apoptosis of human acute myelogenous leukemia stem and progenitor cells. *Apoptosis*, 105(11), pp.4163–4169.

Hachey, S.J. & Boiko, A.D., 2016. Therapeutic implications of melanoma heterogeneity. *Experimental Dermatology*, 25(7), pp.497–500.

Hale, E.K. et al., 2005. Association of melanoma and neurocutaneous melanocytosis with large congenital melanocytic naevi-results from the NYU-LCMN registry. *British Journal of Dermatology*, 152(3), pp.512–517.

Hanahan, D. & Coussens, L.M., 2012. Accessories to the Crime: Functions of Cells Recruited to the Tumor Microenvironment. *Cancer Cell*, 21(3), pp.309–322.

Hanahan, D. & Weinberg, R.A., 2011. Hallmarks of cancer: the next generation. *Cell*, 144(5), pp.646–74.

Harris, M.L. et al., 2013. A Dual Role for SOX10 in the Maintenance of the Postnatal Melanocyte Lineage and the Differentiation of Melanocyte Stem Cell Progenitors. *PLoS Genetics*, 9(7).

Harris, M.L. & Pavan, W.J., 2013. Postnatal lineage mapping of follicular melanocytes with the Tyr::CreER T 2 transgene. *Pigment Cell & Melanoma Research*, 26(2), pp.269–274.

Heidorn, S.J. et al., 2010. Kinase-Dead BRAF and Oncogenic RAS Cooperate to Drive Tumor Progression through CRAF. *Cell*, 140(2), pp.209–221.

Heppner, G.H., 1984. Tumor heterogeneity. *Cancer research*, 44(6), pp.2259–65.

Hodgkinson, C. et al, 1993. Mutations at the mouse micophthalmia locus are associates with defects in a gene encoding a novel basic-helix-loop-helix-zipper protein. *Cell*, 74, pp.395–404.

Hodi, F.S. et al., 2010. Improved Survival with Ipilimumab in Patients with Metastatic Melanoma. *New England Journal of Medicine*, 363(8), pp.711–723.

Hodis, E. et al., 2012. A landscape of driver mutations in melanoma. *Cell*, 150(2), pp.251–263.

Hoek, K.S. et al., 2008. In vivo Switching of Human Melanoma Cells between Proliferative and Invasive States. *Cancer Research*, 68(3), pp.650–656.

Holly, E.A. et al., 1987. Number of melanocytic nevi as a major risk factor for malignant melanoma. *Journal of the American Academy of Dermatology*, 17(3), pp.459–68.

Hoos, A. et al., 2010. Development of Ipilimumab: Contribution to a New Paradigm for Cancer Immunotherapy. *Seminars in Oncology*, 37(5), pp.533–546.

Houben, R. et al., 2011. High-level expression of wild-type p53 in melanoma cells is frequently associated with inactivity in p53 reporter gene assays. *PloS one*, 6(7), p.e22096.

Hsu, P.D. et al., 2013. DNA targeting specificity of RNA-guided Cas9 nucleases. *Nature Biotechnology*, 31(9), pp.827–832.

Huang, F.W. et al., 2013. Highly Recurrent TERT Promoter Mutations in Human Melanoma. *Science*, 339(6122), pp.957–959.

Ikushima, H. et al., 2009. Autocrine TGF-β Signaling Maintains Tumorigenicity of Glioma-Initiating Cells through Sry-Related HMG-Box Factors. *Cell Stem Cell*, 5(5), pp.504–514.

International Agency for Research on Cancer Working Group on artificial ultraviolet (UV) light and skin cancer, 2007. The association of use of sunbeds with cutaneous malignant melanoma and other skin cancers: A systematic review. *International journal of cancer*, 120(5), pp.1116–22.

Jackson, A.L. et al., 2003. Expression profiling reveals off-target gene regulation by RNAi. *Nature Biotechnology*, 21(6), pp.635–637.

Jamal-Hanjani, M. et al., 2017. Tracking the Evolution of Non-Small-Cell Lung Cancer. *The New England journal of medicine*, 376(22), pp.2109–2121.

Jemal, A. et al., 2006. Cancer Statistics , 2006.

Jimbow, K., 1975. Mitotic activity in non-neoplastic melanocytes in vivo as determined by histochemical, autoradiographic, and electron microscope studies. *The Journal of Cell Biology*, 66(3), pp.663–670.

Joseph, E.W. et al., 2010. The RAF inhibitor PLX4032 inhibits ERK signaling and tumor cell proliferation in a V600E BRAF-selective manner. *Proceedings of the National Academy of Sciences*, 107(33), pp.14903–14908.

Joseph, R., Swaika, A. & Crozier, J.A., 2014. Vemurafenib: an evidence-based review of its clinical utility in the treatment of metastatic melanoma. *Drug Design, Development and Therapy*, 8, p.775.

Juhász, M.L.W. & Marmur, E.S., 2015. Reviewing Challenges in the Diagnosis and Treatment of Lentigo Maligna and

Lentigo-Maligna Melanoma. *Rare Cancers and Therapy*, 3(1–2), pp.133–145.

Jung, J., 2014. Human Tumor Xenograft Models for Preclinical Assessment of Anticancer Drug Development. *Toxicological Research*, 30(1), pp.1–5.

Justilien, V. et al., 2014. The PRKCI and SOX2 Oncogenes Are Coamplified and Cooperate to Activate Hedgehog Signaling in Lung Squamous Cell Carcinoma. *Cancer Cell*, 25(2), pp.139–151.

Ka, V.S.K. et al., 2005. The association between large congenital melanocytic naevi and cutaneous melanoma: preliminary findings from an Internet-based registry of 379 patients. *Melanoma research*, 15(1), pp.61–7.

Kan, L. et al., 2007. Dual function of Sox1 in telencephalic progenitor cells. *Developmental Biology*, 310(1), pp.85–98.

Kelly, P.N. et al., 2007. Tumor growth need not be driven by rare cancer stem cells. *Science*, 317(5836), p.337.

Keramari, M. et al., 2010. Sox2 Is Essential for Formation of Trophectoderm in the Preimplantation Embryo M. Pera, ed. *PLoS ONE*, 5(11), p.e13952.

Kim, H.J. & Bar-Sagi, D., 2004. Modulation of signalling by Sprouty: a developing story. *Nature Reviews Molecular Cell Biology*, 5(6), pp.441–450.

Kim, R., Emi, M. & Tanabe, K., 2007. Cancer immunoediting from immune surveillance to immune escape. *Immunology*, 121(1), pp.1–14.

Kirkwood, J.M. et al., 1996. Interferon alfa-2b adjuvant therapy of high-risk resected cutaneous melanoma: the Eastern Cooperative Oncology Group Trial EST 1684. *Journal of clinical oncology : official journal of the American Society of Clinical Oncology*, 14(1), pp.7–17.

Kisseberth, W.C. & Sandgren, E.P., 2004. Polyclonal Development of Mouse Mammary Preneoplastic Nodules. *Cancer Research*, 64(3), pp.857–863.

Kléber, M. et al., 2005. Neural crest stem cell maintenance by combinatorial Wnt and BMP signaling. *Journal of Cell Biology*, 169(2), pp.309–320.

Konishi, N. et al., 1995. Intratumor cellular heterogeneity and alterations in ras oncogene and p53 tumor suppressor gene in human prostate carcinoma. *The American journal of pathology*, 147(4), pp.1112–22.

Koo, B.-K. et al., 2015. Porcupine inhibitor suppresses paracrine Wnt-driven growth of Rnf43;Znrf3 -mutant neoplasia. *Proceedings of the National Academy of Sciences*, 112(24), pp.7548–7550.

Kornberg, R., 1975. Pseudomelanoma. *Archives of Dermatology*, 111(12), p.1588.

Krauthammer, M. et al., 2012. Exome sequencing identifies recurrent somatic RAC1 mutations in melanoma. *Nature genetics*, 44(9), pp.1006–14.

Kreso, A. & Dick, J.E., 2014. Evolution of the Cancer Stem Cell Model. *Cell Stem Cell*, 14(3), pp.275–291.

Laga, A.C. et al., 2010. Expression of The Embryonic Stem Cell Transcription Factor SOX2 in Human Skin. *The American Journal of Pathology*, 176(2), pp.903–913.

Laga, A.C. et al., 2011. SOX2 and nestin expression in human melanoma: An immunohistochemical and experimental study. *Experimental Dermatology*, 20(4), pp.339–345.

Lang, D. et al., 2005. Pax3 functions at a nodal point in melanocyte stem cell differentiation. *Nature*, 433(7028), pp.884–887.

Lapidot, T. et al., 1994. A cell initiating human acute myeloid leukaemia after transplantation into SCID mice. *Nature*, 367(6464), pp.645–648.

Larkin, J. et al., 2015. Combined Nivolumab and Ipilimumab or Monotherapy in Untreated Melanoma. *New England Journal of Medicine*, 373(1), pp.23–34.

Lee, J.T. et al., 2010. PLX4032, a potent inhibitor of the B-Raf V600E oncogene, selectively inhibits V600E-positive melanomas. *Pigment cell & melanoma research*, 23(6), pp.820–7.

Leith, J.T. et al., 1987. Growth properties of artificial heterogeneous human colon tumors. *Cancer research*, 47(4), pp.1045–51.

Lemmon, M.A. & Schlessinger, J., 2010. Cell signaling by receptor tyrosine kinases. *Cell*, 141(7), pp.1117–1134.

Levenberg, S. et al., 2002. Endothelial cells derived from human embryonic stem cells. *Proceedings of the National Academy of Sciences of the United States of America*, 99(7), pp.4391–6.

Levy, C. et al., 2010. Intronic miR-211 Assumes the Tumor Suppressive Function of Its Host Gene in Melanoma. *Molecular Cell*, 40(5), pp.841–849.

Levy, C., Khaled, M. & Fisher, D.E., 2006. MITF: master regulator of melanocyte development and melanoma oncogene. *Trends in Molecular Medicine*, 12(9), pp.406–414.

Li, Y. et al., 2012. Single-cell sequencing analysis characterizes common and cell-lineage-specific mutations in a muscle-invasive bladder cancer. *GigaScience*, 1(1), p.12.

Linder, D. & Gartler, S.M., 1965. Glucose-6-Phosphate Dehydrogenase Mosaicism: Utilization as a Cell Marker in the Study of Leiomyomas. *Science*, 150(3692), pp.67–69.

Livet, J. et al., 2007. Transgenic strategies for combinatorial expression of fluorescent proteins in the nervous system. *Nature*, 450(7166), pp.56–62.

Lovell-badge, R., 2015. Sox2: Biology and Role in Development and Disease.book , p.344.

Lowings, P., Yavuzer, U. & Goding, C.R., 1992. Positive and negative elements regulate a melanocyte-specific promoter. *Molecular and Cellular Biology*, 12(8), pp.3653–3662.

Ma, Y. et al., 2009. Proteomics Identification of Desmin as a Potential Oncofetal Diagnostic and Prognostic Biomarker in Colorectal Cancer. *Molecular & Cellular Proteomics*, 8(8), pp.1878–1890.

Ma, Y. et al., 2010. The relationship between early embryo development and tumourigenesis. *Journal of Cellular and Molecular Medicine*, 14(12), pp.2697–2701.

Macintosh, C.A. et al., 1998. Precise microdissection of human prostate cancers reveals genotypic heterogeneity. *Cancer research*, 58(1), pp.23–8.

Maddipati, R. & Stanger, B.Z., 2015. Pancreatic Cancer Metastases Harbor Evidence of Polyclonality. *Cancer Discovery*, 5(10), pp.1086–1097.

Maertens, O. et al., 2013. Elucidating Distinct Roles for NF1 in Melanomagenesis. *Cancer Discovery*, 3(3), pp.338–349.

Magee, J.A., Piskounova, E. & Morrison, S.J., 2012. Cancer Stem Cells: Impact, Heterogeneity, and Uncertainty. *Cancer Cell*, 21(3), pp.283–296.

Mark Elwood, J. & Jopson, J., 1997. Melanoma and sun exposure: An overview of published studies. *International Journal of Cancer*, 73(2), pp.198–203.

Martello, G. & Smith, A., 2014. The nature of embryonic stem cells. *Annu Rev Cell Dev Biol*, 30, pp.647–675.

Marusyk, A. et al., 2014. Non-cell-autonomous driving of tumour growth supports sub-clonal heterogeneity. *Nature*, 514(7520), pp.54–58.

Marusyk, A. & Polyak, K., 2010. Tumor heterogeneity: Causes and consequences. *Biochimica et Biophysica Acta (BBA) - Reviews on Cancer*, 1805(1), pp.105–117.

McArthur, G.A. et al., 2012. Marked, Homogeneous, and Early [18F]Fluorodeoxyglucose-Positron Emission Tomography Responses to Vemurafenib in BRAF-Mutant Advanced Melanoma. *Journal of Clinical Oncology*, 30(14), pp.1628–1634.

McCaffrey, A.P. et al., 2002. Gene expression: RNA interference in adult mice. *Nature*, 418(6893), pp.38–39.

McCulloch, J.E.T. and E.A., 1961. A Direct Measurement of the Radiation Sensitivity of Normal Mouse Bone Marrow

Cells. *Radiation Reserach*, 14(2), pp.213–222.

McKENNA, J.K. et al., 2006. Lentigo Maligna/Lentigo Maligna Melanoma: Current State of Diagnosis and Treatment. *Dermatologic Surgery*, 32(4), pp.493–504.

Medema, J.P., 2013. Cancer stem cells: The challenges ahead. *Nature Cell Biology*, 15(4), pp.338–344.

Meissner, M., 2005. Defects in the Human Leukocyte Antigen Class I Antigen Processing Machinery in Head and Neck Squamous Cell Carcinoma: Association with Clinical Outcome. *Clinical Cancer Research*, 11(7), pp.2552–2560.

Merritt, A.J., Gould, K.A. & Dove, W.F., 1997. Polyclonal structure of intestinal adenomas in ApcMin/+ mice with concomitant loss of Apc+ from all tumor lineages. *Proceedings of the National Academy of Sciences*, 94(25), pp.13927–13931.

Michaloglou, C. et al., 2005. BRAFE600-associated senescence-like cell cycle arrest of human naevi. *Nature*, 436(August), pp.720–724.

Mittal, D. et al., 2014. New insights into cancer immunoediting and its three component phases—elimination, equilibrium and escape. *Current Opinion in Immunology*, 27(1), pp.16–25.

Miyagi, S. et al., 2008. Consequence of the loss of Sox2 in the developing brain of the mouse. *FEBS Letters*, 582(18), pp.2811–2815.

Mohamed, A. et al., 2013. SOX10 Expression in Malignant Melanoma, Carcinoma, and Normal Tissues. *Applied Immunohistochemistry & Molecular Morphology*, 21(6), pp.506–510.

Molife, R. & Hancock, B.W., 2002. Adjuvant therapy of malignant melanoma. *Critical reviews in oncology/hematology*, 44(1), pp.81–102.

Mollaaghababa, R. & Pavan, W.J., 2003. The importance of having your SOX on: role of SOX10† in the development of neural crest-derived melanocytes and glia. *Oncogene*, 22(20), pp.3024–3034.

Moore, M.A.S., Williams, N. & Metcalf, D., 1973. In Vitro Colony Formation by Normal and Leukemic Human Hematopoietic Cells: Characterization of the Colony-Forming Cells. *J Natl Cancer Inst*, 50(3), pp.603–623.

Mora, J., 2001. Genetic heterogeneity and clonal evolution in neuroblastoma. *British Journal of Cancer*, 85(2), pp.182–189.

Mort, R.L., Jackson, I.J. & Patton, E.E., 2015. The melanocyte lineage in development and disease. *Development*, 142(4), pp.620–632.

Morton, D.L. et al., 2014. Final Trial Report of Sentinel-Node Biopsy versus Nodal Observation in Melanoma. *New England Journal of Medicine*, 370(7), pp.599–609.

Mu, P. et al., 2017. SOX2 promotes lineage plasticity and antiandrogen resistance in TP53- and RB1-deficient prostate cancer. *Science*, 355(6320), pp.1–6.

Muenst, S. et al., 2016. The immune system and cancer evasion strategies: therapeutic concepts. *Journal of Internal Medicine*, 279(6), pp.541–562.

Nakagawa, M. et al., 2008. Generation of induced pluripotent stem cells without Myc from mouse and human fibroblasts. *Nat Biotechnol*, 26(1), pp.101–106.

Niho, S. et al., 1998. Monoclonality of both pale cells and cuboidal cells of sclerosing hemangioma of the lung. *The American journal of pathology*, 152(4), pp.1065–9.

Nilbert, M. et al., 1995. Monoclonal origin of endometriotic cysts. *International journal of gynecological cancer : official journal of the International Gynecological Cancer Society*, 5(1), pp.61–63.

Nishimura, E.K. et al., 2002. Dominant role of the niche in melanocyte stem-cell fate determination. *Nature*, 416(6883), pp.854–860.

Nishimura, E.K., Granter, S.R. & Fisher, D.E., 2005. Mechanisms of hair graying: Incomplete melanocyte stem cell

maintenance in the niche. *Science*, 307(5710), pp.720–724.

Nowak, M.A., 2006. Five Rules for the Evolution of Cooperation. *Science*, 314(5805), pp.1560–1563.

Nowell, P., 1976. The clonal evolution of tumor cell populations. *Science*, 194(4260), pp.23–28.

O'Brien, C.A. et al., 2007. A human colon cancer cell capable of initiating tumour growth in immunodeficient mice. *Nature*, 445(January), pp.111–115.

van Oijen, M.G. & Slootweg, P.J., 2000. Gain-of-function mutations in the tumor suppressor gene p53. *Clinical cancer research : an official journal of the American Association for Cancer Research*, 6(6), pp.2138–45.

Okubo, T., Pevny, L.H. & Hogan, B.L.M., 2006. Sox2 is required for development of taste bud sensory cells. *Genes and Development*, 20(19), pp.2654–2659.

Osawa, M., 2005. Molecular characterization of melanocyte stem cells in their niche. *Development*, 132(24), pp.5589–5599.

Panhard, S., Lozano, I. & Loussouarn, G., 2012. Greying of the human hair: A worldwide survey, revisiting the "50" rule of thumb. *British Journal of Dermatology*, 167(4), pp.865–873.

Paraiso, K.H.T. et al., 2011. PTEN loss confers BRAF inhibitor resistance to melanoma cells through the suppression of BIM expression. *Cancer Research*, 71(7), pp.2750–2760.

Paratore, C. et al., 2001. Survival and glial fate acquisition of neural crest cells are regulated by an interplay between the transcription factor Sox10 and extrinsic combinatorial signaling. *Development*, 128(20), pp.3949–3961.

Pardoll, D.M., 2012. The blockade of immune checkpoints in cancer immunotherapy. *Nature Reviews Cancer*, 12(4), pp.252–264.

Park, I.-H. et al., 2008. Disease-Specific Induced Pluripotent Stem Cells. *Cell*, 134(5), pp.877–886.

Pasquali, S. et al., 2012. Surgeons' Opinions on Lymphadenectomy in Melanoma Patients with Positive Sentinel Nodes: A Worldwide Web-Based Survey. *Annals of Surgical Oncology*, 19(13), pp.4322–4329.

Pattanayak, V. et al., 2013. High-throughput profiling of off-target DNA cleavage reveals RNA-programmed Cas9 nuclease specificity. *Nature biotechnology*, 31(9), pp.839–43.

Patton, E.E. et al., 2005. BRAF Mutations Are Sufficient to Promote Nevi Formation and Cooperate with p53 in the Genesis of Melanoma. *Current Biology*, 15(3), pp.249–254.

Pece, S. et al., 2010. Biological and Molecular Heterogeneity of Breast Cancers Correlates with Their Cancer Stem Cell Content. *Cell*, 140(1), pp.62–73.

Pinner, S. et al., 2009. Intravital Imaging Reveals Transient Changes in Pigment Production and Brn2 Expression during Metastatic Melanoma Dissemination. *Cancer Research*, 69(20), pp.7969–7977.

Pitulescu, M.E. et al., 2010. Inducible gene targeting in the neonatal vasculature and analysis of retinal angiogenesis in mice. *Nature Protocols*, 5(9), pp.1518–1534.

Podsypanina, K. et al., 1999. Mutation of Pten/Mmac1 in mice causes neoplasia in multiple organ systems. *Proceedings of the National Academy of Sciences*, 96(4), pp.1563–1568.

Poetsch, M., Dittberner, T. & Woenckhaus, C., 2001. PTEN/MMAC1 in malignant melanoma and its importance for tumor progression. *Cancer genetics and cytogenetics*, 125(1), pp.21–6.

Pollock, P.M. et al., 2003. High frequency of BRAF mutations in nevi. *Nature Genetics*, 33(1), pp.19–20.

Polyak, K. & Marusyk, A., 2014. Cancer: Clonal cooperation. *Nature*, 508(7494), pp.52–53.

Potter, N.E. et al., 2013. Single-cell mutational profiling and clonal phylogeny in cancer. *Genome Research*, 23(12), pp.2115–2125.

Prahallad, A. et al., 2012. Unresponsiveness of colon cancer to BRAF(V600E) inhibition through feedback activation of EGFR. *Nature*, 483(7388), pp.100–103.

Que, J. et al., 2007. Multiple dose-dependent roles for Sox2 in the patterning and differentiation of anterior foregut endoderm. *Development (Cambridge, England)*, 134(13), pp.2521–31.

Quintana, E. et al., 2008. Efficient tumour formation by single human melanoma cells. *Nature*, 456(7222), pp.593–598.

Quintana, E. et al., 2010. Phenotypic heterogeneity among tumorigenic melanoma cells from patients that is reversible and not hierarchically organized. *Cancer Cell*, 18(5), pp.510–523.

Quintana, E., Eskiocak, U. & Morrison, S.J., Unpublised.

Rabbani, P. et al., 2011. Coordinated activation of wnt in epithelial and melanocyte stem cells initiates pigmented hair regeneration. *Cell*, 145(6), pp.941–955.

Rastrelli, M. et al., 2014. Melanoma: epidemiology, risk factors, pathogenesis, diagnosis and classification. *In vivo (Athens, Greece)*, 28(6), pp.1005–11.

Reid, A.L. et al., 2013. Markers of circulating tumour cells in the peripheral blood of patients with melanoma correlate with disease recurrence and progression. *British Journal of Dermatology*, 168(1), pp.85–92.

Remenyi, A., 2003. Crystal structure of a POU/HMG/DNA ternary complex suggests differential assembly of Oct4 and Sox2 on two enhancers. *Genes & Development*, 17(16), pp.2048–2059.

Rendl, M., Lewis, L. & Fuchs, E., 2005. Molecular Dissection of Mesenchymal–Epithelial Interactions in the Hair Follicle B. Hogan, ed. *PLoS Biology*, 3(11), p.e331.

Reya, T. et al., 2001. Stem cells, cancer, and cancer stem cells. *Nature*, 414(6859), pp.105–11.

Ribas, A. et al., 2012. New Challenges in Endpoints for Drug Development in Advanced Melanoma. *Clinical Cancer Research*, 18(2), pp.336–341.

Richert, S. et al., 1996. Widespread eruptive dermal and atypical melanocytic nevi in association with chronic myelocytic leukemia: case report and review of the literature. *Journal of the American Academy of Dermatology*, 35(2 Pt 2), pp.326–9.

Rigel, D.S. & Carucci, J.A., 2000. Malignant melanoma: prevention, early detection, and treatment in the 21st century. *CA: a cancer journal for clinicians*, 50(4), pp.215-36-40.

Robert, C. et al., 2015. Nivolumab in Previously Untreated Melanoma without BRAF Mutation. *New England Journal of Medicine*, 372(4), pp.320–330.

Roche-Lestienne, C., 2002. Several types of mutations of the Abl gene can be found in chronic myeloid leukemia patients resistant to STI571, and they can pre-exist to the onset of treatment. *Blood*, 100(3), pp.1014–1018.

Roemer, K., 1999. Mutant p53: Gain-of-Function Oncoproteins and Wild-Type p53 Inactivators. *Biological Chemistry*, 380(7–8), pp.879–887.

Roesch, A. et al., 2010. A Temporarily Distinct Subpopulation of Slow-Cycling Melanoma Cells Is Required for Continuous Tumor Growth. *Cell*, 141(4), pp.583–594.

Rudolph, P. et al., 1998. Enhanced expression of Ki-67, topoisomerase IIalpha, PCNA, p53 and p21WAF1/Cip1 reflecting proliferation and repair activity in UV-irradiated melanocytic nevi. *Human pathology*, 29(12), pp.1480–7.

Sanborn, J.Z. et al., 2015. Phylogenetic analyses of melanoma reveal complex patterns of metastatic dissemination. *Proceedings of the National Academy of Sciences*, 112(35), pp.10995–11000.

Sánchez-Mejías, A. et al., 2010. Involvement of SOX10 in the pathogenesis of Hirschsprung disease: Report of a truncating mutation in an isolated patient. *Journal of Molecular Medicine*, 88(5), pp.507–514.

Santini, R. et al., 2014. SOX2 regulates self-renewal and tumorigenicity of human melanoma-initiating cells. *Oncogene*, 33(38), pp.4697–4708.

Sarkar, A. et al., 2016. Sox2 Suppresses Gastric Tumorigenesis in Mice Article Sox2 Suppresses Gastric Tumorigenesis

in Mice. *CellReports*, 16(7), pp.1–13.

Sawada, M. et al., 1994. Clonal analysis of human gynecologic cancers by means of the polymerase chain reaction. *International journal of cancer*, 58(4), pp.492–6.

Schaefer, S.M. et al., 2017. Sox2 is dispensable for primary melanoma and metastasis formation. *Oncogene*.

Schatton, T. et al., 2008. Identification of cells initiating human melanomas. *Nature*, 451(7176), pp.345–349.

Schneider, M.R., Schmidt-Ullrich, R. & Paus, R., 2009. The Hair Follicle as a Dynamic Miniorgan. *Current Biology*, 19(3), pp.R132–R142.

Schwarz, D. et al., 2014. Ezh2 is required for neural crest-derived cartilage and bone formation. *Development*, 141(4), pp.867–877.

Serrone, L. et al., 2000. Dacarbazine-based chemotherapy for metastatic melanoma: thirty-year experience overview. *Journal of experimental & clinical cancer research : CR*, 19(1), pp.21–34.

Shackleton, M. et al., 2009. Heterogeneity in Cancer: Cancer Stem Cells versus Clonal Evolution. *Cell*, 138(5), pp.822–829.

Shah, M. et al., 2010. A role for ATF2 in regulating MITF and melanoma development. *PLoS genetics*, 6(12), p.e1001258.

Shah, S.P. et al., 2009. Mutational evolution in a lobular breast tumour profiled at single nucleotide resolution. *Nature*, 461(7265), pp.809–13.

Shain, A.H. et al., 2015. The Genetic Evolution of Melanoma from Precursor Lesions. *New England Journal of Medicine*, 373(20), pp.1926–1936.

Shain, A.H. & Bastian, B.C., 2016. From melanocytes to melanomas. *Nat Rev Cancer*, 16(6), pp.345–358.

Shakhova, O. et al., 2015. Antagonistic cross-regulation between Sox9 and Sox10 controls an anti-tumorigenic program in melanoma. *PLoS genetics*, 11(1), p.e1004877.

Shakhova, O., 2014. Neural crest stem cells in melanoma development. *Current Opinion in Oncology*, 26(2), pp.215–221.

Shakhova, O. et al., 2012. Sox10 promotes the formation and maintenance of giant congenital naevi and melanoma. *Nature cell biology*, 14(8), pp.882–90.

Shakhova, O. & Sommer, L., 2010. Neural crest-derived stem cells. *stembook.org*, pp.1–20.

Shamblott, M.J. & Clark, G.O., 2004. Cell therapies for type 1 diabetes mellitus. *Expert opinion on biological therapy*, 4(3), pp.269–277.

Shannan, B. et al., 2016. Heterogeneity in Melanoma. In *Cancer treatment and research*. pp. 1–15.

Shin, J. et al., 2012. Sox10 is expressed in primary melanocytic neoplasms of various histologies but not in fibrohistiocytic proliferations and histiocytoses. *Journal of the American Academy of Dermatology*, 67(4), pp.717–26.

Shipitsin, M. et al., 2007. Molecular Definition of Breast Tumor Heterogeneity. *Cancer Cell*, 11(3), pp.259–273.

Slingluff, C.L. et al., 2000. Melanomas with concordant loss of multiple melanocytic differentiation proteins: immune escape that may be overcome by targeting unique or undefined antigens. *Cancer immunology, immunotherapy : CII*, 48(12), pp.661–72.

Smith, J.W., Townsend, D.E. & Sparkes, R.S., 1971. Genetic variants of glucose-6-phosphate dehydrogenase in the study of carcinoma of the cervix. *Cancer*, 28(2), pp.529–32.

Smoller, B.R., 2006. Histologic criteria for diagnosing primary cutaneous malignant melanoma. *Modern pathology : an official journal of the United States and Canadian Academy of Pathology, Inc*, 19 Suppl 2, pp.S34–S40.

Snippert, H.J. et al., 2010. Intestinal Crypt Homeostasis Results from Neutral Competition between Symmetrically

Dividing Lgr5 Stem Cells. *Cell*, 143(1), pp.134–144.

Sommer, L., 2001. Context-dependent regulation of fate decisions in multipotent progenitor cells of the peripheral nervous system. *Cell and Tissue Research*, 305(2), pp.211–216.

Soriano, P., 1999. Generalized lacZ expression with the ROSA26 Cre reporter strain. *Nature Genetics*, 21(1), pp.70–71.

Sosman, J.A. et al., 2011. A phase 2 trial of complete resection for stage IV melanoma. *Cancer*, 117(20), pp.4740–4706.

Southard-Smith, E.M., Kos, L. & Pavan, W.J., 1998. SOX10 mutation disrupts neural crest development in Dom Hirschsprung mouse model. *Nature Genetics*, 18(1), pp.60–64.

Steingrímsson, E., Copeland, N.G. & Jenkins, N.A., 2005. Melanocyte stem cell maintenance and hair graying. *Cell*, 121(1), pp.9–12.

Steingrímsson, E., Copeland, N.G. & Jenkins, N. a, 2004. Melanocytes and the microphthalmia transcription factor network. *Annual review of genetics*, 38, pp.365–411.

Stemple, D.L. & Anderson, D.J., 1992. Isolation of a Stem-Cell for Neurons and Glia From the Mammalian Neural Crest. *Cell*, 71(6), pp.973–985.

Stenn, K.S. & Paus, R., 2001. Controls of Hair Follicle Cycling. *Physiol Rev*, 81(1), pp.449–494.

Straume, O., Sviland, L. & Akslen, L.A., 2000. Loss of nuclear p16 protein expression correlates with increased tumor cell proliferation (Ki-67) and poor prognosis in patients with vertical growth phase melanoma. *Clinical cancer research : an official journal of the American Association for Cancer Research*, 6(5), pp.1845–53.

Tachibana, M. et al., 1996. Ectopic expression of MITF, a gene for Waardenburg syndrome type 2, converts fibroblasts to cells with melanocyte characteristics. *Nature Genetics*, 14(1), pp.50–54.

Takahashi, K. & Yamanaka, S., 2006. Induction of Pluripotent Stem Cells from Mouse Embryonic and Adult Fibroblast Cultures by Defined Factors. *Cell*, 126(4), pp.663–676.

Tammela, T. et al., 2017. A Wnt-producing niche drives proliferative potential and progression in lung adenocarcinoma. *Nature*, 545(7654), pp.355–359.

Taranova, O. V., 2006. SOX2 is a dose-dependent regulator of retinal neural progenitor competence. *Genes & Development*, 20(9), pp.1187–1202.

Teixeira, M.R. et al., 1996. Karyotypic comparisons of multiple tumorous and macroscopically normal surrounding tissue samples from patients with breast cancer. *Cancer research*, 56(4), pp.855–9.

Terzian, T. et al., 2010. p53 prevents progression of nevi to melanoma predominantly through cell cycle regulation. *Pigment Cell & Melanoma Research*, 23(6), pp.781–794.

Thliveris, A.T. et al., 2013. Transformation of epithelial cells through recruitment leads to polyclonal intestinal tumors. *Proceedings of the National Academy of Sciences*, 110(28), pp.11523–11528.

Thliveris, A.T. et al., 2013. Transformation of epithelial cells through recruitment leads to polyclonal intestinal tumors. *Proceedings of the National Academy of Sciences of the United States of America*, 110(28), pp.11523–8.

Thomas, N.E., Berwick, M. & Cordeiro-Stone, M., 2006. Could BRAF mutations in melanocytic lesions arise from DNA damage induced by ultraviolet radiation? *The Journal of investigative dermatology*, 126(8), pp.1693–6.

Thomson, J.A. et al., 1998. Embryonic Stem Cell Lines Derived from Human Blastocysts. *Science*, 1145(1998), pp.1145–1148.

Thurber, A.E. et al., 2011. Inverse expression states of the BRN2 and MITF transcription factors in melanoma spheres and tumour xenografts regulate the NOTCH pathway. *Oncogene*, 30(27), pp.3036–48.

Togawa, Y. et al., 2010. Melanoma in association with acquired melanocytic nevus in Japan: a review of cases in the literature. *International journal of dermatology*, 49(12), pp.1362–7.

Tsao, H. & Niendorf, K., 2004. Genetic testing in hereditary melanoma. *Journal of the American Academy of Dermatology*, 51(5), pp.803–808.

Ulmer, A., 2004. Immunomagnetic Enrichment, Genomic Characterization, and Prognostic Impact of Circulating Melanoma Cells. *Clinical Cancer Research*, 10(2), pp.531–537.

Utikal, J. et al., 2009. Sox2 is dispensable for the reprogramming of melanocytes and melanoma cells into induced pluripotent stem cells. *Journal of Cell Science*, 122(19), pp.3502–3510.

Vanner, R.J. et al., 2014. Quiescent Sox2+ Cells Drive Hierarchical Growth and Relapse in Sonic Hedgehog Subgroup Medulloblastoma. *Cancer Cell*, 26(1), pp.33–47.

Viana, A.C.L.., Gontijo, B.. & Bittencourt, F.V.., 2013. Giant congenital melanocytic nevus [Nevo melanocítico congênito gigante]. *Anais Brasileiros de Dermatologia*, 88(6), pp.863–878.

Viros, A. et al., 2014. Ultraviolet radiation accelerates BRAF-driven melanomagenesis by targeting TP53. *Nature*, 511(7510), pp.478–82.

Visvader, J.E. & Lindeman, G.J., 2008. Cancer stem cells in solid tumours: accumulating evidence and unresolved questions. *Nature reviews. Cancer*, 8(10), pp.755–68.

Vogelstein, B. et al., 1985. Use of restriction fragment length polymorphisms to determine the clonal origin of human tumors. *Science (New York, N.Y.)*, 227(4687), pp.642–5.

Vogelstein, B. & Kinzler, K.W., 2004. Cancer genes and the pathways they control. *Nature Medicine*, 10(8), pp.789–799.

Vogelstein, B. & Kinzler, K.W., 1993. The multistep nature of cancer. *Trends in Genetics*, 9(4), pp.138–141.

Wagner, J.D. et al., 2003. Patterns of Initial Recurrence and Prognosis after Sentinel Lymph Node Biopsy and Selective Lymphadenectomy for Melanoma. *Plastic and Reconstructive Surgery*, 112(2), pp.486–497.

Wakamatsu, Y. et al., 2004. Multiple roles of Sox2, an HMG-box transcription factor in avian neural crest development. *Developmental Dynamics*, 229(1), pp.74–86.

Walsh, D.S. et al., 1998. Patterns of X chromosome inactivation in sporadic basal cell carcinomas: Evidence for clonality. *Journal of the American Academy of Dermatology*, 38(1), pp.49–55.

Wang, K. et al., 1996. BID: a novel BH3 domain-only death agonist. *Genes & Development*, 10(22), pp.2859–2869.

Wang, Y., 2009. Wnt/Planar cell polarity signaling: A new paradigm for cancer therapy. *Molecular Cancer Therapeutics*, 8(8), pp.2103–2109.

Wargo, J.A. & Tanabe, K., 2009. Surgical Management of Melanoma and Other Skin Cancers. *ACS Surgery: Principles and Practice*, 23(2009), pp.565–581.

Weina, K. & Utikal, J., 2014. SOX2 and cancer: current research and its implications in the clinic. *Clinical and Translational Medicine*, 3(1), p.19.

Weinberg, R., 2006. *The Biology of Cancer*,

Weissman, I.L., 2000. Stem cells: units of development, units of regeneration, and units in evolution. *Cell*, 100(1), pp.157–168.

Whittaker, S.R. et al., 2013. A genome-scale RNA interference screen implicates NF1 loss in resistance to RAF inhibition. *Cancer discovery*, 3(3), pp.350–62.

Wilczynski, J.R., 2006. Cancer and Pregnancy Share Similar Mechanisms of Immunological Escape. *Chemotherapy*, 52(3), pp.107–110.

Wong, C.E. et al., 2006. Neural crest–derived cells with stem cell features can be traced back to multiple lineages in the adult skin. , 175(6), pp.1005–1015.

Wu, H., Goel, V. & Haluska, F.G., 2003. PTEN signaling pathways in melanoma. *Oncogene*, 22(20), pp.3113–22.

Xie, K. & Abbruzzese, J.L., 2003. Developmental biology informs cancer: the emerging role of the hedgehog signaling pathway in upper gastrointestinal cancers. *Cancer cell*, 4(4), pp.245–7.

Xu, X. et al., 2012. Single-Cell Exome Sequencing Reveals Single-Nucleotide Mutation Characteristics of a Kidney Tumor. *Cell*, 148(5), pp.886–895.

Yancovitz, M. et al., 2012. Intra- and Inter-Tumor Heterogeneity of BRAFV600EMutations in Primary and Metastatic Melanoma J. M. Brandner, ed. *PLoS ONE*, 7(1), p.e29336.

Yang, H. et al., 2010. RG7204 (PLX4032), a selective BRAFV600E inhibitor, displays potent antitumor activity in preclinical melanoma models. *Cancer research*, 70(13), pp.5518–27.

Yuan, H. et al., 1995. Developmental-specific activity of the FGF-4 enhancer requires the synergistic action of Sox2 and Oct-3. *Genes and Development*, 9(21), pp.2635–2645.

Zaal, L.H. et al., 2004. Classification of congenital melanocytic naevi and malignant transformation: A review of the literature. *British Journal of Plastic Surgery*, 57(8), pp.707–719.

Zalaudek, I. et al., 2011. Frequency of dermoscopic nevus subtypes by age and body site: a cross-sectional study. *Archives of dermatology*, 147(6), pp.663–70.

Zhang, S., 2014. Sox2, a key factor in the regulation of pluripotency and neural differentiation. *World Journal of Stem Cells*, 6(3), p.305.

Zhang, S. & Cui, W., 2014. Sox2, a key factor in the regulation of pluripotency and neural differentiation. *World journal of stem cells*, 6(3), pp.305–11. Zimmerli, D. et al., 2017. Pharmacological interventions in the Wnt pathway: Inhibition of Wnt secretion versus disrupting the protein-protein interfaces of nuclear factors. *British Journal of Pharmacology*.

Zindl, C.L. & Chaplin, D.D., 2010. Tumor Immune Evasion. *Science*, 328(5979), pp.697–698. Zingg, D. et al., 2015. The epigenetic modifier EZH2 controls melanoma growth and metastasis through silencing of distinct tumour suppressors. *Nature Communications*, 6(May 2014), p.6051.

Zipser, M.C. et al., 2011. A proliferative melanoma cell phenotype is responsive to RAF/MEK inhibition independent of BRAF mutation status. *Pigment Cell and Melanoma Research*, 24(2), pp.326–333.